The Dissertation Committee for Yaning Wu Certifies that this is the approved version of the following dissertation:

Establishing a *Drosophila* model for Angelman Syndrome

Committee:

Janice A. Fischer, Supervisor

Jon M. Huibregtse

Paul M. Macdonald

Theresa J. O'Halloran

John C. Sisson

Establishing a *Drosophila* model for Angelman Syndrome

by

Yaning Wu, B.M.; M.S.

Dissertation

Presented to the Faculty of the Graduate School of

The University of Texas at Austin

in Partial Fulfillment

of the Requirements

for the Degree of

Doctor of Philosophy

The University of Texas at Austin

August 2007

Dedication

To my family

for their love and support

Acknowledgements

Looking back on my journey over the past seven years, I cannot help wondering if I would have made it this far without the tremendous help and guidance from Janice Fischer, my wonderful mentor. It was her knowledge, encouragement and patience that help me focus on my research and face whatever challenges I encountered during all these years. This was a once in a lifetime learning experience for me and I will treasure it forever. I am also grateful to my committee members for their insightful criticism and constructive suggestions. My special thanks go to the great former UT undergraduate Monica Suliman. Monica worked with me for two years as an undergraduate student and contributed remarkably to the early stage of this project, even though her work was not included in the dissertation. I also want to thank all the Fischer lab members, past and present, for their help, discussions and friendships.

Establishing a *Drosophila* model for Angelman syndrome

Publication No._____

Yaning Wu, Ph.D.

The University of Texas at Austin, 2007

Supervisor: Janice A. Fischer

Drosophila models for human diseases have helped in advancing our knowledge on human diseases and the discovery of potential treatments. Angelman syndrome is a rare neurological disorder that results in severe mental retardation and loss of motor coordination. The disease is caused by loss-of-function mutations in the *UBE3A* gene encoding a HECT domain ubiquitin protein ligase. *Drosophila dube3a* is the fly homolog of human *UBE3A* and their protein products share ~55% similarity in amino acid sequence along the entire length of the proteins. My goal was to develop a *Drosophila* AS model that will allow us to identify the AS-associated substrate(s) of the *Drosophila UBE3A* homolog and ultimately, to determine why the lack of UBE3A protein causes Angelman syndrome in humans. Dube3a is present in the embryonic, larval and adult central nervous system, including the adult mushroom bodies, which is the center for learning and memory. I have generated *dube3a* knock-out flies and they appear normal externally, but

display abnormal locomotor behaviors. Flies that overexpress wild-type *dube3a* in the nervous system also display locomotion defects, and these overexpression phenotypes are dependent on the presence of a conserved cysteine residue essential for HECT domain E3 enzymatic activity. Targeted overexpression of *dube3a* in the eye, the wing, or ubiquitously causes rough eyes, curly wings and lethality, respectively. These morphological abnormalities in the eye or wing depend on the critical catalytic cysteine of Dube3a. Overexpression of mutant *dube3a* carrying AS-associated point mutations does not elicit such defects, suggesting they act as loss-of-function mutants. Taken together, *dube3a* mutants are a candidate fly model for Angelman syndrome, and the flies that overexpress *dube3a* in the eye or wing are useful for genetic screens to identify the elusive UBE3A substrates relevant to Angelman syndrome.

Table of Contents

List of Tables

List of Figures

Chapter 1: General Introduction

THE UBIQUITIN PATHWAY AND HUMAN DISEASES

Ubiquitin is a 76 amino acid long globular polypeptide, highly conserved from yeast to humans. Covalent attachment of ubiquitin molecules to target proteins provides a dynamic and reversible posttranslational regulation of protein functions. Ubiquitination has been implicated in a variety of cellular processes, such as transcription regulation, cell-cycle control, cell signaling, apoptosis, DNA replication and damage repair, immune response, and protein subcellular localization (Weissman 2001). Malfunctions of the ubiquitin pathway play roles in many human diseases, including neurodegenerative diseases, cancers, and metabolic disorders (Sakamoto 2002; Miller and Wilson 2003). Ubiquitination modifies protein functions in two ways. First, certain poly-ubiquitin chains direct tagged proteins to the proteasome, a multi-subunit proteolytic complex, for degradation. Second, mono-ubiquitination and a subset of polyubiquitin linkages modulate protein functions in ways reminiscent of phosphorylation (Hicke 2001).

The Ubiquitin Conjugating System

Protein ubiquitination occurs through a series of enzymatic reactions usually composed of a ubiquitin-activating enzyme (E1), a ubiquitin-conjugating enzyme or ubiquitin-carrier proteins (E2) and a ubiquitin-protein ligase (E3). Ubiquitin modification is a reversible process. Ubiquitin moieties attached to the target protein can be removed from the substrate, disassembled and recycled by deubiquitinating enzymes.

Ubiquitin-activating enzyme (E1)

Ubiquitin is initially activated by the E1 enzyme in an ATP-dependent manner, resulting in thiolester bond formation between the carboxyl-terminal glycine of the ubiquitin molecule and a conserved cysteine residue in the E1 active site. In *S. cerevisiae*, the *UBA1* gene encodes the 114 kDa Uba1p protein and is essential for yeast cell viability (McGrath et al. 1991). The human E1 enzyme exists in two isoforms, both of which are translated from the same mRNA through alternative translation initiation codons. The 117 kDa E1a isoform is phosphorylated, which regulates its nuclear versus cytoplasmic localization, in a manner that depends on the cell-cycle. The 110 kDa short isoform E1b is not phosphorylated and, in contrast to E1a, has a primarily cytoplasmic distribution. Although these two isoforms are indistinguishable in their E2 recruitment capabilities, their different

localization might provide a mechanism for selecting substrate proteins for ubiquitination (Handley et al. 1991; Handley-Gearhart et al. 1994; Stephen et al. 1996; Shang et al. 2001).

Ubiquitin-conjugating enzyme (E2)

The activated ubiquitin moiety is transferred form the E1 enzyme to an E2 enzyme by forming a thiolester bond between the ubiquitin carboxyl-end glycine and a cysteine in the E2 active site. All E2s share a ~150 amino acid UBC domain containing the conserved cysteine. The E2s can be assigned into four structural classes: class-I E2s consist almost exclusively of the core domain only; class-II E2s have additional carboxyl-terminal sequences; class-III E2s have amino-terminal extensions and class-IV E2s have both amino- and carboxyl end extensions (Plafker et al. 2004). The amino- and/or carboxyl- extended segments might promote interactions with the upstream E1, downstream E3 or even the final substrates (Pickart 2001; Weissman 2001). Although ubiquitin target specificity is thought to depend mainly on E3s (see below), the variety of E2s apparently confers substrate recognition and selection to a certain extent. A single E2 can work with several but not all E3s, and a single E3 can interact with many but not all E2s. Thus, the various permutations and combinations of E2-E3 complexes elicit a plethora of target protein specifications (Weissman 2001). Furthermore,

the observation that the transport receptor importin-11 binds to ubiquitin-loaded class-III E2s, and shuttles them from the cytoplasm to the nucleus, grants an interesting new layer of ubiquitin pathway regulation (Plafker et al. 2004; Zhang and Matunis 2005).

Ubiquitin protein ligases (E3)

The spectrum of E3 ligases is much larger than that of E2 enzymes and new members continue to be identified. In the enzymatic cascade of the ubiquitin pathway, the E3 ligase is the major determinant of substrate specificity. Identification of E3 substrate(s) will help in understanding the ubiquitin pathway and its mechanisms.

There are two major classes of E3s: the HECT (Homologous to E6AP C-terminus) domain E3s and the RING (Really Interesting New Gene) domain E3s. Unlike RING E3s, which bring the E2 to the substrate and facilitate the direct transfer of the ubiquitin moiety from the E2 to the substrate, HECT domain E3s themselves receive the ubiquitin moiety from the upstream E2s and then pass it to the substrates. In the HECT domain, the carboxyl terminal ~350 amino acid sequence, a highly conserved cysteine residue located ~35 amino acids upstream of the C-terminus is the site for thiolester bond-mediated ubiquitin conjugation (Weissman 2001).

HECT domain E3s

HECT domain E3s are modular enzymes, with the divergent amino termini responsible for substrate binding and thus defining target protein specificity, and the carboxyl terminal HECT domain for E2 binding and catalytic ubiquitin transfer in the E2→E3→substrate order. However, as the HECT domains of different HECT enzymes cannot be interchanged, it is likely that HECT domain itself contributes, at least partially, to substrate specification (Rotin et al. 2000; Pickart 2001).

The founder of the HECT domain E3 ligase family is E6AP (E6-associated protein), a ~100 kDa cellular protein. E6AP is encoded by the *UBE3A* gene, and E6AP and UBE3A refer to the same protein product. E6AP was identified as the E3 that mediates tumor suppressor p53 ubiquitination in cervical cancer cells infected by high-risk human papillomavirus HPV16 or HPV18 (Huibregtse et al. 1993; Scheffner et al. 1993). p53 is not an E6AP substrate in normal cells and the recognition of p53 as an E6AP substrate in HPV-infected cells requires the presence of the E6 viral protein. In a sense, E6 hijacks E6AP by changing its substrate specificity. Ubiquitination of p53 by the E6/E6AP complex leads to its proteasomal degradation. In E6AP, the high-risk E6 binding site is composed of 18 amino acids and located ~120 amino acids N-

terminal to the HECT domain (see Figure 2.1) (Huibregtse et al. 1993). The association of E6 with E6AP is the prerequisite step for these two proteins to form a stable complex with p53. The ~240 amino acids long region immediately N-terminal to the HECT domain in E6AP, encompassing the E6 binding motif, is required for p53 binding (Huibregtse et al. 1993; Huibregtse and Beaudenon 1996). How these three proteins physically bind to each other in the p53/E6/E6AP ternary complex is still not clear. E6/E6AP complex also targets the ubiquitin-mediated degradation of hDlg (the human homolog of *Drosophila* Disc large) (Matsumoto et al. 2006; Kuballa et al. 2007) and hScrib (the human homolog of *Drosophila* Scribble) (Nakagawa and Huibregtse 2000). These proteins are tumor suppressor proteins as well and function in epithelial cell polarity regulation. Similar to p53, E6AP only targets the ubiquitination of hScrib and hDlg in the presence of E6. Through mediating the degradation of p53, hScrib and hDlg, E6AP plays an important role in high-risk E6-related carcinogenesis.

Several proteins have been identified as potential constitutive E6AP substrates. HHR23A, a human homolog of the yeast DNA repair protein Rad23, is reported to be an E6-independent target of E6AP (Kumar et al. 1999). The interaction between E6AP and HHR23A is mediated by E6AP N-terminal region, while the E6AP HECT domain is

incapable of HHR23A binding. Several Src family tyrosine kinases, including Blk (B-lymphoid-specific tyrosine kinase) and Src itself, may also be ubiquitinated by E6AP and then subject to proteasome-mediated degradation (Oda et al. 1999). Another potential substrate of E6AP is the multicopy maintenance protein 7 (Mcm7), a subunit of the replication licensing factor (Kuhne and Banks 1998). The direct association of E6AP and Mcm7 is facilitated by the L2G domains present in both proteins (Kuhne and Banks 1998). The L2G domain in E6AP overlaps with the minimal E6-binding site in E6AP, with the L2G consensus sequence (S/TXXXLLG) located inside the E6-binding sequence (see Figure 2.1). E6AP also functions as its own substrate *in vitro* and this process may be promoted by E6 protein in HPV-infected cells (Nuber et al. 1998; Kao et al. 2000). The minimal region of E6AP required for serving as an E6AP substrate is ~570 amino acids long, with the C-terminal end ~100 amino acids away from E6AP C-terminus (Nuber et al. 1998). These available data enforce the idea that the substrate specificity of E6AP is conferred by its N-terminal sequence. However, a common ubiquitination signal shared by all these E6-independent E6AP substrates remains elusive.

In addition to E6AP, only a small portion of HECT domain proteins have been studied in detail about their catalytic activities as well as

substrate recognitions. The majority of such investigated HECT proteins belong to the Nedd4 (neural precursor cell-expressed developmentally downregulated gene 4) subclass HECT domain E3s. In addition to the carboxyl terminal HECT domain, the Nedd4-like proteins have a C2 domain near the amino end and two to four WW domains at the middle of the protein. This Nedd4 subclass is conserved from yeast to human, with one Nedd4-like protein in *S. cerevisiae*, three in *C. elegans* and *D. melanogaster*, and more in human and mouse (Ingham et al. 2004; Shearwin-Whyatt et al. 2006).

Originally identified in protein kinase C and later in various proteins, the C2 or calcium/ lipid binding domains are ~120 amino acids in length and can bind to calcium, phospholipids and other proteins in a calcium-dependent manner. The C2 domains play roles in membrane translocation and functional regulation of the Nedd4 proteins (Plant et al. 1997; Ingham et al. 2004).

WW domains are ~35 amino acids long protein-protein interaction domains with two conserved tryptophan residues ~20 amino acids apart (Harvey and Kumar 1999; Ingham et al. 2004). The WW domains in Nedd4 family E3s mediate the interaction between the substrate and the enzyme by binding to proline-rich motifs in the substrates, such as PPxY

and phosphorylated serine or threonine residues followed by a proline residue (Shearwin-Whyatt et al. 2006). In vitro, WW2 domains from different Nedd4 family members can bind to the same PY motifs and different WW domains from the same E3 have different binding specificity to the same substrate (Harvey and Kumar 1999). As some of the targets of the Nedd4 family E3s don't have apparent WW domain-interacting modules, it was speculated that adaptor proteins carrying PY motifs can recruit the Nedd4 E3s to such atypical substrates (Harvey and Kumar 1999; Shearwin-Whyatt et al. 2006).

The combination of multi-WW domains in Nedd4 family members and the variable protein-binding preference of different WW domains expand the range of cellular proteins that potentially can interact with Nedd4 family proteins, as well as the complexity of tuning Nedd4 family functions (Shearwin-Whyatt et al. 2006).

In addition to the WW domains, the C2 domains of Nedd4-like proteins contribute to localizing the HECT domain proteins, through phospholipid-membrane targeting or binding to accessory protein positioning signals. This provides another level of Nedd4-substrate specificity by regulating the physical juxtaposition of the E3 enzyme and the substrate (Shearwin-Whyatt et al. 2006).

Nedd4 family proteins play roles in an array of cellular processes, including cell signaling, cellular transports, cell-cycle control and transcription regulation. Substrates of Nedd4 family proteins have diverse subcellular distributions and functions. Rsp5p is the only Nedd4-like protein in *S. cerevisiae* and has divergent substrates involved in unrelated cellular processes, including the large subunits of RNA polymerase II, Gap1 (the general amino acid permease), Fur4p (the uracil permease) and Ste2p (the alpha factor receptor) (Rotin et al. 2000; Shearwin-Whyatt et al. 2006). In vertebrates, the TGF-β (Transforming growth factor-β) signaling pathway is tightly controlled by the ubiquitin pathway with the Nedd4-like protein Smurf 1 (Smad ubiquitination-related factor 1), Smurf2 and SCF/Roc1 as the major E3s (Izzi and Attisano 2004). Smurf1 and Smurf2 bind directly to Smad (Sma/Mad related proteins) through the WW-PY modules interaction, and mediate its ubiquitination and degradation. Smad also functions as an adaptor protein to bridge the interaction of Smurf1/2 to other components of the TGF-β pathway, such as the TGF-β receptor and transcription suppressor SnoN, thus leading to their degradation (Ingham et al. 2004; Shearwin-Whyatt et al. 2006). The renal epithelial sodium channel ENaC is the best-studied substrate of mammalian Nedd4-2 and regulates unidirectional flow of the sodium into epithelial cells. ENac is composed

by α, β and γ subunits carrying PY motifs at their carboxyl-termini. Nedd4-2 binds to ENaC through these PY motifs and mediates ENaC ubiquitination and internalization, thus downregulating the cell surface distribution of ENaC (Flores et al. 2003; Snyder 2005).

RING finger domain E3s

The size of the RING finger domain ubiquitin E3 family is much larger than the HECT domain ubiquitin ligase family. The RING finger domain is composed of forty to one hundred amino acids with the linear sequence Cys-X_2-Cys-X_{9-39}-Cys-X_{1-3}-His-X_{2-3}-Cys/His-X_2-Cys-X_{4-48}-Cys-X_2-Cys. The eight conserved cysteine and histidine residues coordinate two zinc ions in a “cross-brace” manner. The RING domain is the site for E2 binding. Other than the RING finger domains, the RING finger proteins have unrelated sequences (Freemont 2000; Fang et al. 2003).

RING finger domain E3s can be categorized into simple RING E3s and complex RING E3s. For simple or single subunit RING domain E3s, such as Cbl (Casitas B-lineage lymphoma), BRCA1 (breast cancer specific tumor suppressor protein 1) and Mdm2 (Murine double minute 2), the E2 binding and the substrate recognition capacities lie in a single protein. It is relatively common, however, for RING E3s to perform their enzymatic activity by forming homodimers or heterodimers through their

RING finger domains or other part of the proteins. For example, BRCA1 forms a heterodimer with BARD1 (BRCA1 associated RING domain 1), which is a more stable and potent E3 than BRCA1 on its own. Similarly, the Mdm2-Mdm4 heterodimer makes a more effective E3 than Mdm2 alone. For complex RING domain E3s, the ubiquitin ligase enzymatic activity is performed by a multisubunit protein complex, such as APC (the anaphase promoting complex) or cyclosome, VHL (the von-Hippel Lindau complex) and SCF (the Skp1-Culin1-F box complex). In these RING E3 complexes, there is one RING finger domain protein, one protein from the Cullin family, and some other proteins that may facilitate substrate interaction. Usually, the RING finger domain subunit recruits the E2, the Cullin protein acts as the scaffolding component and the other subunits are responsible for substrate binding and complex assembly (Hershko and Shapira 2006). Given that RING finger proteins lack apparent homology aside of the RING finger domains, no specific substrate interaction mode can be defined by RING finger E3s (Glickman and Ciechanover 2002; Fang et al. 2003; Lehner et al. 2005).

Deubiquitinating enzymes (DUBs)

Ubiquitination is a reversible process, as the ubiquitin moiety attached to the substrate can be removed or shortened by deubiquitinating enzymes (DUBs). DUBs can be divided into two groups

according to the catalytic mechanism of their protease activity: cysteine proteases and metalloproteases. All DUBs from the metalloprotease group carry the JAMM (Jab1/MPN/Mov34) protease motif. The cysteine protease DUBs can be further divided into four subclasses based on their catalytic domain structure: UCH (ubiquitin carboxyl-terminal hydrolase), USP (ubiquitin-specific protease), OUT (ovarian tumor protease) and MJD (Machado-Joseph disease protease). OUTs, MJDs and JAMM motif proteases are relatively recent members of the DUB family and their functions await further investigations (Amerik and Hochstrasser 2004; Nijman et al. 2005; Millard and Wood 2006). The first described DUBs are UCHs which have a preference for small ubiquitin-attached substrates and are involved mainly in ubiquitin recycling. UCHs also catalyze the processing of ubiquitin precursors translated as polyubiquitin chains or fused ubiquitin-ribosomal protein into singular ubiquitin molecules. USPs forms the largest and most diverse subclass of DUBs. They release ubiquitin from large substrates and disassemble ubiquitin polymer chains (Weissman 2001; Amerik and Hochstrasser 2004; Nijman et al. 2005).

Monoubiquitination versus polyubiquitination

Ub-tagged target proteins take a variety of fates including degradation by the proteasome complex, targeting to certain subcellular

organelles, or alterations in their functions. The destiny of the ubiquitinated targets depends on the number of ubiquitins conjugated onto the substrate, whether they are single ubiquitins or chains, and if chains, the particular lysine residues of ubiquitin used to link the chain (Weissman 2001; Hoppe 2005).

The ubiquitin system was first discovered by its ability to mark cellular proteins for proteasomal degradation. Proteasomal degradation usually requires that the substrate is conjugated with a polyubiquitin chain with at least four ubiquitins. Polyubiquitin chains are formed by attaching the carboxyl-terminal glycine of a ubiquitin monomer to an internal lysine residue of the previously incorporated ubiquitin. In the highly conserved ubiquitin molecule, there are seven internal lysine residues that potentially can be utilized for addition of another ubiquitin. They are Lys^{6}, Lys^{11}, Lys^{27}, Lys^{29}, Lys^{33}, Lys^{48} and Lys^{63} and the most-studied ones are Lys^{11}, Lys^{29}, Lys^{48} and Lys^{63}. Ubiquitin polymers built through Lys^{48} linkage usually serve as an efficient degradation tag and deliver the attached substrate to the 26S proteasomal complex, where the substrates are degraded into small peptides. This is a crucial process for the cell survival, as unwanted or misfolded proteins can be cleared away to ensure proper cellular functioning. Polyubiquitin chains formed with Lys^{63}-linkages usually send target proteins to non-

proteasomal pathways, such as cellular signaling, DNA damage repair, and transcription regulation, presumably through providing binding surfaces for proteins facilitating such processes. Lys^{29}-linkage, Lys^{11}-linkage, Lys^{6}-linkage are also used to generate polyubiquitin chains *in vivo*, although their physiological significances are still unclear (Fang and Weissman 2004; Starita and Parvin 2006; Willis and Patterson 2006).

The ubiquitin pathway targets can be mono-ubiquitinated with a single ubiquitin attached to a substrate lysine residue, or multi-ubiquitinated with multiple lysines of the substrate attached with a single ubiquitin moiety. Mono- or multi-ubiquitination plays a role in modulating target protein activity and is involved in a variety of subcellular processes including endocytosis, protein trafficking, and DNA damage repair (Hicke 2001; Hicke and Dunn 2003; Mukhopadhyay and Riezman 2007).

Ubiquitination and Human Diseases

The enormous number of cellular proteins subject to ubiquitin modification indicates the involvement of the ubiquitin pathway in almost every aspect of subcellular processes. It comes as no surprise that the ubiquitin pathway is interwoven in the pathogenesis of various human diseases, including neurodegenerative diseases, cardiovascular diseases, cancers and metabolic disorders to name just a few

(Sakamoto 2002; Sun 2003; Ardley and Robinson 2004; Herrmann et al. 2004). Understanding the roles played by ubiquitination in the etiology and progression of the human disorders sure will significantly advance our knowledge of these diseases and shed light on developing new treatments to prevent and cure these illnesses. The fact that E3s (together with E2) define substrate specificity and the presence of hundreds of E3s in the human genome means that they are good disease targets. This is also true for DUBs, which cooperate with E3s in fine-tuning the states of ubiquitin pathway substrates. Most of the diseases with a contribution from the ubiquitin pathway can be roughly divided into two categories: diseases caused by dysfunctional substrates of the ubiquitin pathway, and diseases caused by mutations in ubiquitin pathway components— especially the evolutionally diverse ubiquitin ligases and deubiquitinating enzymes.

Diseases caused by mutations of ubiquitin pathway substrates

Nedd4 and Liddle's syndrome

Liddle's syndrome is an autosomal dominant inherited form of hypertension caused by mutations in the carboxyl-terminus of β or γ subunits of ENaC. Subunits of ENaC at the cell surface are multiubiquitinated by Nedd4-2, through the interaction of the PY motifs located at the carboxyl-terminal of the ENaC subunits and the WW2

domains of Nedd4-2. These ubiquitinated ENaC channels may be internalized to downregulate their activity. The Liddle's syndrome-associated ENaC mutations delete or disrupt these PY motifs, and thus prevent Nedd4-2-mediated ubiquitination and downregulation of ENaC cell membrane distribution. Elevated epithelial distribution of ENaC leads to excessive re-absorption of sodium and water in the renal tubules, resulting in chronic hypertension (Staub et al. 1997; Snyder et al. 2004; Wiemuth et al. 2007).

Ubiquitin and neurodegenerative diseases

A hallmark of most neurodegenerative diseases, such as Alzheimer's disease, Huntington's disease, Parkinson's disease and Kennedy disease, is the presence of insoluble intracellular protein aggregates. Involvement of the ubiquitin pathway in such chronic conditions was suggested by the presence of ubiquitin conjugates as well as ubiquitinated cellular proteins in the prominent aggregates. However, the precise role of the ubiquitin system in the pathogenesis of these diseases is still under assessment. The emerging theory is that the ubiquitin-containing aggregates reflect a failure of the ubiquitin pathway to clear toxic cellular proteins because of overstressed proteasomal degradation machinery (Arnaud et al. 2006).

Diseases related to malfunctions of ubiquitin pathway components

Mdm2, E6AP, p53 and cancers

A pivotal coordinator of the cell stress response, cell-cycle control and apoptosis, the p53 tumor suppressor is under tight regulation to maintain a low steady-state cellular level. Under extrinsic stresses such as DNA damage, the p53 level is increased, which leads to the halt of cell-cycle progression and the activation of DNA repair machinery, or apoptosis cascades if the stress is overwhelming. p53 thus protects the cells from undergoing oncogenic transformation. Ubiquitination of p53 plays an important role in the stringent control of p53 level, with the RING finger domain protein Mdm2 as the major E3 that mediates p53 ubiquitination and degradation. Elevated level of Mdm2, especially resulting from gene amplification, is detected in various human cancers. It may cause cancer through over-ubiquitination and degradation of p53, which leads the cells tolerant to DNA damage and undergo tumorigenic transformation (Momand et al. 1998; Onel and Cordon-Cardo 2004; Brooks and Gu 2006; Ciechanover 2006).

Mdm2 is not the only E3 involved in p53 degradation in cancers. As described above, while normally not an E3 for p53, the HECT domain E6AP is geared into mediating p53 degradation through binding viral E6 proteins. As the presence of E6 decrease the levels of p53, the already

low p53 levels predisposes the development of cervical cancer in HPV affected patients.

SCF^{Skp2}, p27 and cancers

Like p53, p27 is another tumor suppressor regulated by the ubiquitin pathway. Downregulation of p27 is related to oral carcinoma, breast cancer, prostate cancer, lung cancer and lymphomas. p27 plays an important role in both cell proliferation and tissue differentiation, through binding and inhibition of cyclinE/CDK2 and cyclinA/CDK2 complex activity. Because these cyclin/CDK2 complexes are essential for initiating the G1 to S phase transition, p27 acts as a negative cell-cycle regulator and arrests cell-cycle progression. SCF^{Skp2} is the ubiquitin ligase that mediates p27 ubiquitination, where the S-phase kinase-associated protein 2 (Skp2) is the F-box protein that recognize p27. An inverse relationship between p27 and Skp2 levels has been demonstrated in several kinds of human cancers. Amplification of the chromosome region containing *skp2* is observed in tumors. The oncogenic potentials of Skp2 was also shown by its ability to transform nude mice and cultured cells (Gstaiger et al. 2001; Hershko et al. 2001; Yokoi et al. 2002; Yokoi et al. 2004).

BRCA1, BARD1 and breast and ovary cancers

Inheritance of a mutant copy of the breast cancer specific tumor suppressor protein 1 (BRCA1) is related to remarkably high susceptibility to breast cancer and ovarian cancer. BRCA1 is a RING finger domain E3 that is involved in DNA damage repair, cell-cycle regulation and transcription activation. The relevance of BRCA1 E3 function to breast cancer is supported by the finding that all mutations related to cancer susceptibility are located in the RING domain. BRCA1 pairs with BARD1 (BRCA1 Associated RING Domain protein1) to form a more stable and efficient E3 heterodimer than BCA1 alone. BARD1 is a RING finger domain protein as well, although no E3 activity has been detected from it alone. BARD1 is also implicated in breast cancer. Although their relevance to cancer predisposition is elusive, many proteins are ubiquitinated by the BRCA1-BARD1 heterodimer *in vitro*, including several histones, RNA polymerase II and p53. Recently, ERα (estrogen receptor α), which is mono-ubiquitinated by BRAC1-BARD1, has been suggested as a substrate for the BRCA1/BARD1 ubiquitin ligase relevant to breast cancer. This might reconcile the discrepancy between ubiquitous BRCA1 expression and the tissue-specific cancer susceptibility of the breast and the ovary (Boulton 2006; Eakin et al. 2007; Huo et al. 2007).

pVHL and von Hippel-Lindau disease

von Hippel-Lindau disease is an autosomal dominant familial cancer syndrome that predisposes individuals to hypervascular tumors in a variety of organs. This disease is cause by mutations of one copy of the *VHL* gene, encoding the VHL tumor suppressor protein. VHL is a subunit of a RING domain E3 complex (ECV or VHL) composed of Cullin2, RBx1/Hrt1, Elongin B (a ubiquitin-like molecule) and Elongin C (a Skp1-related molecule). Among multiple substrates of VHL identified, the transcription factor HIFα (hypoxia-inducible factor 1-α) is the most established target of VHL. Under normoxic or hyperoxic conditions, VHL mediates the ubiquitination and proteasomal degradation of HIFα, whereas under hypoxic conditions, this regulation is inhibited. Through forming a heterodimer with the constitutive HIFβ, HIFα transactivates a broad array of hypoxia-inducible genes, including vascular endothelial growth factor (VEGF), erythropoietin (EPO) and glucose transporter-1 (GLUT1). HIFα-promoted expression of such hypoxia-inducible genes can explain, at least partially, the characteristic hypervascular tumorigenesis in VHL disease, where lack of functional VHL results in high subcellular levels of HIFα due to failure of HIFα ubiquitination and degradation (Haase 2006; Ke and Costa 2006; Ohh 2006).

CYLD and cylindromatosis

Mutations in deubiquitinating enzyme encoding genes are also related to tumorigenesis. Originally identified as the tumor suppressor gene involved in familial cylindromatosis, *cyld* encodes the deubiquitinating enzyme CYLD. Cylindromatosis is an autosomal dominant predisposition to development of multiple benign tumors of the skin appendages. Substrates of CYLD include IKKγ (IκB kinase γ), TRAF2 (Tumor Necrosis Factor Receptor-Associated Factor 2) and TRAF6. CYLD thus negatively regulates the crucial NF-κB pathway associated with inflammation, immunity response and apoptosis. CYLD specifically disbands Lys^{63}-linked polyubiquitin chain, not Lys^{48}-linked ones (Brummelkamp et al. 2003; Kovalenko et al. 2003; Trompouki et al. 2003). Recently, studies done with *cyld*-deficient mice demonstrated that CYLD also removes Lys^{63}-polyubiquitin chain from Bcl-3, and thus hinders its nuclear translocation. As ubiquitination and nuclear accumulation of Bcl-3 is the prerequisite step for activating transcription of a subclass of NF-κB target genes, including *cyclin D1*, CYLD hence modulate the function of the NF-κB pathway in controlling cell proliferation and oncogenesis. (Ikeda and Dikic 2006; Massoumi et al. 2006)

Parkin, UCH-L1 and Parkinson's disease

Autosomal recessive juvenile parkinsonism (AR-JP) is the rare familial form of Parkinson's disease and is linked to mutations in the *parkin* gene which encodes a RING finger domain ubiquitin ligase. AR-JP associated *parkin* mutations abolish the protein's E3 function. It was speculated that subcellular accumulation of one or more substrates of Parkin due to failure in proteasomal degradation is detrimental to dopaminergic neurons and causes Parkinson's disease (Hattori and Mizuno 2004; Wood-Kaczmar et al. 2006). More than ten cellular proteins have been identified as Parkin targets, including α-synuclein, synphilin-1 and parkin-associated endothelin-receptor-like receptor (PAEL). Whether subcellular accumulation of these substrates leads to Parkinson's disease and if so, how, is unclear (Wood-Kaczmar et al. 2006).

Ubiquitin carboxyl-terminal hydrolase L1 (UCH-L1) is another ubiquitin pathway component implicated in Parkinson's disease. UCH-L1 is a deubiquitinating enzyme and mutations in UCH-L1 cause autosomal dominant Parkinson's disease (Wood-Kaczmar et al. 2006). In addition, a polymorphic UCH-L1Ser18Tyr variant displays protective effect again sporadic Parkinson's disease in some ethnic groups, although not others (Mellick and Silburn 2000; Zhang et al. 2000; Levecque et al. 2001;

Satoh and Kuroda 2001; Wang et al. 2002; Elbaz et al. 2003; Miller and Wilson 2003; Wood-Kaczmar et al. 2006; Carmine Belin et al. 2007).

Interestingly, it was found recently, that both parkin and UCH-L1 have dual functionalities. In addition to assembling Lys^{48}-linked polyubiquitin chain onto substrate(s), parkin also promotes formation of Lys^{63}-linked polyubiquitin chains (Doss-Pepe et al. 2005). As for UCH-L1, in addition to its DUB function, it also possesses ubiquitin ligase activity (Liu et al. 2002). Furthermore, a substrate for parkin and UCH-L1 mediated Lys^{63}-linked polyubiquitin chain attachment, α-synuclein, also stimulates assembly of $lysine^{63}$-linked ubiquitin conjugates through an unknown mechanism (Doss-Pepe et al. 2005; Liu et al. 2007). These findings suggest that in addition to compromised ubiquitin-proteasomal degradation, ubiquitination might be interwoven in Parkinson's disease pathogenesis through non-proteasomal pathways as well (Lim et al. 2006).

UBE3A/E6AP AND ANGELMAN SYNDROME

Epidemiology and Clinical Features of Angelman Syndrome

Angelman syndrome (AS) is a neurodevelopmental disorder that affects both sexes. Studies on AS have been reported from various countries, including, but not limited to, United States, Canada, France, Italy, Finland, Demark, Sweden, Switzerland, Russia, Australia, Brazil and Japan (Petersen et al. 1995; Mglinets et al. 1996; Steffenburg et al. 1996; Fung et al. 1998; Malzac et al. 1998; Baumer et al. 1999; Russo et al. 2000; Rapakko et al. 2004; Varela et al. 2004; Saitoh et al. 2005; Dion et al. 2007). The prevalence of AS is estimated to be between 1 in 10,000 and 1 in 20,000 births (Williams 2005). Clinical features of AS include severe developmental delay, mental retardation, speech impairment, ataxic gaits and jerky movements. The abandoned original name, “happy puppet” syndrome, reflects the characteristic happy and social nature of AS patients and the easiness in provoking excessive and sometimes inappropriate laughing from the affected children. Seizures, sleep disorders, microcephaly, abnormal EEG patterns and subtle dysmorphic facial features, such as wide-opening mouth, large chin and deep-set eyes, are also seen in some patients (Clayton-Smith and Laan 2003; Williams 2005).

Genetic Mechanisms of Angelman Syndrome

Angelman syndrome is caused by genetic defects in the chromosome 15q11-q13 region, which is subject to genomic imprinting of the paternal chromosome (Clayton-Smith and Laan 2003; Sahoo et al. 2005). To date, AS cases are divided into five classes according to the genetic mechanisms leading to this disorder: (I) Large interstitial deletion of the maternal chromosome 15q11-q13 region. This kind of defect is the most prevalent and found in ~70% of AS cases. The majority of the deletions are 3~4Mb in size. (II) Paternal uniparental disomy (UPD), where both copies of chromosome 15 are paternal-derived. This occurs in ~5% of AS patients. Given that the 15q11-13 region is subject to paternal silencing, in these individuals, gene(s) related to AS are not expressed from either chromosome. (III) Imprinting defects (ID), which account for ~5% of all AS cases. In those cases, maternal copies of the gene(s) relevant to AS in the 15q11-13 region are silenced through abnormal imprinting. (IV) *UBE3A* mutations. The *UBE3A* gene is located in the 15q11-13 region. In ~10% of AS cases, mutations in this gene have been found. These mutations could be point mutations, small (<15bp) deletions or insertions. (V) Unknown. For 10% of the AS patients, no chromosome 15 abnormality has been detected (Russo et al. 2000; Lossie et al. 2001; Lalande and Calciano 2007).

Correlations between the genetic mechanisms and clinical severity are also observed. In comparison to other classes, patients from Class I and Class V display more severe symptoms, such as frequent seizures and absence of speech. Class II and Class III patients are the least severe cases. Class IV lies in the middle of Class I/V and Class II/III (Lossie et al. 2001; Clayton-Smith and Laan 2003; Lalande and Calciano 2007). The underlying molecular mechanism for such phenotypic discrepancies present in different AS classes is not clear. For Class I, it was speculated that haplo-insufficiency of other genes encompassed in the 15q11-13 deletion contributes to the severe clinical manifestations (Lossie et al. 2001; Clayton-Smith and Laan 2003).

UBE3A, residing in the 15q11-13 region was identified as the pathogenic gene of AS in 1997, as intragenic *UBE3A* mutations were isolated from AS patients lacking of maternal deletion, paternal UPD or imprinting defects in the vital 15q11-13 region (Kishino et al. 1997; Matsuura et al. 1997). The fact that class IV patients display typical AS phenotypes argues that absence or disruption of expression of *UBE3A* from the maternally inherited chromosome (the only one that expresses *UBE3A*) is the cause of the major clinical deficits in AS cases through known genetic mechanisms (class I~IV). For the Class V (unknown) group, there may be mutations in the non-coding region of *UBE3A*.

Another possibility is that the patients in this class carry mutations in other genes controlling *UBE3A* expression or function, such as genes in the ubiquitin pathway that might interact and modify UBE3A function. It is equally likely that mutations in genes encoding UBE3A substrates or other downstream components are responsible for AS development in the group (Lossie et al. 2001; Clayton-Smith and Laan 2003).

Current Hypothesis for Pathogenesis of Angelman Syndrome

The *UBE3A* gene encodes the UBE3A (also known as E6AP, see above) ubiquitin protein ligase. The genomic DNA sequence for *UBE3A* covers more than 120kb, composed of sixteen exons (Kishino and Wagstaff 1998). There are three isoforms of UBE3A/E6AP resulting from alternative splicing, which are different at their amino-termini (Yamamoto et al. 1997). It is not clear which isoform is the predominant one in the brain, nor if they are differentially relevant to AS. All AS-associated *UBE3A* mutations affect all three isoforms. The majority of all *UBE3A* mutations known to date (Table 1.1) are frameshifts and nonsense mutations, resulting in premature stop codons and carboxyl-terminally truncated proteins (Kishino et al. 1997; Matsuura et al. 1997; Fung et al. 1998; Malzac et al. 1998; Tsai et al. 1998; Baumer et al. 1999; Fang et al. 1999; Huang et al. 1999; Moncla et al. 1999; Russo et al. 2000; Lossie et al. 2001; Burger et al. 2002; Rapakko et al. 2004). As the

HECT domain is carboxyl-terminal, this suggests that these mutations are loss-of-function mutations and that the impairment of UBE3A/E6AP ubiquitin ligase function is critical to the disease state (Lalande and Calciano 2007). In addition, missense mutations or other mutations that alter amino acids have been identified (Table 1.1). For three of such mutations, S349P, R506C and M802MI (in-frame insertion of an isoleucine), the clinical manifestations are not distinguishable from patients carrying frameshift or nonsense mutations (Malzac et al. 1998; Baumer et al. 1999). For the C21Y missense mutation, however, milder clinical phenotypes were reported (Matsuura et al. 1997; Fang et al. 1999). No clinical phenotypic descriptions for the remainder of the AS-associated amino acid changes are available.

A simple model for how UBE3A/E6AP deficiency leads to AS phenotypes is that loss-of-function UBE3A/E6AP mutants fail to ubiquitinate and subsequently degrade its normal substrate(s). The subcellular accumulation of the substrate protein(s) is detrimental for neuronal development and/or function and leads to AS. Another possibility is that UBE3A/E6AP mono-ubiquitinates its substrate(s), thus modulating their functions. As biochemical experiments indicate that the polyubiquitin chains produced by UBE3A/E6AP are Lys48-linked (Wang and Pickart 2005), the first model seems to be the most likely one.

Frameshift Mutations

Site	Mutation	Reference
Exon 8	645insA	Malzac et al. 1998
Exon 8	762–763insGA	Baumer et al. 1999
Exon 8	856delG	Fang et al. 1999
Exon 9	897insA	Russo et al. 2000
Exon 9	904del5	Fang et al. 1999
Exon 9	946delAG	van den Ouweland et al.1999
Exon 9	980delAG	Lossie et al. 2001 Fang et al. 1999
Exon 9	1296insT	Baumer et al. 1999
Exon 9	1461del14	Malzac et al. 1998
Exon 9	1522delG	Malzac et al. 1998
Exon 9	1552delA	Lossie et al. 2001 Fang et al. 1999
Exon 9	1559del7	Fang et al. 1999
Exon 9	1694del4	Fang et al. 1999
Exon 9	1930del 2	Lossie et al. 2001
Exon 9	1930delAG	Matsuura et al. 1997 Fung et al.1998 Fang et al. 1999 Rapakko et al. 2004
Exon 9	2037del10	Malzac et al. 1998
Exon 10	2230del26insA	Malzac et al. 1998
Exon 11	2376delG	Baumer et al. 1999
Exon 12	2527insA	Malzac et al. 1998
Exon 12	2544insA	Russo et al. 2000
Exon 12	2567ins4	Fang et al. 1999
Exon 16	3027insT	van den Ouweland et al.1999
Exon 16	3033insA	Malzac et al. 1998
Exon 16	3076ins4	van den Ouweland et al.1999
Exon 16	3086ins5	Kishino et al. 1997 Malzac et al. 1998
Exon 16	3092delA	Lossie et al. 2001
Exon 16	3093del 4	Fang et al. 1999 Lossie et al. 2001 Rapakko et al. 2004
Exon 16	3120ins16	Baumer et al. 1999
Intron 9	IVS9-8A→G	Kishino et al., 1997 Malzac et al. 1998

Nonsense Mutations

Site	Mutation		Reference
Exon 9	1085G→T	E167X	Russo et al. 2000
Exon 9	1500G→A	W305X	Fang et al. 1999
Exon 9	1835C→T	R417X	Lossie et al. 2001 Fang et al. 1999

			Matsuura et al.,1997
Exon 9	2030C→T	R482X	Malzac et al. 1998 Lossie et al. 2001 Russo et al. 2000
Exon 9	2033 A→T	R483X	Lossie 2001
Exon 9	2185T→G	Y533X	Fang et al. 1999
Exon 15	2890G→A	W768X	Tsai et al.,1998 Fang et al. 1999
Missense Mutations/In-frame Insertions or Deletions			
Site	**Mutation**		**Reference**
Exon 8	648G→A	C21Y	Lossie et al. 2001 Fang et al. 1999 Matsuura et al.,1997
Exon 9	902A→C	T106P	Rapakko et al. 2004
Exon 9	975T→C	I130T	Rapakko et al. 2004
Exon 9	1631T→C	S349P	Malzac et al. 1998
		L502P	Huang et al. 1999
Exon 9	2102C→T	R506C	Baumer et al. 1999
		E550L	Huang et al. 1999
Exon 15	2929del3	F782Δ	Fang et al. 1999
Exon 15	2992ins3	M802MI	Malzac et al. 1998
Exon 15	2997T→A	I804K	Fang et al. 1999
Exon 16	3142del15	Elongated protein	Fang et al. 1999
Other AS-associated Mutations			
Site	**Mutation**		**Reference**
Intron11	-12del7		van den Ouweland et al.1999
Benign Polymorphisms			
Site	**Mutation**		**Reference**
Exon 8	702G→A	R39H	Malzac et al. 1998
Exon 9	1118G→A	A178T	Matsuura et al.,1997 Malzac et al. 1998 Baumer et al. 1999 Fang et al. 1999 Rapakko et al. 2004
Exon 9	1144A→G	silent mutation	Lossie et al. 2001
Exon 16	3'UTRdel14		Fung et al. 1998; Baumer et al. 1999
Intron6	-47insT		Lossie et al. 2001
Intron7	GATGAT→GAT		Fang et al. 1999
Intron12	T→C		Baumer et al. 1999

Table 1.1: Benign polymorphism and Angelman syndrome-related mutations in *UBE3A*. Nucleotide and amino acid positions are according to GenBank U84404 (UBE3A isoform1, the smallest isoform).

Although several proteins have been identified as the constitutive substrates of E6AP or UBE3A, including HHR23A, Blk and Mcm7 (see above). The relevance of these substrate(s) to the pathophysiology of AS is unclear.

Mouse Models for Angelman Syndrome

Several AS mouse models have been established and provide valuable research tools for study of this disorder**.** Mouse chromosome region 7C containing the mouse *UBE3A* gene corresponds to human chromosome 15q11-13 and is also subject to imprinting. The first AS model utilizes mice with partial paternal disomy of chromosome 7 (UPD). These mice display AS analogous phenotypes, such as growth retardation, deficient locomotor skills, hyperactivity, reduction in brain weight and a salient AS-characteristic EEG abnormality (Cattanach et al. 1997). RNA *in situ* hybridization analyses using these paternal UPD mice demonstrate preferential expression of the maternal murine *UBE3A* copy in Purkinje cells, hippocampal neurons and mitral cells of the olfactory bulbs (Albrecht et al. 1997). This is among the first reports of brain-specific imprinting of mammalian *UBE3A*, which also highlights the association of AS-like phenotypes with certain brains regions. Mice carrying a large chromosome 7C deletion (Gabriel et al. 1999) or

imprinting defect (Gabriel et al. 1999; Wu et al. 2006) are also reported as models of AS. In addition, two *UBE3A*-specific knock-out mouse models have been generated through targeted inactivation of *UBE3A* (Jiang et al. 1998; Miura et al. 2002). Impaired behaviors of these mice mimic AS phenotypes: locomotor dysfunctions, defective hippocampus-dependent learning and abnormal EEG are observed with both maternal chromosome *UBE3A*-deficiencent models. Predominant expression of *UBE3A* from the maternally inherited chromosome in the hippocampus and the cerebellar Purkinje cell layer is also confirmed in these *UBE3A* knock-out mice. Sleep disorders are also detected in the *UBE3A* maternal chromosome-deficient mice model developed by Miura et al. (2002). Jiang et al. (1998) also described the presence of inducible seizures and impaired hippocampal long-term potentiation (LTP) in their mouse model, which first suggested a potential correlation between the cognitive deficits in AS and aberrant LTP. Further investigations of these mice led to the proposal that disruption of calcium/calmodulin-dependent kinase type 2 (CaMKII) activity regulations is related to the LTP deficit in AS mice, and very likely the mental retardation symptoms in AS humans. Significantly decreased enzymatic activities of protein phosphatases 1 (PP1) or PP2A, the major phosphatases for CaMKII may be responsible for the misregulation of CaMKII. In the AS mouse brain, elevated phospho-CaMKII at sites Thr285 and Thr305 and reduced CaMKII

activity is detected in the hippocampus, even though the total level of CaMKII is unaltered (Weeber et al. 2003). Remarkably, many AS-like phenotypes caused by murine maternal chromosome *UBE3A*-deficiency are rescued by the presence of CaMKII Thr305Val/Thr306A, whose mutations prevent the inhibitory phosphorylation of CaMKII (van Woerden et al. 2007). This suggests that CaMKII malfunction contributes to the overall neurological defects in AS. Neither CaMKII nor its phosphatases PP1/PP2A are likely the direct target of UBE3A/E6AP-mediated ubiquitination/degradation, as no changes in total concentrations of CaMKII or these phosphatases are detected in brains of the mouse model (Weeber et al. 2003). The crucial cellular protein(s) that link the UBE3A/E6AP mutations to CaMKII function remain mysterious.

Drosophila DISEASE MODELS

Reasons for Utilizing the Fruit Fly to Model Human Diseases

For more than a hundred years, *Drosophila melanogaster* (the fruit fly) has been an appealing model organism to study all kinds of biological phenomena. The well-developed genetic tools available and the completion of the fly genome project make the fruit fly an attractive system for doing both forward and reverse genetics. An emerging theme is to use the fruit fly to model human diseases, given that many pathogenic genes of human disorders have conservative homologs in the fly. By comparing the human genome and the *D. melanogaster* genome, it was reported that over 75% of the known human disease genes can find their orthologs in the fly genome (Rubin et al. 2000; Reiter et al. 2001).

Investigation of the genetic and molecular functions of the fly counterparts of such pathogenic genes can be achieved by making gene-specific knock-out mutants or by ectopically expressing the fly or/ and the human genes using the bipartite *Gal4-UAS* system (Brand and Perrimon 1993). The latter is especially amenable to genetic manipulation with the vast collection of *Gal4* drivers enabling the highly specialized temporal and spatial expression of the transgenes in virtually

any fly tissue. Many genes, even those without apparent morphological knock-out phenotypes, when misexpressed with the *Gal4-UAS* system, give rise to morphological defects. These easy-to-screen-for phenotypes can be used as backgrounds for genome-wide genetic modifier screens. In addition to the traditional mutagens, such as EMS and X-ray radiation, to generate *de novo* mutations throughout the entire genome, the availability of growing collections of isogenized deficiency chromosomes and P element insertion lines will speed up the screen processes and the discovery of genes in the disease pathways. The identification of genes in the pathways of the human disease homologs will lead to the understanding of the functions of the disease genes and shed light on the underlying mechanism of disease pathogenesis. For many disease genes that are essential for fly viability, the powerful FLP-FRT technique enables the study of classical homozygous knock-out mutants in special tissues in the otherwise heterozygous flies (Golic 1991).

Drosophila models for neurodevelopmental diseases, neurodegenerative diseases and cancers have been well established (Bilen and Bonini 2005; Cauchi and van den Heuvel 2006). The realization that the functions of the heart, the kidney and the immune system are conserved from fly to human also makes the fruit fly a promising model system for cardiovascular diseases, kidney diseases

and infectious diseases (Bier and Bodmer 2004; Brumby and Richardson 2005; Marsh and Thompson 2006; Sanchez-Martinez et al. 2006; Vidal and Cagan 2006; Ocorr et al. 2007). These models not only provide a platform for *in vivo* analyses of the developmental and cellular behaviors of diseases genes and proteins, they also provide rapid and economic testing systems for therapeutic drugs.

Fly Models for Neurodegenerative Diseases

"Neurodegenerative diseases" is the collective description for over thirty clinical disorders caused by progressive loss of neurons. Characteristic symptoms for this class of diseases are ataxia and declining cognitive function (dementia). The representative neuropathological feature for these conditions is the formation of intracellular filamentous aggregates. The major protein components of the intracellular inclusions differ among neurodegenerative diseases. Prevalence of these devastating chronic neurological disorders rises over time, given the lengthened life expectancy of man and the fact that most of them are late-onset. No effective treatments are currently available (Ardley and Robinson 2004; Marsh and Thompson 2004; Troulinaki and Tavernarakis 2005). A growing list of neurodegenerative diseases modeled in fly includes Huntington's disease (HD), Alzheimer's Disease (AD), Parkinson's Disease (PD), Amyotrophic Lateral Sclerosis

(ALS), Spinocerebellar Ataxia (SCA), Kennedy disease (KD) and hereditary spastic paraplegia (HSP) (Merry 2005; Cauchi and van den Heuvel 2006).

Fly models for Polyglutamine diseases

Polyglutamine (PolyQ) diseases, with HD as the classical representative, refer to a group of disorders caused by CAG codon expansion, resulting in the incorporation of abnormally long glutamine stretches in the affected proteins. Such aberrant proteins are the major components of nuclear inclusions, a typical pathological feature shared by the PolyQ diseases. Most diseases in this collection show autosomal dominant inheritance, except Kennedy disease, which is X-linked (Merry 2005; Mutsuddi and Rebay 2005; Cauchi and van den Heuvel 2006).

Fly models for HD and other PolyQ diseases were generated by misexpression of full-length or truncated human PolyQ-expanded proteins, such as Huntingtin (Htt) protein for HD (Jackson et al. 1998; Lee et al. 2004), androgen receptor (hAR) for KD (Chan et al. 2002; Takeyama et al. 2002), and ataxin-1, ataxin-3 and ataxin-7 for SCA-1 (Fernandez-Funez et al. 2000), SCA-3/Machado-Joseph disease (Warrick et al. 1998) and SCA-7 (Latouche et al. 2007) respectively. In fact, direct expression of excessive epitope tagged polyQ peptide is

sufficient to introduce neuropathology (Kazemi-Esfarjani and Benzer 2000; Marsh et al. 2000). Mutant phenotypes exhibited by these fly models mirror well the central characteristics of PolyQ diseases in many aspects. For example, the presence of distinguishing nuclear inclusions in affected cells and late on-set progressive cell degeneration are highly proportional to the number of the CAG repeats. Decreased life span and locomotor activity were demonstrated in fly models, when mutant proteins were targeted for nervous system expression (Warrick et al. 1998; Marsh et al. 2000; Lee et al. 2004; Latouche et al. 2007).

These fly models have made enormous contributions to identifying molecular mechanisms underlying the pathophysiology. Unbiased genetic screens for dominant modifiers of neurodegenerative eye phenotypes of the fly models (Fernandez-Funez et al. 2000; Kazemi-Esfarjani and Benzer 2000; Bilen et al. 2006) have revealed various cellular pathways and processes involved in the polyQ-mediated neuronal degeneration. Protein folding chaperone proteins have been isolated as genetic modifiers of the eye defects in both the SCA-1 model (Fernandez-Funez et al. 2000) and the tag-polyQ peptide model (Kazemi-Esfarjani and Benzer 2000). The ubiquitin pathway is implicated in the neuronal pathogenesis, as ubiquitin and other Ub pathway components were isolated in the SCA-1 screen (Fernandez-Funez et al.

2000). Transcriptional factors compose another group of modulators of the SCA-1 eye phenotype (Fernandez-Funez et al. 2000). This offers persuasive support for the relevance of transcriptional regulation to polyQ disease, as the toxicity of the nuclear inclusions was speculated to repress transcription. An interesting class of genetic modifiers is made up of genes involved in RNA regulation. While several RNA binding proteins were recovered in the SCA-1 screen (Fernandez-Funez et al. 2000), the involvement of microRNA pathway in neurodegeneration were first described in a similar screen for genes that alter the SCA-3 eye phenotype (Bilen et al. 2006).

These fly models also provide an *in vivo* system for evaluating candidate genes speculated to play roles in polyQ disease pathogenesis as well. The possible relevance of histone acteylation/ deacetylation balance-monitored transcription control (Steffan et al. 2001; Taylor et al. 2003), post-translational protein modification and protein folding (Warrick et al. 1999; Chan et al. 2002; Steffan et al. 2004) as well as the microRNA pathway (Bilen et al. 2006) to polyQ-mediated degeneration were examined in fly polyQ models.

Drosophila polyQ models are also valued for their efficiency in low-cost *in vivo* screens for promising therapeutic molecules identified

through high-throughout biochemical screens (Kaltenbach et al. 2007). Even though it might seem intimidating to utilize invertebrates for selecting future drugs, the therapeutic effects of the histone deacetylase (HDAC) inhibitors in the fly (Steffan et al. 2001) were comparable to those in the mouse (Ferrante et al. 2003; Hockly et al. 2003). This argues strongly for the potentials of the fly model for preliminary *in vivo* chemical assessment.

Fly models for Alzheimer's disease

AD is the leading cause of senile dementia, with two cardinal histopathological markers— the extracellular amyloid plaques composed of the β-amyloid peptides (Aβs) and tau protein-based intracellular neurofibrillary tangles. Aβs are the proteolytic fragments of the amyloid precursor protein (APP), which is cleaved by β-secretase and Presenilin-based γ-secretase. There are two forms of Aβs, $A\beta_{40}$ and $A\beta_{42}$. It was proposed that excessive production of the sticky $A\beta_{42}$, due to increased APP expression or aberrant APP cleavage, initiates AD pathogenesis (Bilen and Bonini 2005; Cauchi and van den Heuvel 2006).

Given that fly APP lacks sequence homology at the Aβ region (Rosen et al. 1989), fly AD models have been established through misexpression of $A\beta_{42}$ or human APP, which leads to neurodegenerative

defects, such as compromised locomotor ability and shortened life span. These models provide *in vivo* evidence for the proposed mechanism of APP processing and Aβ toxicity (Finelli et al. 2004; Greeve et al. 2004; Iijima et al. 2004; Crowther et al. 2005). They are also useful for screening/assaying genetic modifiers of Aβ neurotoxicity (Finelli et al. 2004; Kinghorn et al. 2006) or pharmacological ones (Greeve et al. 2004; Crowther et al. 2005).

Furthermore, research in *Drosophila* provides insights into the physiological functions of fly and human APP homologs in neurons (Torroja et al. 1999; Torroja et al. 1999; Gunawardena and Goldstein 2001; Merdes et al. 2004; Leyssen et al. 2005; Rusu et al. 2007). These findings may well be extended into mouse or human systems, as exemplified by the involvement of APPs in axonal transport in both flies and vertebrates (Torroja et al. 1999; Gunawardena and Goldstein 2001; Stokin et al. 2005). The fruit fly also provides an practical system for analyzing the normal function of Presenilin (Lu et al. 2007) as well as *in vivo* molecular properties of AD-related *presenilin* mutants (Ye and Fortini 1999; Seidner et al. 2006).

Neurofibrillary tangles composed of hyperphosphorylated tau, a microtubule-binding protein, are another characteristic pathological

feature of AD. Parallel to Aβ fly models, misexpression of normal or mutant human tau in flies were used for probing the mechanism of tau-associated neurodegeneration (Wittmann et al. 2001; Jackson et al. 2002; Chee et al. 2005). Although, the tau proteins in these models are hyperphosphorylated, no neurofibrillary tangles were observed. These thus provide *in vivo* evidence for the uncoupling of these two cellular events. A genetic screen for modifiers of tau toxicity (Ghosh and Feany 2004) recovered a large class of protein kinases and phosphatases, suggesting that phosphorylation of tau is important. These screen results are dramatically different from the types of modifiers yield from the polyQ model screen (as above). This significant difference suggests that divergent molecular mechanisms underline neurodegenerative diseases sharing overlapping clinical and pathological features. As with all fly disease models, the tau overexpression flies were used for candidate gene analyses as well (Jackson et al. 2002; Ghosh and Feany 2004).

Fly model for Parkinson's disease

The discoveries of PD causative genes related to the rare forms of familial PD help in advancing our knowledge of pathogenesis of both hereditary and sporadic PD. The list of these PD genes includes *α-synuclein*, *parkin*, *DJ-1*, *PTEN-induced putative kinase 1* (*Pink-1*), and LRRK2/PARK8 (Wood-Kaczmar et al. 2006). Except for *α-synuclein*,

there are fly homologs for these PD causative genes (Whitworth et al. 2006). α-synuclein mutations are associated with autosomal dominant PD. Misexpression of human wild-type and mutant (A30P, A53T) *α-synuclein* in *Drosophila* leads to the first and most intensively studied fly PD model. *α-synuclein* overexpression recapitulate dopaminergic neuron loss, the appearance of intraneuronal proteineous aggregates resembling PD Lewy's body, and locomotor deficits features of PD (Feany and Bender 2000). In search for a means to alter α-synuclein toxicity, it was found that heat-shock chaperones will do just that. α-synuclein toxicity was alleviated genetically by HSP70 overexpression. Moreover, drugs that induce chaperone overexpression also alleviate α-synuclein toxicity (Auluck and Bonini 2002; Auluck et al. 2002). The phosphorylation state of α-synuclein is also crucial for its neurotoxicity (Whitworth et al. 2006).

Loss of *Pink, parkin*, and *DJ-1* are linked to autosomal recessive PD. Research on their fly homologs have shed light on the physiological functions of these genes as well as on the underlying mechanisms for PD pathogenesis. Disruption of either *Drosophila parkin* (Greene et al. 2003; Pesah et al. 2004; Whitworth et al. 2005) or *dPink1* alone (Clark et al. 2006; Park et al. 2006; Yang et al. 2006) leads to muscle degeneration, selective loss of dopaminergic neurons, reduced life span

and male sterility. Mitochondrial dysfunctions underscore these loss-of-function phenotypes. Interestingly, overexpression of *parkin* rescues the phenotypes of the *pink* mutant, thus putting *parkin* downstream of *pink* in the genetic pathway involving mitochondrial regulation. The roles of fly DJ-1 orthologs in oxidative stress responses are implicated consistently in various studies (Menzies et al. 2005; Meulener et al. 2005; Park et al. 2005; Yang et al. 2005). Mitochondrial malfunction and oxidative stress have long been interwoven in the pathophysiology of neurodegenerative disease. The availability of fly models for PD will continue to provide vast opportunities to address such relevance in great detail.

Fly Models for Neurodevelopmental Diseases

Drosophila fragile X models

Fragile X syndrome (FXS) is the leading cause of inherited mental retardation. This disorder is caused by mutations that disrupt the expression of *Fragile X mental retardation* gene (*FMR1*). *FMR1* encodes the RNA binding protein FMRP. In human and mouse, there are two close paralogs of *FMR1*, *FXR1* and *FXR2*, and all three constitute the *FMR1*/*FXR* gene family. Although the functions of FXR1P and FXR2P have yet to be resolved, at least in the mice model, double *FXR2* and *FMR1* knock-out mice display stronger behavioral phenotypes than single knock-out mice of either gene alone, suggesting some functional

interactions or redundancy between these paralogs (Spencer et al. 2006). In *Drosophila*, there is only one *FMR1* ortholog, *Drosophila fragile X related* (*dfxr*) gene (Zhang et al. 2001), also called *dfmr1* (Wan et al. 2000). DFXR protein exhibits comparable degrees of identity and similarity to all three mammalian FMR1/FXR protein family members (Zhang et al. 2001). Since the first cloning of *dfxr* (Wan et al. 2000) and the characterization of *dfxr* knock-out flies (Zhang et al. 2001; Inoue et al. 2002; Lee et al. 2003), the fly fragile X models have made a huge contribution to understanding the functions of FMRP and the possible mechanisms of FXS pathogenesis.

Loss-of-function *dfxr* mutants are viable and demonstrate locomotor defects at both larval and adult stages, as tested in the larval crawling assay and adult flight test (Xu et al. 2004; Zhang et al. 2004). Adult *dfxr* mutants are also arrhythmic, underlining the role of *dfxr* in circadian output regulation (Dockendorff et al. 2002; Inoue et al. 2002; Morales et al. 2002). Aberrant courtship behavior is also observed in *dfxr* mutants (Dockendorff et al. 2002). The role of DFXR in regulating the structure of synapses or neuronal processes was suggested by the neurite overgrowth and overbranching phenotypes seen in different types of neurons (Zhang et al. 2001; Dockendorff et al. 2002; Lee et al. 2003; Michel et al. 2004). Conversely, overexpression of *dfxr* using the

Gal4-UAS system results in defects opposite to those in *dfxr* knock-outs. The behavioral and neuronal architectural defects displayed by *dfxr* loss-of-function mutants parallel with what is observed in FXS patients and *FMR1* knock-out mice (Comery et al. 1997; Irwin et al. 2001; Irwin et al. 2002), suggesting the evolutionary conservation of FMRP function from fly to human.

Systemic microarray analyses have identified more than four hundred mRNAs associated with FMRP in the mouse brain, providing a daunting repertoire of potential targets of FMRP (Brown et al. 2001). The fly models provide an amenable *in vivo* system for sorting out the physiological mRNA target(s) responsible for fragile X. In fact, various mRNAs have been identified as the *in vivo* targets of DFXR in the fly nervous system, including (1) *futsch* mRNA, which encodes the fly homolog of microtubule-associated protein 1B (MAP1B), whose translation is repressed by DFXR (Zhang et al. 2001); (2) *pickpocket1* mRNA, encoding PPK1 from the degenerain/epithelial sodium channel family, which is involved in DFXR regulation of the larval crawling behavior (Xu et al. 2004); (3) mRNA encoding the Rho GTPase dRac1 (Lee et al. 2003). As it was also proposed that dRac1 controls DFXR activity through acting on the *Drosophila* homolog of Cytoplasmic FMRP-interacting protein/Sra-1 (Schenck et al. 2003), these data suggest

dRac1 and DFXR constitute a feedback loop; (4) mRNA encoding Profilin (Reeve et al. 2005). Both dRac1 and Profilin are involved in actin skeleton dynamics and it was suggested that dRac1 and DFXR work cooperatively in Profilin regulation (Reeve et al. 2005).

Defects related to *dfxr* deficiency outside the nervous system were also investigated in *Drosophila*, and DFXR targets in such tissues were discovered (Zhang et al. 2004; Costa et al. 2005; Deshpande et al. 2006; Monzo et al. 2006). *trailer hitch* mRNA was isolated as a target of dFMRP during the cleavage stage of fly embryogenesis (Monzo et al. 2006) and *orb* mRNA is a target for DFXR regulation in the ovary (Costa et al. 2005).

Drosophila FXS models also contribute to the isolation of DFXR-interacting proteins (Zarnescu et al. 2005; Zhang et al. 2005) and cellular complexes. The emergence of DFXR's likely involvement in the RNAi and microRNA pathways is due to the co-isolation of DFXR, Argonaute 2 and other components of the RNAi machinery in cellular complexes (Caudy et al. 2002; Ishizuka et al. 2002). The functional relevance of DFXR and RNAi is confirmed, at least to some extent, by the observation that Argonaute 2 and DFXR collaborate in *ppk1* mRNA level

control (Xu et al. 2004), and *argonaute* 1 genetically interacts with *dfxr* (Jin et al. 2004).

In many cases, discoveries about FMRP were made first in the fly, and confirmed later in the mouse. For example, the identification of mammalian MAP1B mRNA as a target of murine FMRP and its requirement in microtubule dynamics in the neuron (Lu et al. 2004) extends the corresponding finding in fly (Zhang et al. 2001). Second, after the association of DFXR and RNAi pathway was first unveiled in *Drosophila*, the interaction between mammalian FMRP and microRNAs and RNAi pathways was demonstrated as well (Jin et al. 2004; Plante et al. 2006). Third, the isolation of *dlgl* (*Drosophila lethal (2) giant larvae*) as a modifier of *dfxr* phenotype in a genetic screen guides the finding that FMR and Lgl physical associate with each other in a macromolecule complex in both flies and mice during neural development (Zarnescu et al. 2005). These examples highlight the virtues of the fly FXS models, which complement well the mouse models and act as forerunners for modeling other neurodevelopmental diseases in *Drosophila*.

Establishing a *Drosophila* model for Angelman syndrome

Although *UBE3A* mutations were identified as the cause of Angelman syndrome ten years ago, at present nothing more is

understood about the biochemical nature of disease. The UBE3A substrate(s) relevant to Angelman syndrome are still elusive.

While *UBE3A* mutant mice provide an excellent model for Angelman syndrome in many regards, the mouse system has its inherent limitations in dissecting the biological processes that go awry in *UBE3A* deficiency. For example, it is impractical in mice to do a mutagenesis screen to identify the normal substrate(s) of *UBE3A*.

The *UBE3A* gene is conserved among higher eukaryotes. Gene *CG6190* annotated by the *Drosophila* genome project appears to be the fly homolog of *UBE3A*. The similarity between human UBE3A and *Drosophila* UBE3A (Dube3a) proteins is ~50% with the majority of the conserved amino acids clustering in the HECT domain. No mutant allele of the *dube3a* gene is characterized and its function in fly development is unknown.

My goal is to develop a *Drosophila* AS model that will allow us to identify the AS-associated substrate(s) of the *Drosophila UBE3A* homolog and ultimately, to determine why the lack of UBE3A protein causes Angelman syndrome in humans. This knowledge could lead to

methods for early diagnosis and possibly treatment to control or prevent the disease.

Chapter 2: Generation and Molecular Characterization of *dube3a* Alleles

INTRODUCTION

The goal of the research is to develop a *Drosophila* model of Angelman syndrome that will be useful for identification of UBE3A substrates relevant to the disease in the future. To do so, I need to determine if disruption of the fly *UBE3A* homolog will causes AS-like defects in flies. Because human AS is caused by loss-of-function mutations in *UBE3A*, to obtain loss-of-function mutants of the fly *UBE3A* homolog and to analyze their phenotypes is a crucial first step in the establishment and validation of the fly AS model.

RESULTS AND DISCUSSION

A Blast search of either the human UBE3A full-length protein sequence or that of its HECT domain (carboxyl-terminal 350 amino acids) against the *Drosophila* genome reveals fourteen fly HECT domain proteins (Table 2.1). Among them, the annotated CG6190 protein is the most likely homolog of human UBE3A. These two proteins share 55 percent similarity in their overall amino acid sequences and 71 percent similarity over their HECT domains (Figure 2.1). Unlike other fly HECT domain proteins, CG6190 protein has no other characteristic protein

#	Gene	Cytological position	Protein domains/ regions other than the HECT domain present in the encoded proteins
1.	CG17735	82D5	WWE domain ARM repeat
2.	CG3099	8F21	--
3.	CG3356	60C21	IQ calmodulin-binding region
4.	CG4238	22B9	Filamin/ABP280 repeat
5.	CG5087	66F11	IQ calmodulin-binding region
6.	CG5604	31C4	Ankyrin repeats mib/herc2 domain ARM repeat Sad1/UNC-like C-terminal
7.	**CG6190**	**68B12**	**--**
8.	CG8184	13E8	UBA domain WWE domain DUF908 domain DUF913 domain
9.	CG9153	61F6 1	RCC1 repeats
10.	HERC2	19C5	RCC1 repeats UBA domain Cytochrome b5 mib/herc2 domain
11.	Hyd	85E5	RCC1 repeats UBA domain PABP unique domain Zinc finger, N-recognin
12.	Nedd4	74D2	C2 domain WW domain
13.	Smurf	54C12	C2 domain WW domain
14.	Su(dx)	22C1	C2 calcium/lipid-binding region WW domain

Table 2.1: List of fourteen *Drosophila* HECT domain protein encoding genes in the fly genome. Among these HECT domain protein genes, *CG6190* is the most like homolog of human *UBE3A*.

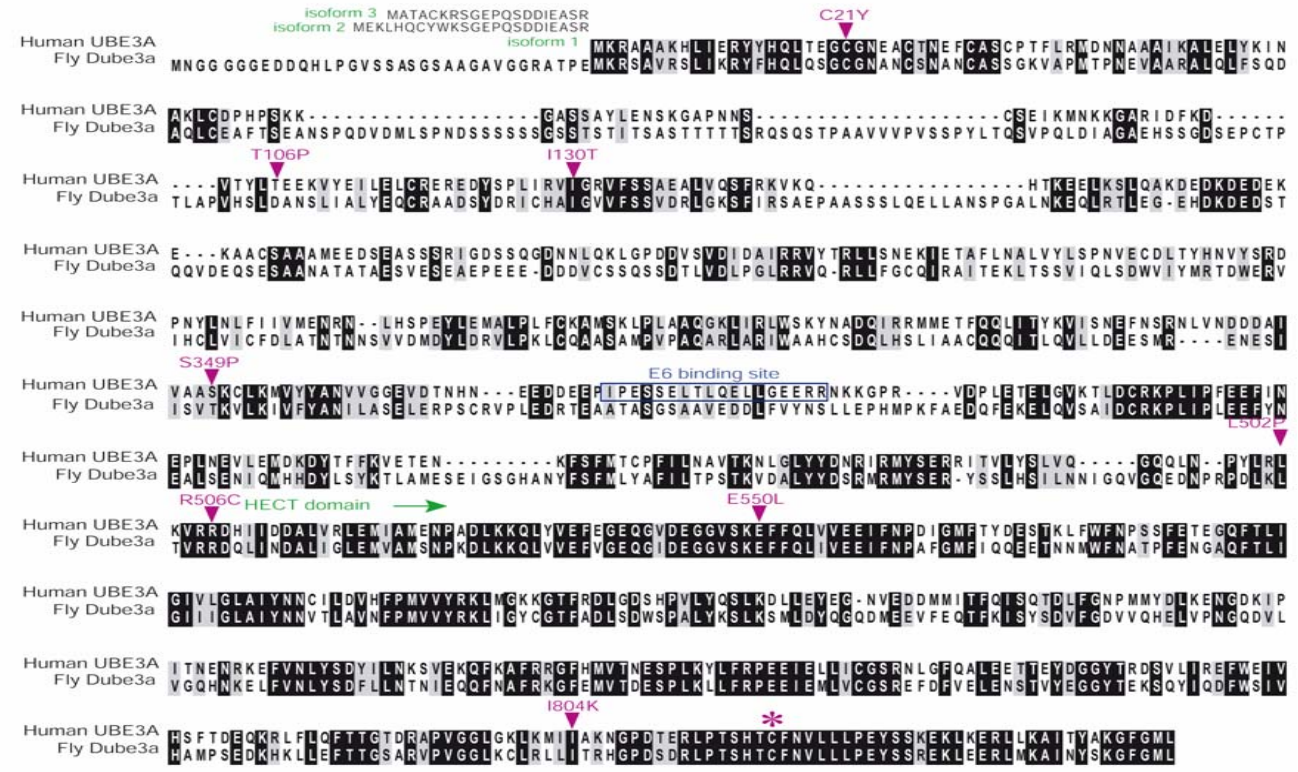

Figure 2.1: Conservation of amino acid sequences of fly Dube3a and human UBE3A. Shown are the amino acid sequences of the three human UBE3A isoforms (Yamamoto et al. 1997), and the single *Drosophila melanogaster* Dube3a protein aligned using MacVector 9.0. Grey shading indicates similarity, and black shading identities. The two proteins are 39% identical and 55% similar overall, and the HECT domain is 56% identical and 71% similar. Missense amino acid changes in Angelman syndrome patients are indicated in purple, and the asterisk indicates the catalytic Cysteine residue.

domains outside the HECT domain (Table 2.1). This is similar to human UBE3A, except that that UBE3A has a 18 amino acids long E6 binding site/ L2G box, which is not conserved in fly CG6190 protein (Figure 2.1).

CG6190 gene is located at position 68B1 on the left arm of chromosome 3 and has not been characterized molecularly. The structure of *CG6190* is derived from computational analyses of the genomic DNA sequence and available EST data (http://flybase.bio.indiana.edu/reports/FBgn0061469.html, Figure 2.2, Table 2.2). The *CG6190* gene is also referred as *dube3a* (Reiter et al. 2006), which highlights the orthological connection between *Drosophila dube3a* and human *UBE3A*.

Due to alternative mRNA splicing, there are three different human UBE3A isoforms that differ at their N-termini (Yamamoto et al. 1997). There is no evidence for alternate isoforms of the fly protein, as ESTs identify only one *dube3a* mRNA (Figure 2.2, Table 2.2). Using RT-PCR and DNA sequence determination, I found this mRNA in embryos, larvae and adults (not shown). Virtual translation of the *dube3a* mRNA starting at the first in-frame Met residue results in a protein whose second Met residue, 34 codons downstream, aligns well with the initiation codon of human UBE3A isoform 1. I think that the first Met codon is likely to be

#	EST	Align to *dube3a* cDNA	Expression Pattern
1.	EN06317	2511-2938	Cultured cell-line
2.	RE02013	24-216	Embryo
3.	RE26015	24-604	Embryo
4.	RE27977	24-481	Embryo
5.	RE28250	30-608	Embryo
6.	RE28274	30-664	Embryo
7.	RE29433	25-671	Embryo
8.	RE33980	21-478	Embryo
9.	RE36891	24-474	Embryo
10.	RE50278	24-589	Embryo
11.	RE62574	19-723	Embryo
12.	RE66965	16-555	Embryo
13.	RE69002	30-610	Embryo
14.	LD04717	44-437	Embryo
15.	LD11513	19-706	Embryo
16.	LD15749	68-639	Embryo
17.	LD21888	24-3644	Embryo
18.	LD23356.3'	3327-3645	Embryo
19.	LD23356.5'	766-1491	Embryo
20.	LD26168	68-701	Embryo
21.	LD26277	3169-3429	Embryo
22.	LD27716	766-1341	Embryo
23.	LD31792	55-628	Embryo
24.	LD33078	1-763	Embryo
25.	LD36547	47-582	Embryo
26.	LD38041	1-544	Embryo
27.	LD47770	31-581	Embryo
28.	EK132730	2070-2516	Embryo/ larval imaginal disc/ adult head
29.	EK190022	3061-3262	Embryo/ larval imaginal disc/ adult head
30.	LP23042	19-736	Larvae/pupae
31.	EC39982	2705-3240	Larval third instar stage fat body
32.	LP09860	65-580	Larvae/pupae
33.	LP05352	1135-1758	Larvae/pupae
34.	GM03445.3'	3077-3654	Ovary germarium-stage 6
35.	GM03445.5'	1788-2480	Ovary germarium-stage 6
36.	GM25309	44-642	Ovary germarium-stage 6
37.	AT01473	65-735	Testes, adult
38.	AT02553	73-493	Testes, adult
39.	AT05579	481-1268	Testes, adult
40.	AT10666	86-665	Testes, adult
41.	AT16565	1539-1851	Testes, adult
42.	AT19959	96-423	Testes, adult
43.	AT20594	120-856	Testes, adult
44.	AT23227	147-548	Testes, adult
45.	AT24587	73-819	Testes, adult
46.	AT24638	73-459	Testes, adult
47.	AT28915	482-1164	Testes, adult
48.	AT30647	120-786	Testes, adult
49.	AT30695	34-736	Testes, adult
50.	AI945680	2948-3246	Testes, adult
51.	BE976277	805-1359	Testes, adult

Table 2.2: List of *dube3a* ESTs.

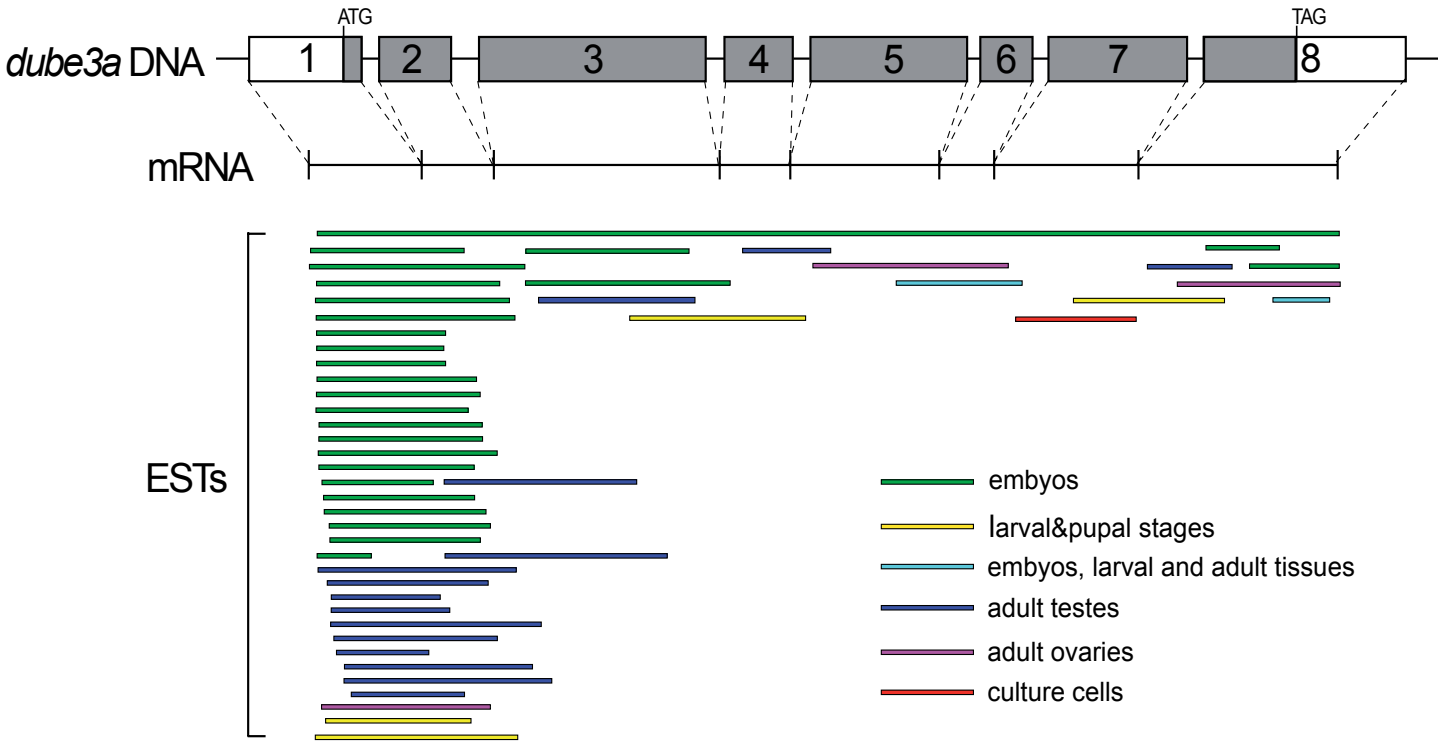

Figure 2.2: Genomic organization of *dube3a* and ESTs for *dube3a*. *dube3a* ESTs have been isolated from various fly tissues and developmental stages, including adult ovary and testis, embryos, larvae, pupae. In addition, one *dube3a* EST fragment was isolated from cultured cells. There is no evidence for alternative splicing of *dube3a*, as ESTs available so far identify only one *dube3a* mRNA.

used for two reasons. First, human isoforms 1 and 2 have N-termini that extend upstream of the initiator Met in isoform 1 (Figure 2.1). Second, I find an extended open-reading-frame in each of the eleven *Drosophila* species whose genomic DNA sequences were analyzed (Figure 2.3).

A P-element allele of *dube3a* was generated by the BDGP (Berkeley Drosophila Genome Project) Gene Disruption Project. It is inserted in the 5'-UTR of *dube3a*, ~300bp upstream of the putative translation start site. Genomic location of this EP line was confirmed by PCR and DNA sequencing. The original EP allele is homozygous viable and no noticeable external phenotype is observed in EP homozygotes or *in trans* to several deficiency chromosomes carrying large chromosomal deletions, uncovering the region containing *dube3a* (*Df (3L) vin5* [68A02-03; 69A01-03], *Df (3L) vin2* [67F02-03; 68D06] or *Df (3L) vin66* [68A02-03; 68D03]). In comparison to w^{1118} controls, the presence of the *EP* insertion in the 5'-UTR of *dube3a* does not affect the transcription level of *dube3a* significantly, as shown in RT-PCR. Generation and analysis of *dube3a* knock-out mutants enable us to understand its endogenous functions.

By mobilizing the *EP (3)3124* element with $\Delta 2\text{-}3$ transposases, ~250 individual hop-out lines were generated (Figure 2.4). None of them

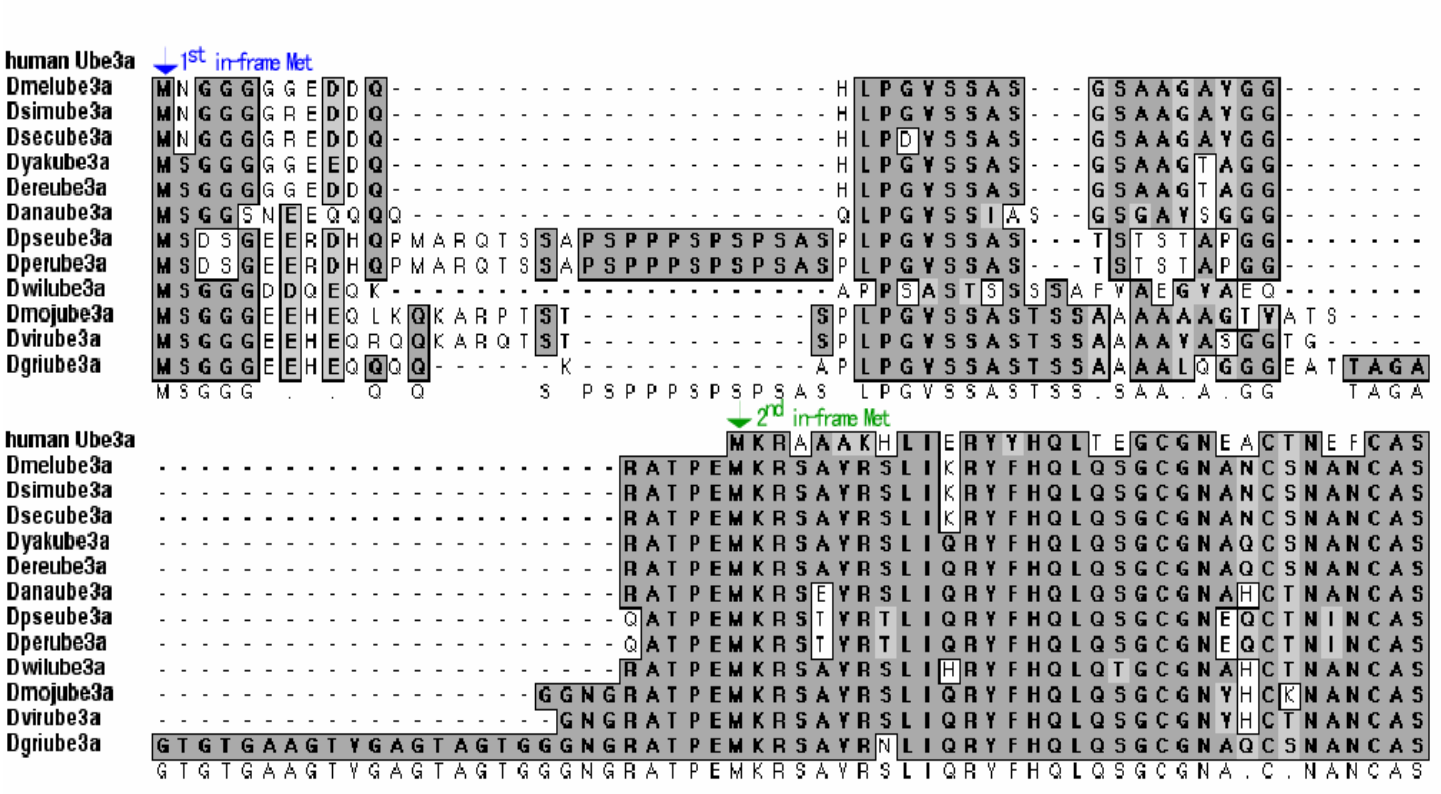

Figure 2.3: The first Met codon in Dube3a computed open reading frame is likely to be the start codon of the endogenous Dube3a protein. We BLASTed the first 50 amino acids of the *melanogaster* sequence against eleven *Drosophila* species' genome sequences, and all of them have an in-frame Met codon upstream of the one that aligns with human UBEA isoform 1. As in Figure 2.1, the N-termini of human isoforms 2 and 3 extend upstream of the initiator Met in isoform 1.

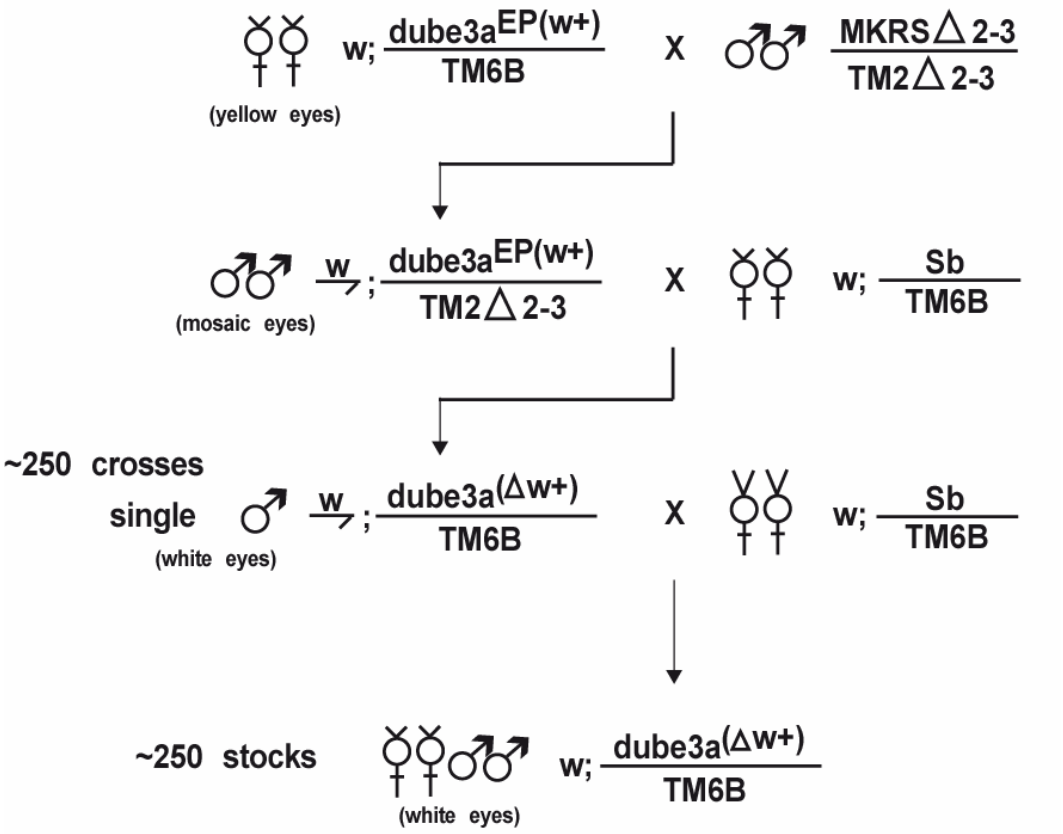

Figure 2.4: Fly cross scheme for the generation of *dube3a* mutants by mobilizing the *EP(3)3214* element inserted into the 5'-UTR of the *dube3a* gene. The *dube3a* alleles generated from this attempt are *dube3a*^{8O} and *dube3a*^{6J}

are homozygous lethal or lethal *in trans* to deficiency chromosomes uncovering the *dube3a* region. No obvious external morphological defects were present in these flies. As murine *UBE3A* knock-out homozygous mice are viable with neurological defects (Jiang et al. 1998), I reasoned that flies lacking *dube3a* expression would be viable likewise. PCR-based identification was performed on these hop-out lines to find lines carrying deletions around the *EP* insertion site. Two imprecise excision mutations in *dube3a* were recovered and named as *dube3a*^{6J} and *dube3a*^{8O}. Through PCR and DNA sequencing, the breakpoints of each mutant were confirmed molecularly. *dube3a*^{6J} has a ~1.7kb deletion within *dube3a*, uncovering the region from the *EP* insertion site to the middle of *dube3a* exon 4. *dube3a*^{8O} contains a ~2.4kb deletion, which extends from exon 1 of *CG7600*, an uncharacterized gene just upstream of *dube3a*, to exon 3 of *dube3a* (Figure 2.6). Flies homozygous for either *dube3a* allele are viable and fertile with no obvious external morphological defects. This is true also for either *dube3a*^{6J}/*Df (3L) vin5* flies or *dube3a*^{8O}/*Df (3L) vin5* flies.

RT-PCR results (not shown) from flies that are either *dube3a*^{8O} homozygotes or *dube3a*^{8O}/*Df (3L) vin5 trans*-heterozygotes showed that there is no or just trace amounts of *dube3a* mRNA present in these flies. Therefore, *dube3a*^{8O} is a strong or null allele of *dube3a*. It might disrupt

function of the nearby gene, *CG7600*, as well (Figure 2.6). In *dube3a*^{6J} homozygous flies, the remaining *dube3a* exons are still transcribed. This is consistent with the fact that while the *dube3a* transcription start point is gone in *dube3a*^{8O}, it is still present in the *dube3a*^{6J} chromosome and thus enables transcription initiation.

Dube3a protein expression levels of both *dube3a*^{6J} and *dube3a*^{8O} in third instar larval eye discs were assayed by Western blots with polyclonal anti-Dube3a anti-sera (see Chapter3 for description of these antibodies). These anti-sera were generated in rats and guinea pigs against the recombinant full-length Dube3a. In *w*^{1118} controls, one band corresponding to the size of the putative Dube3a protein (~107 kD) was detected. In contrast, no band was detected in the *dube3a*^{8O} homozygous sample, which is expected to make no Dube3a protein. This result also confirmed the specificity of the anti-Dube3a antisera, generated against full-length Dube3a, in Western blot assays. The amounts of total proteins loaded on the gel from each sample are roughly the same according to tubulin controls. In the *dube3a*^{6J} sample, no band was visible either (Figure 2.6).

Two additional *dube3a* alleles were generated from an isogenized *EP(3)3214* chromosome (Figure 2.5). They are *dube3a*^{15B} and

dube3a^{6PE} (Figure 2.6). They were also characterized through DNA sequencing and Western blotting. *dube3a*^{6PE} is a precise excision allele, with the *EP* insertion removed completely and no nucleotide deletion or insertion left behind. Like *dube3a*^{8O} and *dube3a*^{6J}, *dube3a*^{15B} is an imprecise excision allele bearing an ~1.2kb deletion, starting from the *EP* insertion site to the middle of *dube3a* exon3. Western blotting with polyclonal anti-Dube3a anti-sera showed no band in *dube3a*^{15B} protein extracts and the amount of Dube3a in the *dube3a*^{6PE} preparation is comparable to the w^{1118} controls (Figure 2.6).

CONCLUSIONS

Among the fourteen fly HECT domain proteins, *CG6190* or *dube3a*, is clearly more similar to UBE3A in amino acid sequence than are the other thirteen (Figure 2.1, Table 2.1). The two protein sequences are conserved along the entire length of the proteins and the C-terminal HECT domain is more highly conserved. Unlike human UBE3A, which is subject to alternative splicing and has three N-terminal different isoforms, Dube3a is most likely encoded by one open reading frame and is 973 amino acid long (Figure 2.1).

By mobilizing an EP element in the 5'UTR of *dube3a*, four *dube3a* alleles were generated and characterized through DNA sequencing

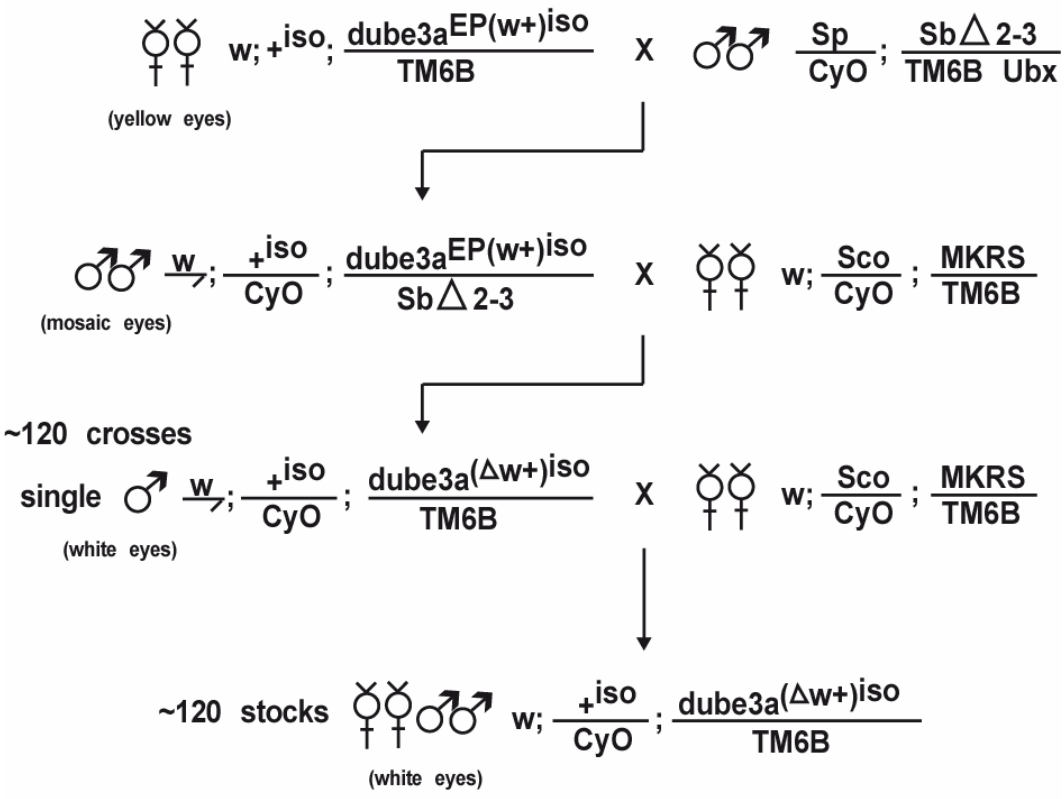

Figure 2.5: Fly cross scheme for the generation of *dube3a* mutants by mobilizing the *EP(3)3214* element inserted into the 5'-UTR of the *dube3a* gene. The *dube3a* alleles generated from this attempt are *dube3a*^{15B} and *dube3a*^{6PE}.

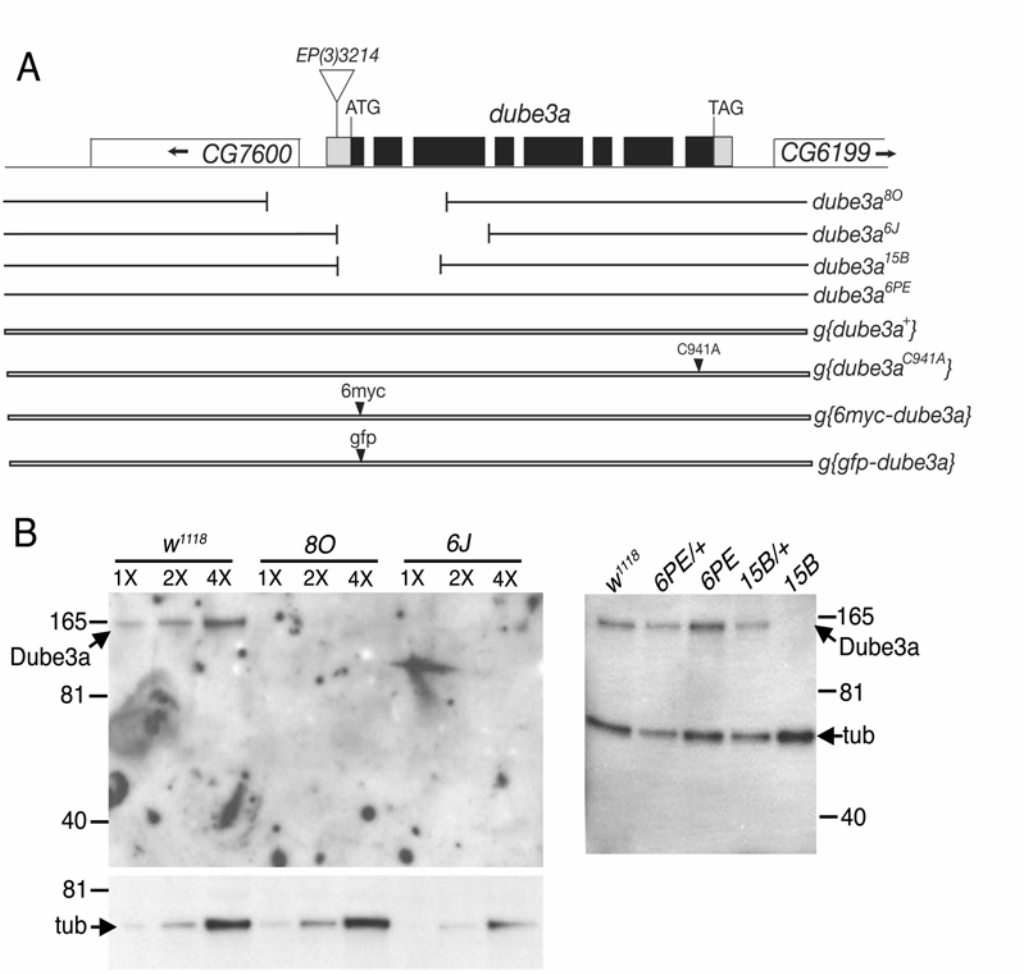

Figure 2.6: Wild-type and mutant *dube3a* alleles. (*A*) A diagram of the *dube3a* genomic region is shown at top (not to scale). There are ~400 bp between *CG6700* and *dube3a*, and ~200 bp between *CG6199* and *dube3a*. Boxes are exons; black indicates coding region and grey indicates non-coding regions. Four *dube3a* alleles generated by excision of *EP(3)3214* are shown. The extents of the deletions in the mutant alleles are indicated. The four black bars beneath indicate the ~12.9 kb genomic DNA fragments in each of four transgenes. (*B*) Shown are blots of eye disc protein extracts from third instar larvae of the genotypes indicated. The blots were probed with guinea pig anti-Dube3a and anti-tubulin as a loading control. 1X, 2X, and 4X indicate different amounts (7.5, 15 and 30ul respectively) of the same protein extract. For the blot on the right, in each lane, 35ul protein extracts from third instar larvae of the corresponding genotypes were loaded.

and Western blotting analyses. Two of them are likely null alleles and they are homozygous viable and fertile with no morphological defects that are obvious externally. As humans with Angelman syndrome as well as *UBE3A* knock-out mice are viable and more-or-less normal externally, the viable phenotype of these *dube3a* knock out mutants is consistent with the idea that *Drosophila dube3a* is the homolog of human *UBE3A*.

These *dube3a* loss-of-function mutants will be analyzed to determine if they have mutant phenotypes suggestive of a neural function for *dube3a* and similar to those seen in *UBE3A* deficient people and mice (see Chapter 4). The results will determine if *Drosophila dube3a* mutants are a valid model for Angelman syndrome.

Chapter 3: Dube3a Protein Expression Patterns and Subcellular Localizations

INTRODUCTION

Human *UBE3A* is transcribed in a variety of tissues and cell types, including the brain, heart, skeletal muscle, liver, pancreas, kidney, lung, adrenal gland, intestine, placenta (Sutcliffe et al. 1997; Vu and Hoffman 1997; Rougeulle and Lalande 1998), fibroblasts, lymphoblasts (Nakao et al. 1994), and foreskin keratinocytes (Huibregtse et al. 1993). *UBE3A* is also expressed in the brain (Rougeulle and Lalande 1998). While bi-allelic expression of *UBE3A* was demonstrated in all other human tissues and cell types examined, in the brain, *UBE3A* is predominantly transcribed from the maternal allele (Rougeulle et al. 1997; Vu and Hoffman 1997).

Transcripts of murine *UBE3A* were detected in extensive mouse brain sections, liver and testis (Albrecht et al. 1997; Sutcliffe et al. 1997). Unlike in other tissues or brain regions, in the murine hippocampus and the cerebellar Purkinje cell layer, the maternal copy of *UBE3A* is transcribed preferentially (Albrecht et al. 1997; Jiang et al. 1998; Miura et al. 2002). Analyses of the *UBE3A* expression pattern in embryonic mice

indicate that UBE3A is expressed broadly early in embryogenesis and later concentrates in neural tissue (Albrecht et al. 1997).

Knowing the expression patterns and cell-type specificity of *dube3a* during fly development would shed light on its potential function. Most importantly, expression of *dube3a* in the fly nervous system will provide validation for the establishment of a fly AS model, which is based on the speculation that the mechanisms underlining the functions of fly UBE3A orthologs in the neuronal cells are conserved from fly to human. Particular attention would be paid to the expression of *dube3a* in the mushroom bodies (MB), the seat of learning and memory (Roman and Davis 2001; Heisenberg 2003). Whether endogenous *dube3a*, and most likely its substrate(s) as well, are expressed in fly tissues amenable to convenient and efficient genetic screens, such as the eye and the wing, will also test the feasibility of future modifier screens based on phenotypic abnormalities in these tissues.

RESULTS AND DISCUSSION

dube3a mRNA Expression Patterns

As stated in Chapter 2, transcription of *dube3a* in fly embryos, larvae and adults were revealed by RT-PCR experiments. RT-PCR also

indicated that *dube3a* mRNA is present in larval eye discs, suggesting its substrate(s) may also present in this tissue.

Dube3a Proteins Expression Patterns

Means of protein expression pattern detection

Anti-Dube3a polyclonal antisera

Two different antisera (one in rat and one in Guinea pig) were generated against full-length Dube3a made in bacteria. Rat anti-Dube3a polyclonal antisera were used for tissue immunostaining whenever possible. The specificity of these antisera for immunostainings was tested by staining larval antenna-eye disc complex containing *dube3a*^{8O} or *dube3a*^{6J} homozygous clones. Labeling was observed in the wild-type areas but not the null clone areas (Figure 3.1). When used for embryo immunostaining, Dube3a was absent in *dube3a*^{8O} embryos while present in the wild-type embryos, which further confirmed the tissue specificity of anti-Dube3a (Figure 3.2). In addition, as described in Chapter 2, the specificity of these rat anti-Dube3a antisera was also verified on Western blots. The specificity of the guinea pig anti-Dube3a antibody was verified on Western blots as well, although it did not work for immunolocalization in tissues.

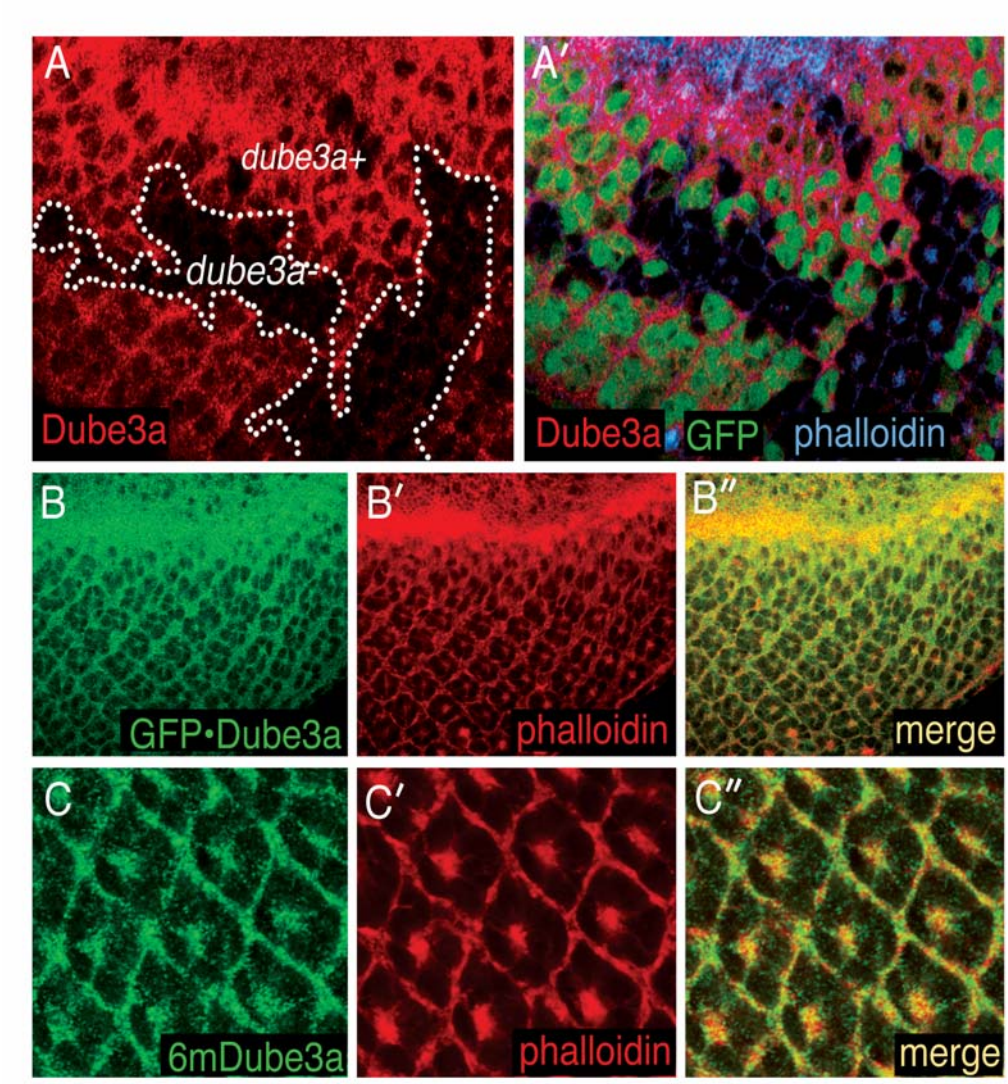

Figure 3.1: Dube3a expression in larval eye discs. Confocal immuno-fluorescence images of third instar larval eye discs are shown. (*A, A'*) A *dube3a*^{8O} homozygous clone surrounded by *dube3a*^{8O}*/dube3a*$^{+}$ cells is shown in a disc labeled with rat anti-Dube3a. Little or no Dube3a (red) is detected in the clone, indicating that the antibody is specific for Dube3a. Dube3a is ubiquitous and cytoplasmic in the eye disc outside the clone. Identical Dube3a expression patterns were observed with anti-Dube3a on wild-type eye discs (*A, A'*), with anti-GFP on eye discs containing a *ggfp-dube3a* transgene (Figure 2.4) that expresses GFP-Dube3a (*B-B''*), and with anti-Myc on eye discs containing a *g6myc-dube3a* transgene (Figure 2.4) that expresses 6mDube3a (*C-C''*). Dube3a appears to be associated with the plasma membrane partially.

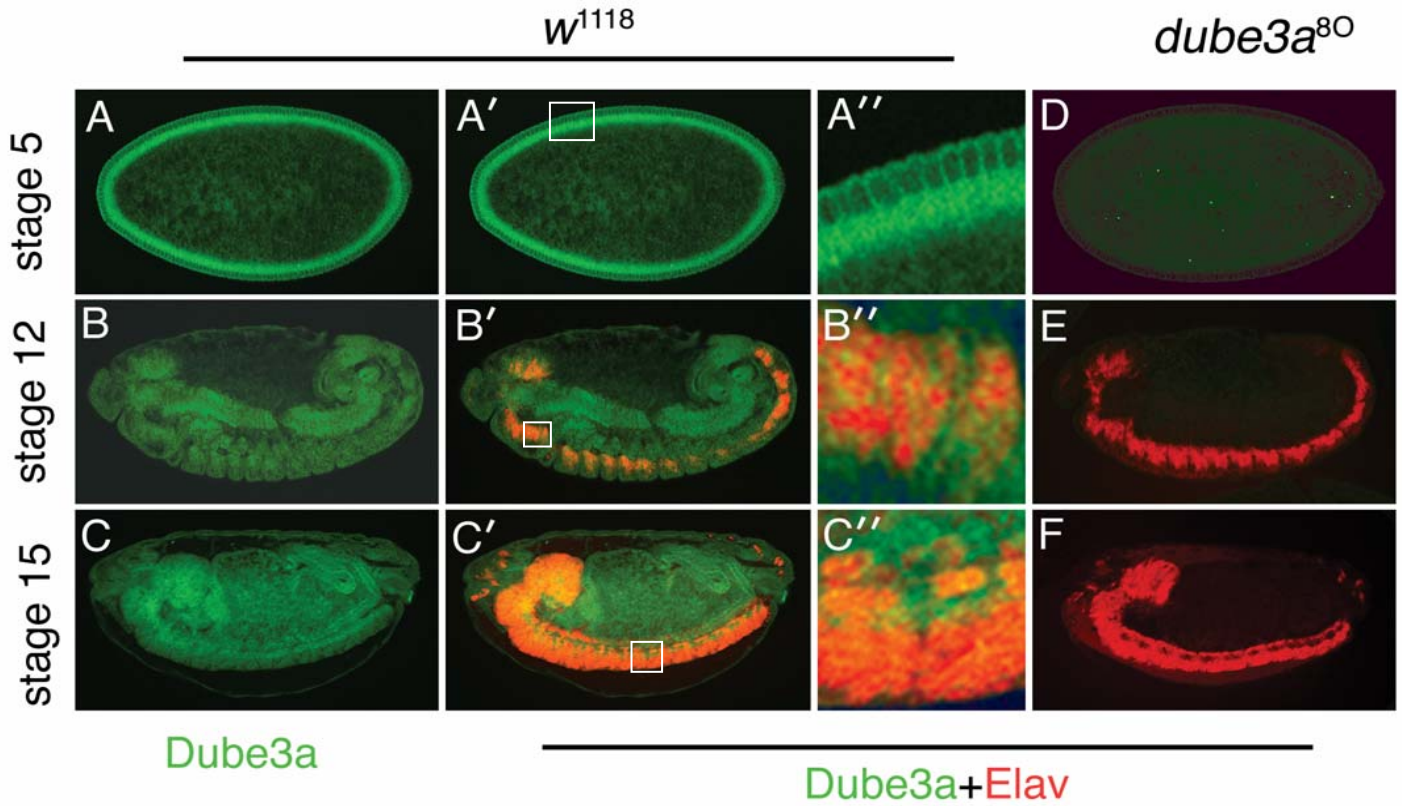

Figure 3.2: Dube3a expression in embryos. Confocal immunofluorescence images are shown. (*A-C"*) *dube3a*$^{+}$ embryos labeled with Dube3a (green) and Elav (red); *A-A"* are the same embryo; *A* shows Dube3a, *A'* is a merge of Dube3a and Elav, and *A"* is an enlargement of part of *A'* (Same for *B-B"* and *C-C"*). (*D-F*) *dube3a*^{8O} embryos; no Dube3a is detected.

g6mdube3a and *ggfpdube3a* transgenes

In addition to the anti-Dube3a antibodies, an alternative way to look at the expression pattern of Dube3a is to use flies carrying large genomic transgenes encoding either 6mDube3a (6×MycDube3a) or GFPDube3a and anti-Myc antibodies or anti-GFP antibodies. These 6XMyc and GFP tag sequences were inserted in-frame into the 5' ends of the *dube3a* open reading frames (Figure 2.6).

Tissue expression patterns of the endogenous Dube3a protein

Embryos

During embryogenesis, Dube3a protein can be detected from stage 5 to later stages (earlier stages were not analyzed). Ubiquitous distribution of Dube3a protein is observed, and its expression is detected in the embryonic nervous system, identified by double-labeling with anti-Elav, which labels all neurons (Figure 3.2).

Larval eye discs

In larval eye-antenna discs, Dube3a protein has a ubiquitous distribution and does not display cell-type specificity (Figure 3.1).

Expression patterns of 6mDube3a and GFPDube3a fusion protein

Embryos

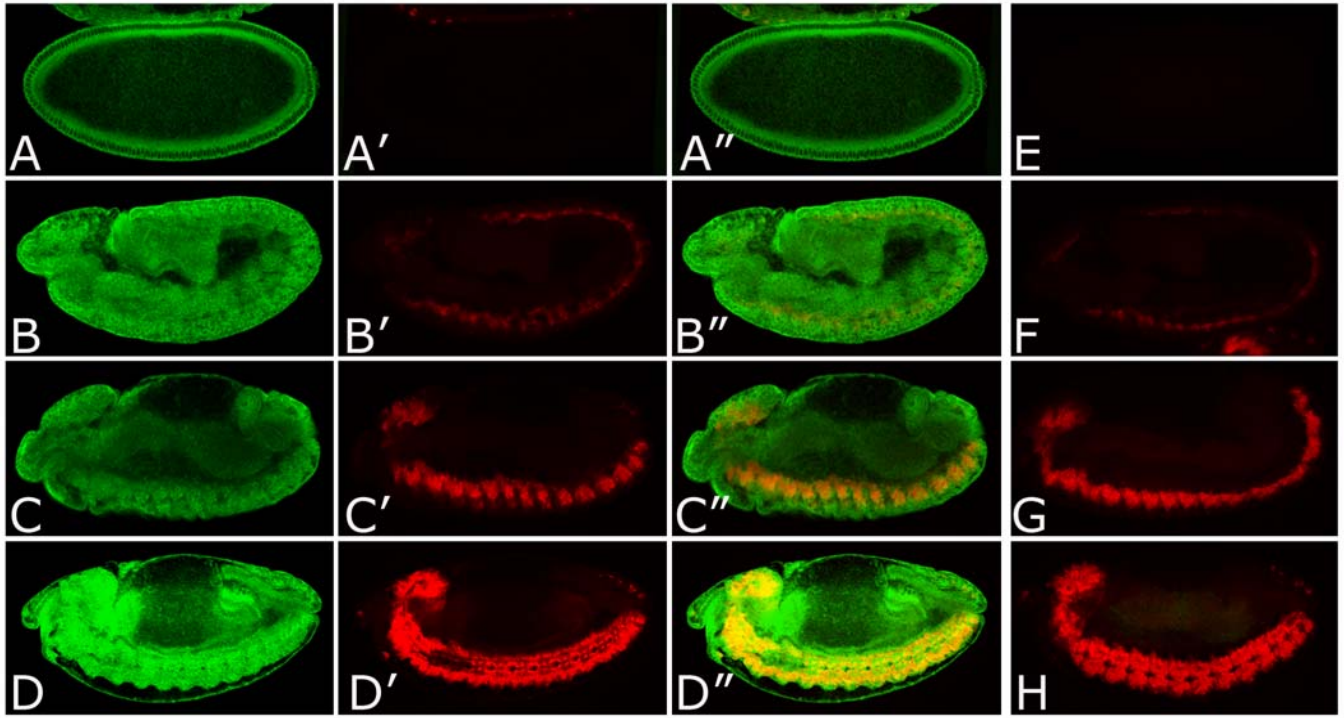

Figure 3.3: 6mDube3a expression in embryos. Confocal immunofluorescence images are shown. (*A-D"*) embryos containing a *g6myc-dube3a* transgene that expresses 6mDube3a are labeled with anti-Myc (green) and anti-Elav (red); *A-A"* are the same embryo; *A* shows 6mDube3a, *A'* shows Elav, and *A"* is a merge of 6mDube3a and Elav (Same for *B-B"*, *C-C"* and *D-D".*) (*E-H*) w^{1118} embryos (without a *g6myc-dube3a* trans-gene); in contrast to Elav (red), no 6mDube3a is detected. The 6mDube3a expression patterns are identical to those of endogenous Dube3a (Figure 3.2).

Anti-Myc immunostainings of *g6mdube3a* embryos resembles anti-Dube3a w^{1118} embryo staining results. The anti-Myc staining patterns were absent in w^{1118} embryo controls (Figure 3.3).

Larval eye discs

Immunostainings of *g6mdube3a* larval eye discs with anti-Myc and immunostainings of *ggfpdube3a* larval eye discs with anti-GFP show comparable results to anti-Dube3a w^{1118} eye disc immunostaining (Figure 3.1).

Larval central nervous system

6mDube3a protein has a ubiquitous distribution in the larval central nervous system with pronounced expression in the neuroblasts and their immediate progeny. Very low levels of expression are observed in differentiated neuronal cells and glia. These observations were made by labeling the *g6mdube3a* larval brains with anti-Myc, and co-labeling either with anti-Elav, which labels all neuronal nuclei (Figure 3.4), or nuclear GFP (from *UAS-nucGFP*) driven by various neuronal *Gal4* drivers. For both *l(3)31-1-Gal4* and *Mz1060-Gal4*, the GAL4 proteins were expressed in the neuroblasts and their immediate progeny (Figure 3.5). *Cha-Gal4* expresses GAL4 specifically in cholinergic neurons. *OK6-Gal4* is a motor neuron-specific *GAL4* driver. *Repo-Gal4* is a glial cell-

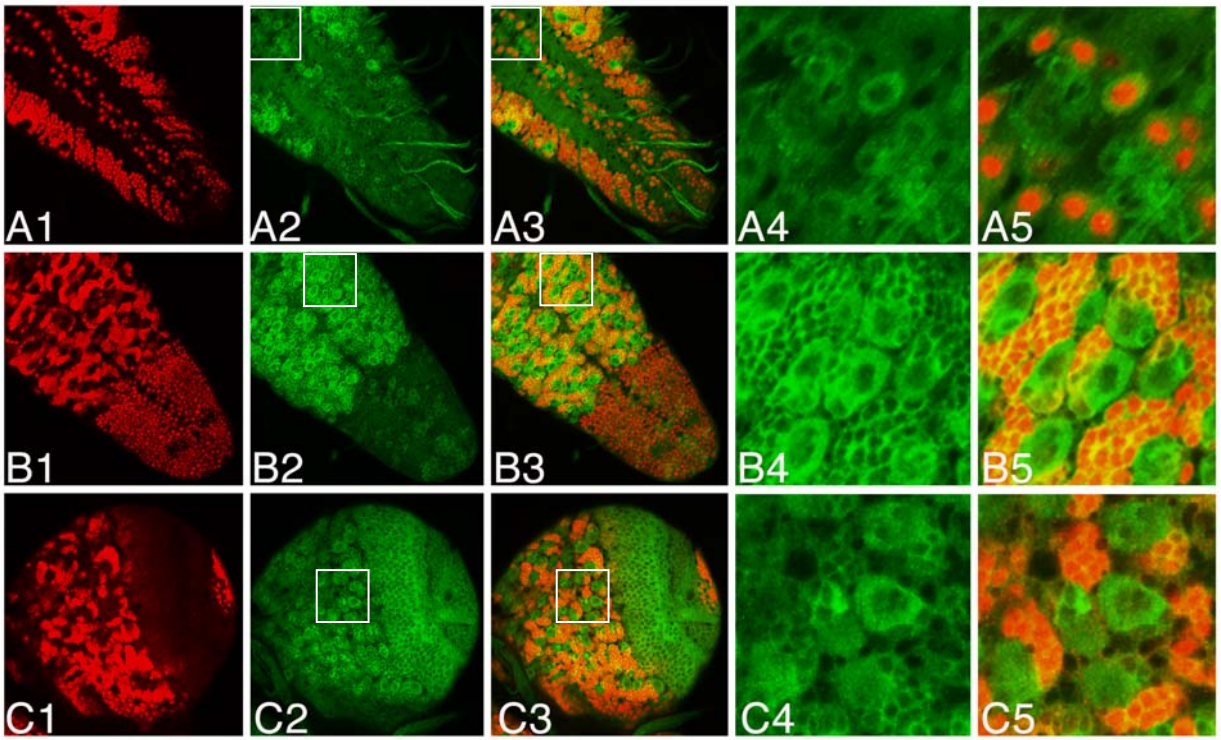

Figure 3.4: 6mDube3a expression in larval central nervous system. Confocal immunofluorescence images are shown. In all rows, panels 4 and 5 are enlargements of the same regions of panels of 2 and 3, respectively. (*A-C*) 6mDube3a (green) and Elav (red). (*A1-A5*) Apical view of ventral nerve cord. 6mDube3a is present in the Elav+ cells, and also in other cells. (*B1-B5*) Basal view of ventral nerve cord. 6mDube3a is present in neuroblast (NB) cytoplasm and in that of surrounding Elav+ progeny. (*C1-C5*) Larval brain is shown. 6mDube3a is present mainly in NBs and is also in surrounding Elav+ progeny. The neuroblast distribution of 6mDube3a is confirmed as in Figure 3.5.

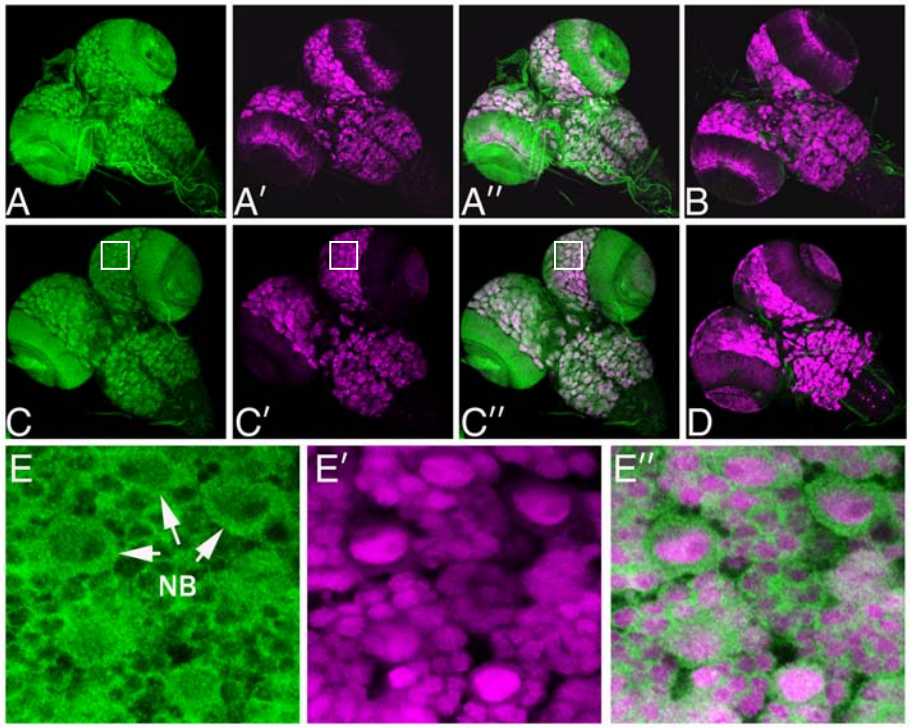

Figure 3.5: 6mDube3a expression in the neuroblasts of larval central nervous system. Confocal immunofluorescence images are shown. 6mDube3a (green) and Nuclear GFP (purple). Nuclear GFP is expressed from *UAS-nucgfp* driven by *Mz1060-Gal4* (*A'-A''* and *B*) or *l(3)31-Gal4* (*C'-C''*, *E'-E''* and D). *A''* is a merge of *A* and *A'* (Same for *C''* and *E''*). *E-E''* are enlargements of the same regions of panels *C-C''*, respectively. Both *Mz1060-Gal4* and *l(3)31-Gal4* mark neuroblasts and neurons; 6mDube3a is present in these marked cells in larval CNSs containing a *g6myc-dube3a* transgene(*A'-A''* and *C'-C''*), but not in larval CNSs without (*B* and *D*).

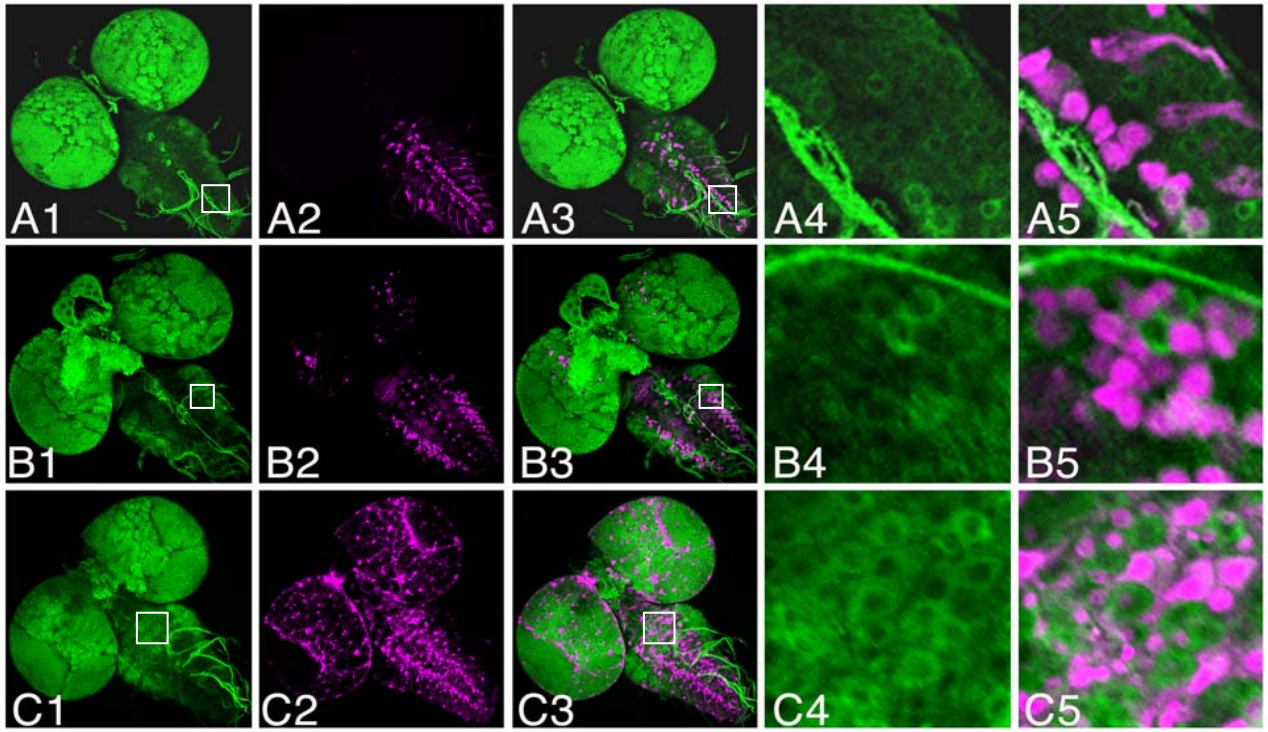

Figure 3.6: Low levels of 6mDube3a in differentiated neurons and glial cells in larval central nervous system. Confocal immunofluorescence images of the apical view of ventral nerve cord are shown. In all rows, panels 4 and 5 are enlargements of the same regions of panels of 1 and 3, respectively. Dube3a (green) and Nuclear GFP (purple). Nuclear GFP (purple) is expressed from a Gal4 driver and *UAS-nucgfp*. Low level 6mDube3a are present in *OK6-Gal4* marked motor neurons (*A1-A5*); *cha-Gal4* marked cholinergic neurons (*B1-B5*); *repo-Gal4* marked glia (*C1-C5*).

specific *GAL4* driver (Figure 3.6). Background signal from anti-Myc is insignificant in the central nervous system of w^{1118} larvae, which lacks the *g6mdube3a* transgene and serves as a negative control (Figure 3.5 B, D as examples).

Adult brain

As in larval brains, 6mDube3a is expressed broadly in the adult brain as shown by co-labeling the *g6mdube3a* adult brain with anti-Myc and anti-Elav (Figure 3.7).

In contrast with larval brains (not shown), 6mDube3a is expressed at particularly high levels in the adult mushroom bodies (MB), the *Drosophila* brain center for associative learning and memory. Such 6mDube3a mushroom body expression patterns were confirmed by co-labeling with *OK201Y-Gal4>UAS-GFP* or *OK107-Gal4>UAS-GFP*, where both *OK201Y-Gal4* and *OK107-Gal4* are mushroom body drivers (Figure 3.7).

Subcellular localization of Dube3a, 6mDube3a

The subcellular localizations of Dube3a, 6mDube3a and GFPDube3a were also observed in the above tissue stainings. All these Dube3a proteins are mainly cytoplasmic (Figure 3.1-3.7).

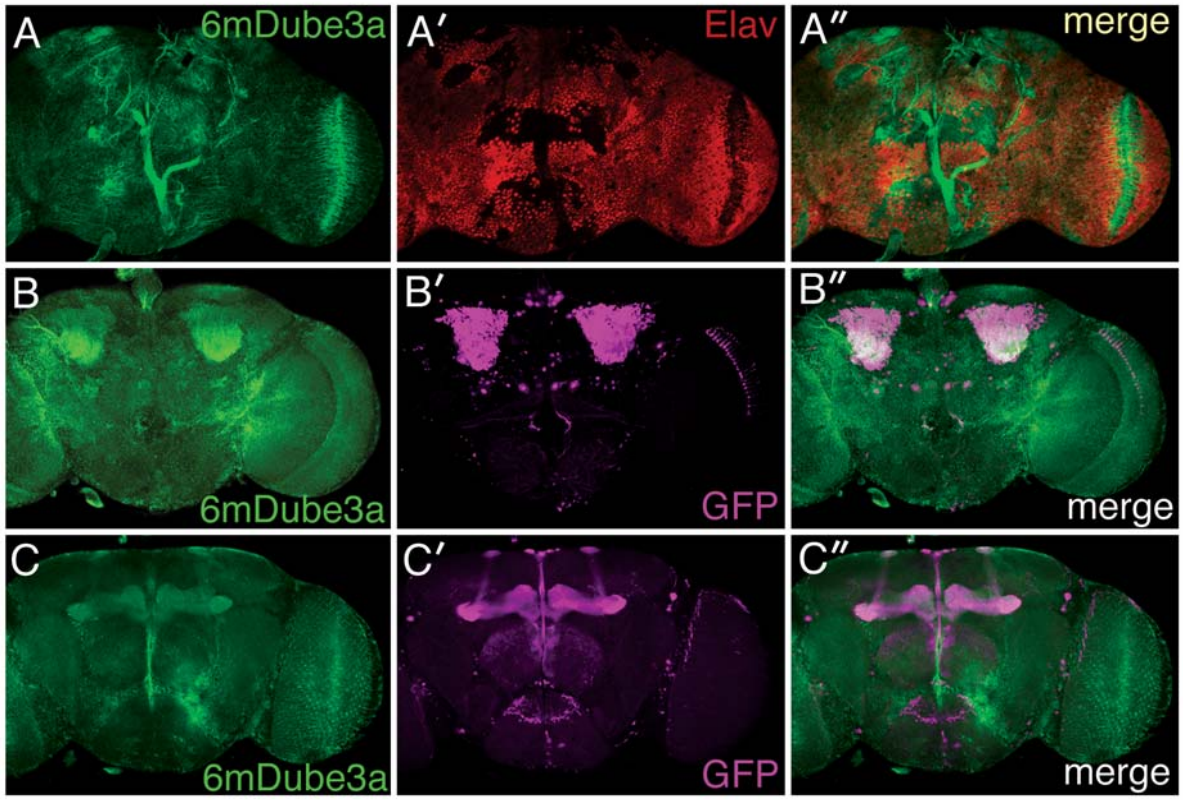

Figure 3.7: 6mDube3a expression in adult brains. Confocal immunofluorescence images are shown. (*A-A"*) Dube3a is expressed broadly in brain cell cytoplasm, as compared to Elav in all neural nuclei. (*B-C"*) Mushroom bodies (purple) are marked by nuclear GFP expressed by *OK201Y>UAS-nucgfp*. *B* and *C* panels show different planes. High levels of Dube3a are present in mushroom bodies.

CONCLUSIONS

In summary, similar to the expression of vertebrate UBE3A, Dube3a protein is mainly cytoplasmic (Huibregtse, personal communication), and is expressed broadly through out fly development. Expression of Dube3a or 6mDube3a (encoded by *g6mdube3a* genomic transgenes) is detected in the nervous system at the embryo, larval and adult stages. In the adult brain, high levels of Dube3a are present in the adult mushroom bodies. As Angelman syndrome affects brain function, these results are consistent with the idea that *Drosophila dube3a* is the homolog of human *UBE3A*.

The expression of Dube3a in the developing eye (larval eye disc), also suggest that the substrates of Dube3a may be present in this tissue. Thus, the overexpression eye phenotype described in Chapter 5 might be particular useful as a screen background for isolating Dube3a substrates.

Chapter 4: *dube3a* Mutant Flies Have Locomotor Defects

INTRODUCTION

As *dube3a* null mutants are homozygous viable, they can be assessed for neurological phenotypes resembling those of AS patients. The four clinical features that occur in all AS cases are developmental delay, movement or balance disorder, unique behaviors and speech impairment. Seizures and microcephaly are also present in a large proportion of AS (Williams et al. 2006).

Two established and commonly used assays for adult locomotor behaviors in flies are the flight test and the climbing test. In consideration of the large impact of genetic background on fly behavioral performance, wild-type (*dube3a*^{6PE}) and *dube3a* mutant (*dube3a*^{15B}) flies isogenic for the two major autosomes were analyzed in parallel. As motor coordination can be affected by age, wild-type and mutant flies of similar ages were compared over a range of ages.

As Angelman patients also experience seizures, the *dube3a* mutant flies were tested in the bang sensitivity and heat shock assay for this tendency. In these assays, flies are examined for paralysis after severe mechanical shaking or heat exposure (Zhang et al. 2002).

In AS cases, the major brain components affected are the hippocampus and cerebellum, which are involved in learning and memory and motor coordination, respectively. The corresponding *Drosophila* brain centers are the mushroom bodies (Roman and Davis 2001; Heisenberg 2003) and the central body complex (Strauss 2002). I thus examined if there are morphological abnormalities in these structures in *dube3a* knock-out mutants.

RESULTS AND DISCUSSION

The ability of *dube3a* flies to initiate flight was tested with a flight assay described (Benzer 1973; Palladino et al. 2002). In brief, flies were dumped through a glass funnel into a glass graduated cylinder with the inside surface coated by mineral oil. Strong fliers would start flight immediately at the opening of the funnel and strike to the side of the cylinder near the top. Weak fliers, on the other hand, would initiate flight later and land near the bottom. The flight tests were done on flies 3-4 days old and 7-8 days old. Approximately 300 flies were tested for each genotype at each time point and the results were counted as described in Palladino et al. (2002). The overall flight abilities of *dube3a* mutant and control flies were analyzed with the student's t-test. When tested at 3-4 days old, *dube3a*^{15B} flies initiate flight as robustly as *dube3a*^{6PE} (wild-

type). At age 7-8 days, however, *dube3a*^{15B} are weaker fliers compared to *dube3a*^{6PE}. The flight impairment in *dube3a* mutants is small but statistically significant, and absolutely consistent in several repeated experiments (Figure 4.1).

The locomotor activity of *dube3a* mutants was also tested in a climbing assay as described (Orso et al. 2005) with some modifications. The flies tested were collected one day after eclosion. Twenty adult flies were kept in food vials to age. Upon the day of testing, the flies were transferred into empty plastic vials and gently tapped down to the bottom of the vials and the percentage of flies climbing up to the 3cm line in 3 seconds were recorded with a digital camera. The climbing tests were performed on files at day 3-4 and 8-9 after eclosion. For each genotype, ~300 flies were tested and the results were analyzed by the student's t-test. When tested at either 3-4 days or 8-9 days old, *dube3a*^{15B} flies were less able to climb in comparison to *dube3a*^{6PE} controls (Figure 4.2).

To determine if the climbing defects in *dube3a*^{15B} mutants are due solely to disruption of *dube3a* function, or if effects on expression of the nearby gene *CG7600* (Figure 2.6) might also contribute to the mutant

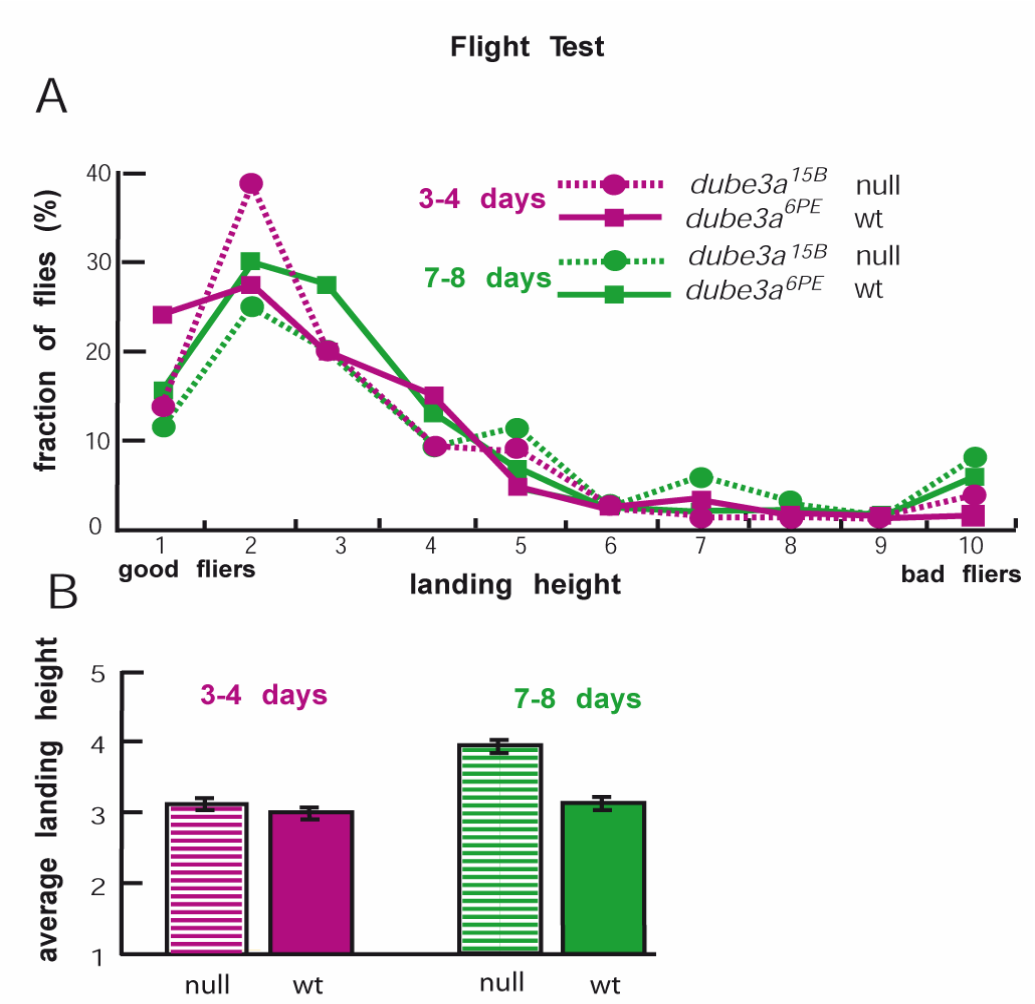

Figure 4.1: Defective flight initiation in *dube3a* mutants. Results of flight tests on two populations of ~300 flies each of different ages are shown. Very similar results were obtained in two repeats of this experiment. (*A*) The percentage of flies at each of 10 possible landing heights is shown. (*B*) The results in *A* are presented in bar graph form. The error bars are standard error. Using the t-test, the difference in performance between 7-8 day old wt and *dube3a* mutant flies is statistically significant ($P<0.01$).

phenotypes, I generated two transgenes, one with wild-type genomic DNA containing the *dube3a* gene (*gdube3a*$^{+}$), and the other an identical genomic DNA fragment, except for a missense mutation in the codon for the critical catalytic cysteine residue in Dube3a (*gdube3a*^{C941A}) (Figure 2.6). Transformants were generated with each construct, and their genetic backgrounds were homogenized by rounds of backcrossing with *dube3a*^{15B}.

Homozygotes for *dube3a*^{15B} carrying a single copy of either *gdube3a*$^{+}$ or *gdube3*^{C941A} were tested in the climbing assay, along with *dube3a*^{6PE} homozygous flies and *dube3a*^{15B} homozygous flies. I found that the wild-type *gdube3a*$^{+}$ transgene restores wild-type climbing ability to the *dube3a*^{15B} mutant flies, whereas the mutant *gdube3*^{C941A} transgene has no rescuing activity (Figure 4.2).

These results suggest that the climbing defect of *dube3a*^{15B} is caused by disruption of *dube3a* function and that flies lacking *dube3a*$^{+}$ activity have reduced motor control (Figure 4.2). Furthermore, the ability of the wild-type *gdube3a*$^{+}$ transgene, but not the *gdube3*^{C941A} mutant, to rescue the climbing phenotype in *dube3a* mutant flies suggest that the involvement of *dube3a* in locomotion control depends on the ubiquitin E3 activity of Dube3a.

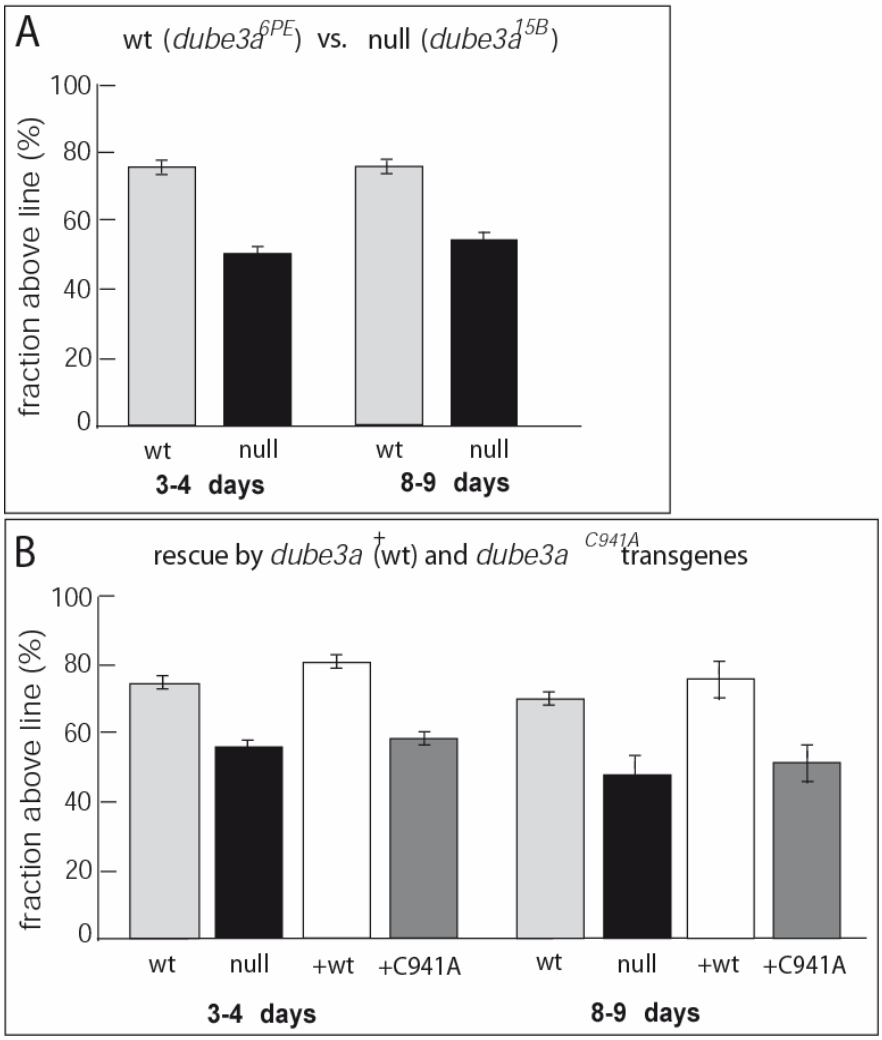

Figure 4.2: Defective climbing ability in *dube3a* mutants. Results of climbing tests are shown. In all panels, the results are averages of 16-18 different trials, each performed on separate populations of ~20 flies. Error bars are standard error calculated considering each trial as a single experiment. Statistical significance was determined using the t-test. (*A*) At both ages tested, *dube3a* mutants perform worse than wild-type flies ($P<0.05$). (*B*) At both ages tested, a *gdube3a+* transgene (Figure 2.4) rescues the *dube3a* mutant climbing defect to wild-type ($P<0.05$), while a *gdube3aC941A* mutant transgene (Figure 2.4) provides no rescue activity ($P>0.15$).

Two tests to induce seizures were performed. First, I performed a Bang sensitivity test (for response to mechanical stress) on wild-type and *dube3a* mutant flies at age 2-3 days or 7-8 days. Second, a heat shock assay (for response to temperature stress) was performed on wild-type and *dube3a* mutant flies at age 3-4 days or 8-9 days. Neither wild-type nor *dube3a* mutants showed any signs of paralysis in either assay. No incidence of seizure has been induced in *dube3a* null flies under mechanical or heat stresses. This is in line with the fact that seizure is not present in all AS cases (Williams et al. 2006). Actually, attempts to induce seizure in AS mouse models have yield discrepant results. While inducible seizure were shown in the *UBE3A* deficiency mouse model constructed by Jiang et al. (1998), it was absent in the *UBE3A* knockout mice generated by Miura et al. (2002). The reason for such differences observed is unclear. Possibly, different genetic backgrounds could have an effect on mouse behaviors (Miura et al. 2002).

The morphology of the adult brains of *dube3a*^{15B} and the *dube3a*^{6PE} flies was examined by staining with anti-Elav and anti-Fasciclin II. Anti-Fasciclin labels the adult mushroom bodies and well as the ellipsoid body of the central complex. No obvious morphological differences were detected between wild-type and *dube3a* mutant flies

(not shown). This observation is consistent with those made in AS mouse models: no apparent morphological change in hippocampus and cerebellum, the mammalian brain regions related to learning and memory and locomotor coordination (Jiang et al. 1998; Miura et al. 2002).

CONCLUSIONS

Similar to Angelman syndrome patients and AS mouse models, *dube3a* knock-out flies display locomotor dysfunction, including reduced flight coordination and climbing ability. These results suggest that the functions of fly Dube3a and human UBE3A may be similar and loss of UBE3A homologs in flies or human results in locomotor defects. Thus, *dube3a* mutants provide a candidate fly model for Angelman syndrome.

Chapter 5: Dube3a Overexpression Causes Morphological and Behavioral Phenotypes

INTRODUCTION

For genes with redundant roles in fly development, or mutants with no apparent morphological phenotypes, like *dube3a*, study of some aspects of their functions is facilitated by overexpressing these genes and analysis of the overexpression mutant phenotypes. This can be achieved with the well-established binary *UAS-Gal4* system (Brand and Perrimon 1993). A large collection of *Gal4* drivers with different temporal and tissue specificities is accessible in the *Drosophila* research community. There are two purposes to my Dube3a overexpression experiments. First, I want to generate morphological phenotypes useful for structure/function analysis of the Dube3a protein. These flies will also be useful later in modifier screens designed to reveal Dube3a substrates. Second, I want to know how sensitive the nervous system is to changes in the level of Dube3a substrates.

The fly tissues used most commonly for targeting *UAS*-transgene expression are the eye or the wing. The advantages of using these tissues are: (1) The ease of observing the severity of the phenotypes in these tissues in living flies under a stereo microscope; (2) The

dispensibility of these structures for fly viability and fertility. Even flies with no eyes or wings can be maintained and used in future analyses. (3) Efficient tissue specific *Gal4* drivers are available for eye and wing expression. In addition to provide valuable hints for the function of the RNA or protein products encoded by the *UAS*-transgenes, these attractive features of eye/wing specific expression are highly treasured as starting points for genetic modifier screens. Genetic and biochemical interactions between the gene of interest and the mutants isolated in such modifier screens can be further investigated in other tissues, such as the nervous system. One successful example is the isolation of the tumor suppressor *lethal (2) giant larvae* (*dlgl*) gene as a genetic suppressor of the *dfxr* gain of function rough eye phenotype. Genetic interaction and physical association between *dlgl* and *dfxr* in neural development was confirmed (Zarnescu et al. 2005).

In addition, excessive expression of Dube3a in the nervous system might provide crucial hints about the *in vivo* function of Dube3a in the nervous system. This is of great significance as the long-term interest in establishing a *Drosophila* Angelman syndrome model is to promote the understanding of Dube3a/UBE3A function and their AS-relevant substrate(s).

RESULTS AND DISCUSSION

Ubiquitous overexpression of *dube3a* results in lethality

Ectopic overexpression of *UAS-dube3a*$^{+}$ transgene under the *tubulin-Gal4* driver causes lethality. *tubulin-Gal4* enables the ubiquitous expression of the *UAS-dube3a* in all fly tissues and all developmental stages.

dube3a overexpression leads to eye and wing abnormalities

Flies carrying one copy of the eye-specific *GMR-Gal4* driver and one copy of a *UAS-dube3a*$^{+}$ transgene have rough external eyes. While no apparent defects are present in the developing photoreceptor clusters in the *GMR-Gal4>UAS-dube3a*$^{+}$ larval eye discs, the adult retina is completely disorganized as shown in adult eye sections (Figure 5.1).

Flies carrying one copy of the *UAS-dube3a*$^{+}$ transgene and one copy of the wing-specific *MS1096-Gal4* driver have curly wings (Figure 5.1).

As position in the genome can influence transgene expression level, I tested five independent *UAS-dube3a*$^{+}$ transformant lines and they all result in lethality with *tubulin-Gal4*, eye roughness under *GMR-Gal4* and curly wings with *MS1096-Gal4*.

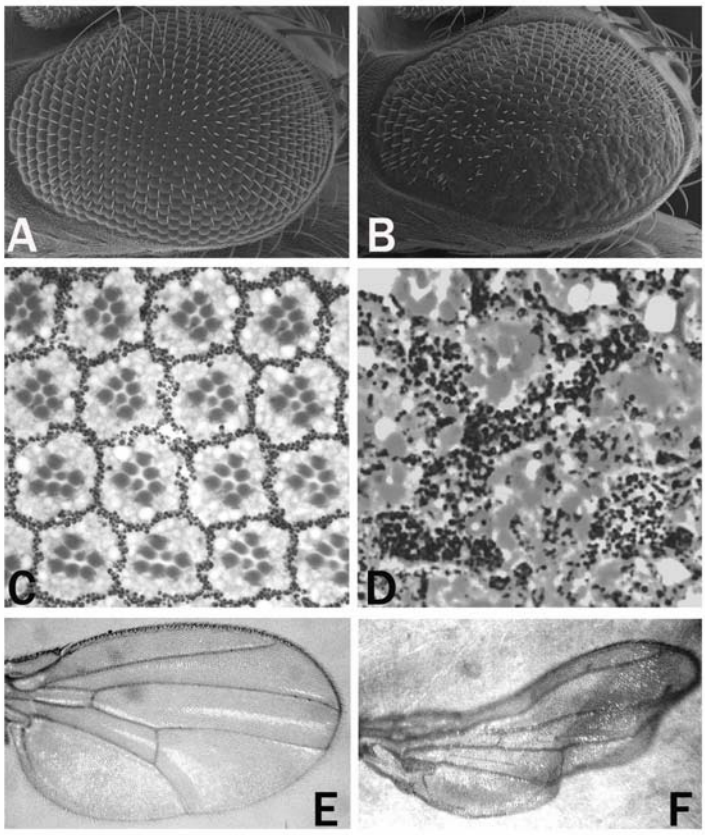

Figure 5.1: Morphological defects in flies that overexpress *dube3a*$^{+}$ in the eye or wing. Shown are external eyes (*A*, *B*), tangential sections of adult retinas (*C, D*), and wings (*E, F*) of flies that are wild-type (*A*, *C*, *E*) or overexpress the *UAS* transgene indicated with the eye-specific Gal4 driver (*GMR-Gal4*) or the wing-specific driver (*MS1096-Gal4*) (*B*, *D*, *F*). In flies with either the *UAS* or the Gal4 driver alone, eyes and wings are wild-type. (*A*, *E*) Eyes are irregular and wing tissue is curly. (*B*, *F*) Eyes and wings are wild-type. (*C*, *D*) Wild-type retinas contain organized hexagonal facets, each with eight photoreceptors arranged in a trapezoid (*C*). Retinal morphology is severely disrupted by Dube3a^{+} over-expression (*D*). In flies that overexpress *dube3a*^{C941A}, eyes and wings look wild-type.

***dube3a* overexpression defects require its potential E3 activity**

It was a common concern that ectopic overexpression of a transgene might lead to non-specific phenotypes. To assess if the *dube3a*$^{+}$ overexpression phenotypes are relevant to the physiological function of Dube3a, a *UAS-dube3a*^{C941A} transgene, encoding a mutant protein Dube3a^{C941A}, was generated and tested for its ability to elicit corresponding mutant defects. In Dube3a^{C941A}, the essential cysteine941 residue in the HECT domain (Figure 2.1), where the ubiquitin moiety passed down from the upstream E2s conjugates to the HECT E3s, is replaced by an alanine residue. For human UBE3A/E6AP, substitution of the equivalent cysteine820 to alanine abolishes the capability of E6AP to form a thiolester bond with ubiquitin (Huibregtse et al. 1995; Talis et al. 1998). I found that Dube3a^{C941A} behaves in flies like a loss-of-function mutant form of Dube3a^{+}. Overexpression of Dube3a^{C941A} (from either of two transformant lines) in the eye or the wing does not obviously affect their morphology. Likewise, ubiquitous expression of Dube3a^{C941A} does not kill the flies.

Also, as mentioned later in Chapter 6, overexpression of N-terminally *3xmyc*-tagged versions of Dube3a^{+} and Dube3a^{C941A} results in phenotypes (Figure 6.2) identical to those with their untagged

counterparts, when the expression level of 3mDube3a proteins are comparable.

These results suggest that the *dube3a* overexpression phenotypes are not artificial but depend on Dube3a's potential E3 function.

Excessive Dube3a activity in the nervous system results in abnormal behaviors

Overexpression of *UAS-dube3a*$^{+}$ in the developing and adult nervous system under the control of the pan-neural *Elav-Gal4* driver leads to deficiencies in movement coordination in adult flies. This movement defect was quantified using the climbing assay.

In one experiment (Figure 5.2 A), the climbing ability of flies harboring the *Gal4* driver transgene only, the *UAS-dube3a*$^{+}$ transgene only, or flies with both transgenes that thus express high levels of Dube3a^{+} were compared. As in Figure 5.2 A, flies overexpressing Dube3a^{+} have reduced climbing ability, and that the defect is more severe in older flies.

In order to determine if the mutant phenotype caused by Dube3a overexpression is due to the catalytic activity of the protein rather than to a non-specific effect, the climbing activity of flies that overexpress Dube3a^{C941A}, and flies that overexpress wild-type Dube3a from either of two different *UAS-dube3a* insertions were assayed. At all ages tested, each wild-type Dube3a overexpresser performs less well than the Dube3a^{C941A} overexpresser (Figure 5.2 B). In addition, the climbing ability of flies overexpressing Dube3a^{C941A} is similar to that of flies that express Gal4 alone.

Thus, neural overexpression of Dube3a, but not Dube3a^{C941A}, impairs climbing. This suggests that in the nervous system, Dube3a overactivity, presumably through over-ubiquitination of its substrates, is detrimental.

As both lack of Dube3a activity or excess Dube3a activity in the nervous system lead to similar, not opposite, neurological defects, I speculated that the fly nervous system is sensitive to the level of the substrate(s) of Dube3a. It is also possible that the subcellular accumulation of the substrate(s) (due to failure in being ubiquitinated and degraded) and the decreased levels of the substrate(s) (due to excessive ubiquitination and degradation) affect different subcellular

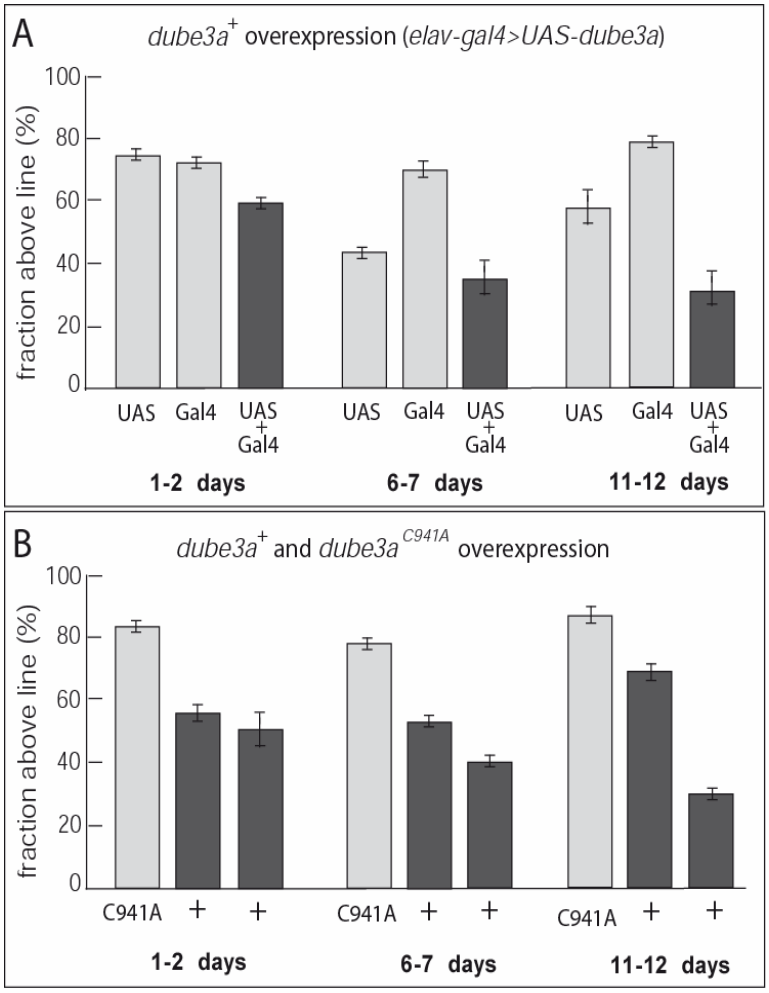

Figure 5.2: Defective climbing ability in flies that overexpress *dube3a*$^{+}$ in the nervous system. Results of climbing tests are shown. In all panels, the results are averages of 16-18 different trials, each performed on separate populations of ~20 flies. Error bars are standard error calculated considering each trial as a single experiment. Statistical significance was determined using the t-test. (*A*) At all ages tested, overexpression of *dube3a*$^{+}$ in the nervous system results in climbing defects (P<0.01 for Gal4 alone vs. Gal4+*UAS*). The smaller effect of *UAS* alone on climbing is likely due to its expression without the Gal4 driver. (*B*) At all ages tested, overexpression of *dube3a*$^{+}$ as in *A* from either one of two transgenes decreases climbing ability from wild-type levels, while overexpression of *dube3a*^{C941A} has no effect (P<0.01 for either *dube3a*$^{+}$ line vs. *dube3a*^{C941A}).

events in the neurons, but both result in similar gross neurological abnormality, such as climbing defects observed in the flies.

CONCLUSIONS

We have shown that overexpression of *UAS-dube3a* in the eye, the wing or ubiquitously, leads to severe morphological malformations, or lethality, respectively. Furthermore, extra Dube3a activity in the nervous system impairs climbing. All these overexpression defects depend on the presence of the critical catalytic cysteine in the HECT domain. These experiments implicate that like human UBE3A, fly Dube3a behaves as a HECT E3 ligase and its activity relies on the crucial cysteine residue in the HECT domain.

These gain-of-function mutant phenotypes provide invaluable tools for further study of *dube3a* and *UBE3A*. For example, I can now test how Angelman syndrome-associated *dube3a* mutants behave in the overexpression assay (see Chapter 5). Also, I could ask if wild-type and mutant *UBE3A* lead to defects similar to *dube3a* when overexpressed in *Drosophila* (see Chapter 6).

In addition, these gain-of-function mutant phenotypes are of great potential to be used as the background for genetic screens for

identification of Dube3a substrates and other genes in the pathway. However, as it is not clear that if Dube3a maintains its substrate specificity under the overexpression states, the candidate genes isolated in such screen needs to be analyzed in the *dube3a* loss-of-mutants to test if they are physiological substrate of Dube3a (and UBE3A) relevant to AS (also see Chapter 8).

Chapter 6: Overexpression of *dube3a* Carrying Angelman Syndrome Mutations

INTRODUCTION

Among the known AS-associated human *UBE3A* mutations, which are mostly frameshifts and nonsense mutations, there are eight missense point mutations, seven of which occur at amino acid residues conserved between Dube3a and UBE3A/E6AP. They are *UBE3A*^{C21Y}, *UBE3A*^{I130T}, *UBE3A*^{S349P}, *UBE3A*^{L502P}, *UBE3A*^{R506C}, *UBE3A*^{E550L} and *UBE3A*^{I804K} (Figure 2.1). If corresponding mutations impair fly *dube3a* function, this would provide further evidence for conservation of function between human UBE3A and the fly Dube3a ortholog. The *dube3a* overexpression phenotypes dependent on its potential E3 function provide an *in vivo* assay for evaluating whether Dube3a missense mutant proteins are functional.

RESULTS AND DISCUSSION

Four *dube3a* transgenes encoding AS-associated Dube3a mutants were generated, namely, *UAS-3mdube3a*^{C55Y}(corresponding to human *UBE3A*^{C21Y}), *UAS-3mdube3a*^{T447P}(corresponding to *UBE3A*^{S349P}), *UAS-3mdube3a*^{R626C}(corresponding to *UBE3A*^{R506C}), and *UAS-3mdube3a*^{I925K}(corresponding to *UBE3A*^{I804K}). All these *UAS*-transgenes

were *3×myc*-tagged at their N-termini to facilitate further expression level analyses on Western blots.

Whether the presence of the 3×Myc tag affects Dube3a protein function was first tested with *UAS-3mdube3a*$^{+}$ and *UAS-3mdube3a*^{C941A} controls. These two *3×myc*-tagged transgenes behave the same as *UAS-dube3a*$^{+}$ and *UAS-dube3a*^{C941A} respectively. When driven by *tubulin-Gal4*, *GMR-Gal4* or *MS1096-Gal4*, the *UAS-3mdube3a*$^{+}$ transgene leads to lethality, eye roughness and curly wings, and the *UAS-3mdube3a*^{C941A} transgene causes no mutant phenotypes (Figure 6.1, Figure 6.2). Comparable expression levels of 3mDube3a^{+} and 3mDube3a^{C941A} proteins were detected on Western blots with *GMR-Gal4>UAS-3mdube3a* larval eye disc extracts (Figure 6.2).

For each of the four *UAS-3mdube3a* transgenes encoding AS-associated missense alleles, at least three unique transformant lines were tested to minimize the possibility of position effects on transgene expression levels. The protein expression levels of these transgenes were also assayed on anti-Myc Western blots with protein extracts prepared from *GMR-Gal4>UAS-3mdube3a* larval eye discs (not shown).

None of the *UAS-3mdube3a* transgenes led to overexpression phenotypes when driven by *GMR-Gal4* or *tubulin-Gal4*, except *UAS-3mdube3a*^{T447P}, which showed variable results (Figure 6.2). Four of six *UAS-3mdube3a*^{T447P} transgenic lines, at least one of which expresses similar levels of 3mDube3a^{T447P} protein to 3mDube3a^{+} and 3mDube3a^{C941A}, result in no phenotypes. However, the other two of the six *UAS-3mdube3a*^{T447P} transgenic lines causes lethality when driven by *tubulin-Gal4* and one of them leads to rough eyes when driven by *GMR-Gal4*. Both 3mDube3a^{R626C} and 3mDube3a^{I925K} behave identically to the catalytically inactive 3mDube3a^{C941A} protein in this overexpression assay; the mutant proteins accumulate to similar levels as wild-type protein, but do not cause mutant phenotypes (Figure 6.2). 3mDube3a^{C55Y} also behaves like 3mDube3a^{C941A} in that it fails to cause phenotypes, but its level of accumulation is lower than that of 3mDube3a^{C941A} and 3mDube3a^{+}.

In addition, the *UAS-3mdube3a* transgenic lines expressing comparable level of 3mDube3a^{T447P}, 3mDube3a^{R626C} and 3mDube3a^{I904K} and the *UAS-3mdube3a*^{C55Y} transgenic line with the highest 3mDube3a^{I904K}-expressing level were tested for their ability to induce the curly wing phenotype under *MS1096-Gal4*. As consistent with the *GMR-*

Figure 6.1: Morphological phenotypes of flies that overexpress different *UAS-3mdube3a* transgenes in the eye and wing. Shown are external eyes (*A*-*G*) and wings (*H*-*N*) of flies that are wild-type (*A*, *H*), or those carrying a copy of either *GMR-Gal4* or *MS1096-Gal4* and a copy of one of the *UAS-3mdube3a* transgenes: *UAS-3mdube3a*^{WT} (*B*, I), *UAS-3mdube3a*^{C55Y}(*C*, *J*), *UAS-3mdube3a*^{T447P} (*D*, *K*), *UAS-3mdube3a*^{R626C} (*E*, *L*), *UAS-3mdube3a*^{I925K} (*F*, *M*), or *UAS-3mdube3a*^{C941A} (*G*, *N*). Eyes and wing abnormalities are only observed in 3mdube3a^{+} overexpression. The expression levels of these *UAS-3mdube3a* transgenes are demonstrated in Figure 6.2 (*B*) and the transformant lines used for each transgene are indicated in Figure 6.2 (*A*).

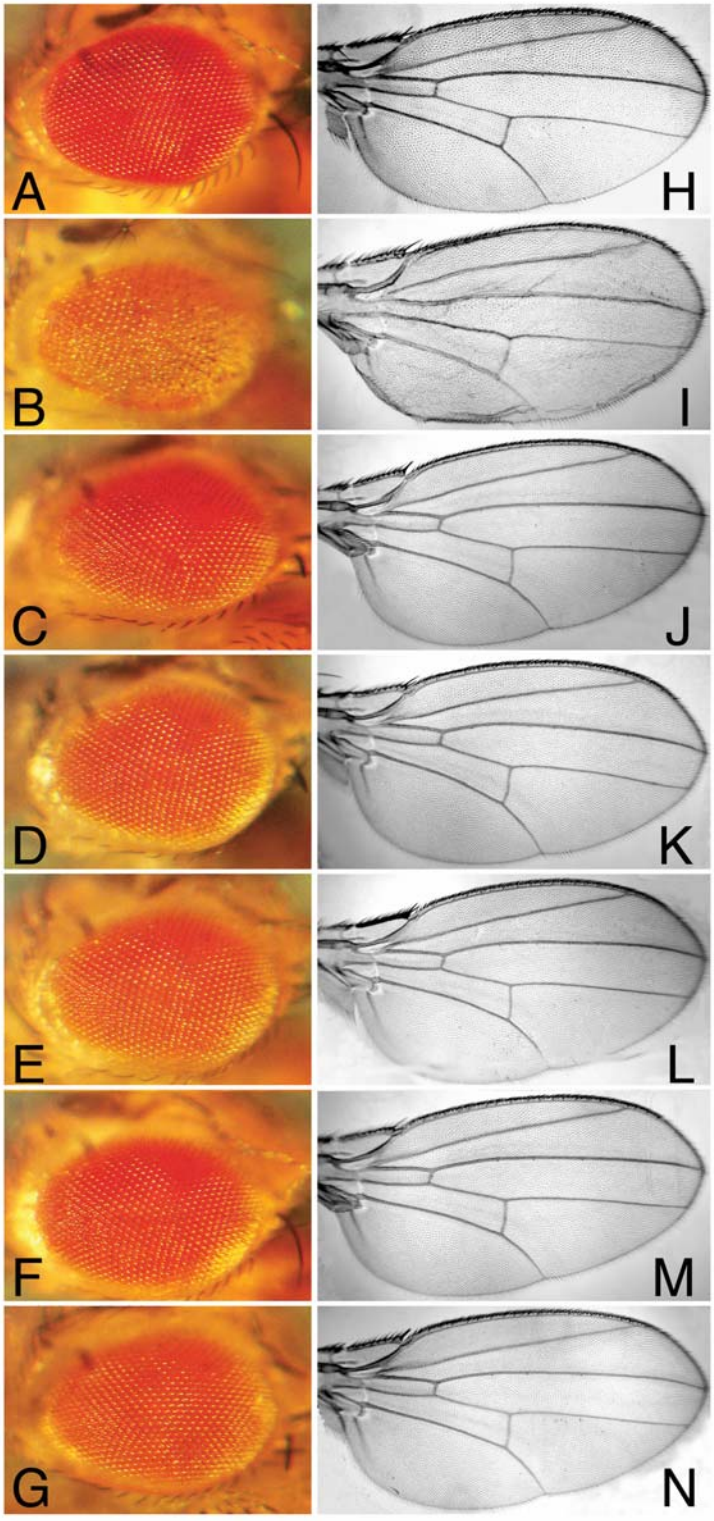
A
H
B
I
C
J
D
K
E
L
F
M
G
N

A Overexpression of 3mDube3a proteins

mutation	lines	eye	wing	ubiquitous	blot
wild-type	1-4	rough	curly	lethal	line1
C941A	1-3	normal	normal	viable	line1
C55Y (hC21Y)	1-6, 8	normal	ND	viable	
	7	normal	normal	viable	line7
T447P (hS349P)	1-3	normal	normal	viable	line3
	6	normal	ND	viable	
	4	normal	normal	lethal	
	5	rough	curly	lethal	
R626C (hR506C)	1, 6	normal	normal	viable	line6
	2-5, 7-8	normal	ND	viable	
I925K (hI804K)	6, 8	normal	normal	viable	line6
	2-5, 7	normal	ND	viable	

B 3xmyc-tagged Dube3a proteins

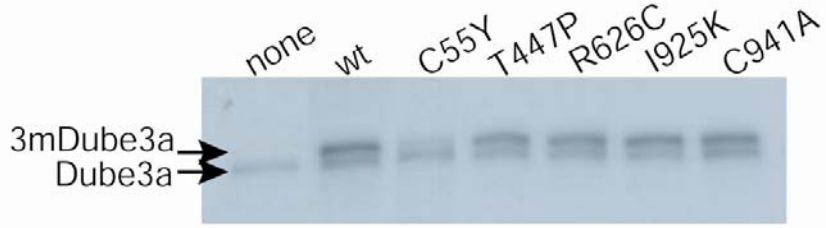

Figure 6.2: Angelman syndrome missense mutations are loss-of-function mutations in *dube3a*. (*A*) A tabulation of the phenotypes that result from expression of six different *UAS-3mdube3a* transgenes in the eye (*GMR-Gal4*), wing (*MS1096-Gal4*), or ubiquitously (*tubulin-Gal4*). The "mutation" column indicates which missense mutation is present in the fly gene (human isoform1 counterpart in parentheses). The "lines" column indicates independent transformant lines assayed. The "eye", "wing", and "ubiquitous" columns indicate whether or not expression resulted in a mutant phenotype. Shaded rows indicate lines that resulted in no phenotypes. The "blot" column indicates the transformant lines with their protein expression level displayed in the blot in (*B*) and their overexpression phenotypes displayed in Figure 6.1. (*B*) A blot of eye disc protein extracts from flies with no transgene (none), or flies with a *GMR-Gal4* and a *UAS* line expressing wild-type 3mDube3a (wt), or one of the five missense mutant 3mDube3a proteins indicated. The blot was probed with guinea pig anti-Dube3a, so that endogenous protein serves as an internal loading control.

Gal4 and *tubulin-Gal4* results, no curly wing defects were observed in these flies (Figure 6.1).

In vitro biochemical properties of the human UBE3A counterparts to Dube3a^{I925K} (UBE3A^{I804K}), Dube3a^{C55Y} (UBE3A^{C21Y}), and Dube3a^{T447P} (UBE3A^{S349P}) have been studied (Cooper et al. 2004). Unlike Dube3a^{I925K}, which is apparently stable in flies, UBE3A^{I804K} is an unstable protein *in vitro*. Dube3a^{C55Y}, however, is cannot be overexpressed to a high level, suggesting that it might be an unstable protein in flies. Its human counterpart UBE3A^{C21Y} is also unstable *in vitro*. Finally, while Dube3a^{T447P} is partially active in flies, *in vitro* UBE3A^{S349P} cannot ubiquitinate the substrate HHR23A. Perhaps this difference in the fly and *in vitro* assays is because the assays measure Ub ligase activity on different substrates.

CONCLUSIONS

In summary, the fly counterparts of the four AS missense alleles tested behave as loss of function mutations in the fly. This is supportive of the idea that *dube3a* and *UBE3A* are functional homologs and that AS is caused by loss of UBE3A function.

Chapter 7: Expression of Human *UBE3A* in *Drosophila*

INTRODUCTION

As overexpression of wild-type fly Dube3a leads to mutant phenotypes, the possibility of inducing similar defects through overexpressing human UBE3A was examined. There are three human UBE3A isoforms that differ at their N-termini resulting from alternative splicing. They are 875aa long isoform 2, 872aa long isoform 3, and the 853aa long isoform1 (Figure 2.1). It is not known whether any one of the isoforms predominates in the human brain (especially in the hippocampus and the Purkinje cells). Whether the subtly different N-termini are functionally significant is also unclear.

RESULTS AND DISCUSSION

UAS-UBE3A^{iso2+} and *UAS-UBE3A*$^{iso1+}$ transgenes were generated, encoding the wild-type UBE3A isoform2 and UBE3A isoform 1 proteins, respectively. When driven by *GMR-Gal4* (eye), *MS1096-Gal4* (wing) or *tubulin-Gal4* (ubiquitous), none of these transgenes causes mutant phenotypes.

To determine whether this was due to a failure to overexpress the UBE3A proteins, a *3Xmyc*-tagged *UAS-3mUBE3A*$^{iso1+}$ transgene was

generated and two independent transformant lines were obtained. When expression of the *UAS* was driven with any of the three *Gal4* drivers, these lines behaved identically to those expressing untagged UBE3A proteins: no mutant phenotypes resulted. By mobilizing the *UAS* insertion in these two lines, I generated 20 different lines with the *UAS* construct in different positions in the genome. When expressed using the ubiquitous *Gal4* driver, only one line showed a lethal phenotype. Two more *3Xmyc*-tagged *UAS-3mUBE3A* transgenes were made as well. They are *UAS-3mUBE3A*^{iso1C21Y} and *UAS-3mUBE3A*^{iso1S347P}. Protein extracts of several lines of these *3Xmyc*-tagged transgenes were assayed on Western blots for the level of 3mUBE3A, and the protein levels were vanishingly low compared to the levels of 3mDube3a (Figure 7.1). I have not determined why the human protein fails to accumulate appreciably in the fly. Nevertheless, I conclude that at least using the human *UBE3A* gene, it is extremely difficult to express UBE3A in *Drosophila*.

CONCLUSIONS

Recently, Reiter et al. (2006) identified *Drosophila* Pebble (a guanine nucleotide exchange factor) as one of twenty proteins whose levels are increased when human UBE3A (isoform 2) is overexpressed in the fly head. In addition, UBE3A transgenes expressed in the fly eye

A Ectopic expression of human UBE3A proteins

UAS-transgene	#lines	eye	wing	ubiquitous
UBE3A^{iso2+}	3	normal	normal	viable
UBE3A^{iso1+}	3	normal	normal	viable
3mUBE3A^{iso1+}	2	normal		viable
	19			viable
	1	normal		lethal
3mUBE3A^{iso1C21Y}	1	normal		viable
3mUBE3A^{iso1S349P}	3	normal		viable

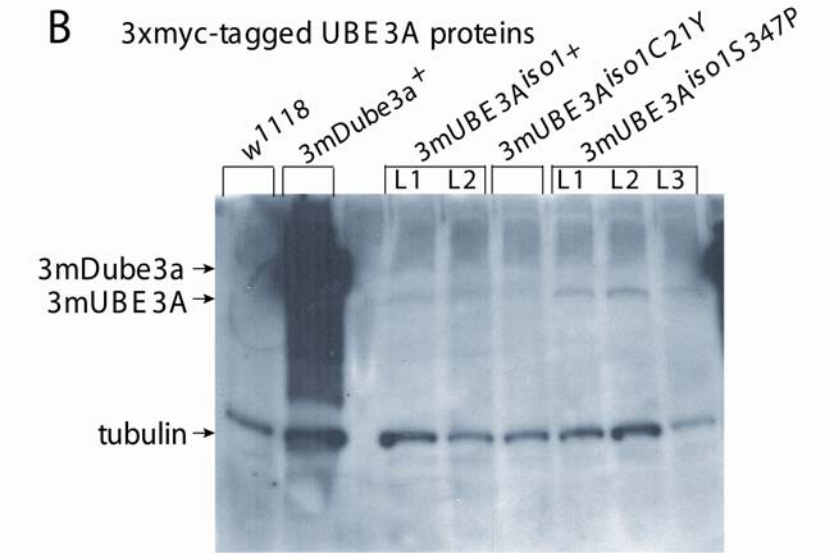

Figure 7.1: Human UBE3A proteins could not be overexpressed in *Drosophila*. (*A*) A tabulation of the phenotypes that result from ectopic expression of five different *UAS* transgenes encoding human UBE3A in the eye (*GMR-Gal4*), wing (*MS1096-Gal4*), or ubiquitously (*tubulin-Gal4*). The layout of the table is the same as the one in Figure 6.2 A. (*B*) A blot of eye disc protein extracts from flies with no transgene (w^{1118}, negative control), or flies with a *GMR-Gal4* and a *UAS* line expressing wild-type 3mDube3a (positive control), or a UAS line encoding 3mUBE3A proteins as indicated. The blots were probed with mouse anti-Myc and anti-tubulin, which serves as an internal loading control. The transgenic lines underlined in (*A*) are the ones used for this blot (L1, L2 or L3 for each one of the three 3mUBE3A proteins).

were able to suppress Pebble overexpression phenotypes. The results of further experiments using the fly and mouse models suggest that the mouse Pebble homolog, ECT2 (epithelial cell transforming sequence 2), may be a direct target of UBE3A. At present, we cannot reconcile our inability to overexpress human UBE3A with their results.

Chapter 8: Overall Conclusions and Future Directions

OVERALL CONCLUSIONS

The data described here provide strong evidence for the idea that *dube3a* is the *Drosophila* homolog of human *UBE3A* and that *dube3a* mutants could serve as a fly model for Angelman syndrome. First, as the most likely fly homolog of human *UBE3A*, *Drosophila dube3a* is present in the fly nervous system at the embryonic, larval and adult stages and high level expression of Dube3a is present in the adult mushroom bodies, the brain components involved in associative learning and memory. Second, I have generated *dube3a* null mutants and they appear normal externally, but display abnormal locomotor behaviors. Third, overexpression of Dube3a causes morphological or behavioral phenotypes dependent on the HECT domain function. Finally, most of the missense mutations identified in Angelman syndrome patients are in amino acid residues conserved between the human UBE3A protein and *Drosophila* Dube3a protein. When four of such mutations were introduced into Dube3a, these mutants act as loss-of-function alleles.

The development of a *Drosophila* AS model will help to elucidate the underlying mechanism of AS pathogenesis, especially in identifying the substrates of *dube3a* and *UBE3A* relevant to AS. Unfortunately, the

unique imprinting feature of AS could not be studied in the fly model, as there is not similar CpG island-related imprinting in flies.

FUTURE DIRECTIONS

Genetic Screens to Identify *dube3a* Substrate(s) and Other Genes in the Pathway

Genetic screens using the *dube3a* overexpression eye phenotype or wing phenotype can now be carried out to identify the substrate(s) of *dube3a* and possibly other genes involved in the same pathway. As the overexpression defects are dependent on the potential E3 function of Dube3a, a plausible explanation for these overexpression phenotypes is that overexpressing *dube3a* in the eye or the wing, where endogenous *dube3a*, and most likely its substrate(s) as well are present, results in excessive ubiquitination and then excessive degradation of these target protein by the proteasome. The decrease in the substrate levels interferes with certain processes in eye/wing development and results in rough eyes or curly wings. If this speculation is correct, then the substrates potentially could be isolated using genetic screens. For example, a loss-of-function mutation in a substrate gene would be expected to behave as a dominant enhancer of the eye or wing phenotype, while overexpression of the substrate gene would be expected to suppress the phenotypes. Mutations in genes that facilitate

the ubiquitin pathway or positively regulate *dube3a* expression or function could also be recovered in such genetic screens.

Various genetic screen strategies are available. Large scale EMS screens have the highest potential to identify most of the genes involved in the relevant molecular pathways and cellular processes. However, the follow-up mapping processes to identify the genes carrying EMS-induced mutations could be rather intensive and usually rely on the mutants having a lethal or morphological phenotype on their own.

The large collections of P-element (loss-of-function) or EP-element (loss-of-function and gain-of-function) insertions and the isogenic deficiency kits could help to eliminate these drawbacks, although the EP-element and P-element lines do not cover as much the genome as a saturated EMS screen would. In addition to providing loss-of-function mutants as the P-element or deficiency collections, the EP stocks can be used for analyzing gain-of-function phenotypes of adjacent genes simply by crossing into a *Gal4* driver.

I think that the best choice for the first genetic screen would be the isogenic deficiencies. Isogenic P-elements could be used to find

genes within the deficiencies. In parallel, the EP collections could be used for a screen for gain-of-function modifiers.

Testing If UBE3A Substrates Identified So Far Are Dube3a Substrates in the Nervous System

Another great advantage to the fly model is that the potential relevance of a Dube3a substrate to AS may be tested easily through a variety of genetic and biochemical experiments.

Overexpression in the brain of Dube3a substrates relevant to AS should phenocopy the motor dysfunction observed in *dube3a* loss-of-function mutations. This powerful assay may be used immediately to test whether the UBE3A substrates already identified biochemically (the Src family tyrosine kinase Blk, the excision repair protein HHR23, the replication licensing factor Mcm7 and Pebble/ECT2) are relevant to AS.

We can also examine if the loss-of-function mutations in these candidate Dube3a substrates enhance the Dube3a overexpression eye or wing defects. Conversely, overexpression of these substrates simultaneously with Dube3a may alleviate the eye or wing malformations caused by Dube3a overexpression.

Whether the cellular concentration of the substrate is altered in *dube3a* null or overexpressing flies can be assesses both *in vivo* and *in vitro*, if antibodies are available. Additionally, whether the substrate is ubiquitinated in the presence or absence of Dube3a can be analyzed on Western blots.

Ultimately, the mouse homologs of promising potential substrates found in the fly assays may be tested similarly in the mouse models for AS.

Appendix: Materials and Methods

Drosophila stocks

Drosophila stocks generated for this project

w; dube3a^{6PE} / TM6B
w; dube3a^{15B} / TM6B
w; dube3a^{6J} / TM6B
w; dube3a^{8O} / TM6B
w; gdube3a^{+} / CyO; dube3a^{15B} / TM6B
w; gdube3a^{C941A} / CyO; dube3a^{15B} / TM6B

w; ggfpube3aL2 / TM6B
w; ggfpdube3aL3 / TM6B

w; g6mdube3aL2 / CyO
w; g6mdube3aL3/ TM6B
w; g6mdube3aL2; g6mdube3aL3, nucGFP / TM6B

w; UASt-dube3a^{+}L1 / CyO
w; UASt-dube3a^{+}L2 / TM6B
w; UASt-dube3a^{+}L3 / TM6B
w; UASt-dube3a^{+}L6 / TM6B
w; UASt-dube3a^{+}L 8/ CyO

w; UASt-dube3a^{C941A}L1 / TM6B
w; UASt-dube3a^{C941A}L2 / TM6B

w; UASt-3mdube3a^{+}L1 (on 2nd)
w; UASt-3mdube3a^{+}L2 / TM6B
w; UASt-3mdube3a^{+}L3 / TM6B
w; UASt-3mdube3a^{+}L4 / TM6B

w; UASt-3mdube3a^{C55Y}L1 / CyO
w; UASt-3mdube3a^{C55Y}L2 / TM6B
w; Sco / CyO; UASt-3mdube3a^{C55Y}L3 / TM6B
w; Sco / CyO; UASt-3mdube3a^{C55Y}L4/ TM6B
w; UASt-3mdube3a^{C55Y}L5/ CyO; MKRS / TM6B
w; UASt-3mdube3a^{C55Y}L6 / CyO; MKRS / TM6B
w; UASt-3mdube3a^{C55Y}L7 / CyO; MKRS / TM6B
w; UASt-3mdube3a^{C55Y}L8 / CyO; MKRS / TM6B

w; UASt-3mdube3a^{T447P}L1 / TM6B
w; UASt-3mdube3a^{T447P}L2 / CyO; MKRS / TM6B
w; UASt-3mdube3a^{T447P}L3 / CyO; MKRS / TM6B
w; UASt-3mdube3a^{T447P}L4 / CyO; MKRS / TM6B
w; UASt-3mdube3a^{T447P}L5 / CyO; MKRS / TM6B
w; UASt-3mdube3a^{T447P}L6 / CyO; MKRS / TM6B

w; UASt-3mdube3a^{R626C}L1 (on 2nd)
w; UASt-3mdube3a^{R626C}L2 / CyO
w; UASt-3mdube3a^{R626C}L3 / TM6B
w; UASt-3mdube3a^{R626C}L4 / TM6B
w; UASt-3mdube3a^{R626C}L5 / TM6B
w; UASt-3mdube3a^{R626C}L6 / TM6B
w; UASt-3mdube3a^{R626C}L7 / TM6B
w; UASt-3mdube3a^{R626C}L8 / TM6B

w; UASt-3mdube3a^{I925K}L2 / CyO; MKRS / TM6B
w; UASt-3mdube3a^{I925K}L3 / CyO; MKRS / TM6B
w; UASt-3mdube3a^{I925K}L4 / CyO; MKRS / TM6B
w; UASt-3mdube3a^{I925K}L5 / TM6B
w; UASt-3mdube3a^{I925K}L6 / TM6B
w; UASt-3mdube3a^{I925K}L7 / CyO; MKRS / TM6B
w; UASt-3mdube3a^{I925K}L8 / TM6B

w, UASt-3mdube3a^{C941A}L1 (on X-ch)
w; UASt-3mdube3a^{C941A}L2 / CyO
w; UASt-3mdube3a^{C941A}L3 / TM6B

w; UASt-UBE3A^{iso2+}L1 / CyO
w; UASt-UBE3A^{iso2+}L2 / TM6B
w; UASt-UBE3A^{iso2+}L3 / TM6B

w; UASt-UBE3A^{iso1+}L1 / TM6B
w; UASt-UBE3A^{iso1+}L2 (on 2nd)
w; UASt-UBE3A^{iso1+}L3 (on 2nd)

w; UASt-3mUBE3A^{iso1+}L1 (on X-ch)
w; UASt-3mUBE3A^{iso1+}L2 (on 2nd)

w; UASt-3mUBE3A^{iso1C21Y} (on 2nd)

w; UASt-3mUBE3A^{iso1S349P}L1 (on 2nd)
w; UASt-3mUBE3A^{iso1S349P}L2 / TM6B

w; UASt-3mUBE3A^{iso1S349P}L3 / TM6B

Stocks obtained from Bloomington stock center or other resources

w; dube3a$^{EP(3)3214}$ / TM6B
w; Cha-GAL4.7.4 / CyO, sevRas1
w; repo-Gal4 / TM3, Sb
w; OK6-Gal4 *(from Dr. Bing Zhang)*
w; OK107-Gal4
w; OK201Y-Gal4
MZ1060-Gal4; sbb$^{e(2)03432}$ / CyO *(from Dr. Marla Sokolowski)*
sbb$^{e(2)03432}$ / CyO-GFP; l(3)31-Gal4 / TM6C *(from Dr. Marla Sokolowski)*

Fischer lab fly stocks

OregonR
w^{1118}
yw
w; GMR-Gal4
w, MS1096-Gal4
yw; tubulin-Gal4/ TM3
w; Elav-Gal4 (on 3rd)
w; UAS-nucGFP8
Sp/ CyO; TM6, Ubx / SbΔ2-3
TM2Δ2-3 / MKRSΔ2-3
w; Sb/TM6B
w; Sco/CyO; MKRS/TM6B

Molecular Biology. All oligonucleotides were from Integrated DNA Technologies (Coralville, IA). PCR was performed using PCR Supermix (Invitrogen Corporation, Carlsbad, CA). DNA sequences of all PCR products were determined, and automated fluorimetric methods were used (ICMB DNA facility, UT Austin). Genomic DNA isolation was as described (Hamilton and Zinn, 1994).

Confirmation of EP(3)3214 insertion site by PCR
PCR was done with genomic DNA isolated from *EP(3)3214* homozygotes as the template and the primer pairs: 5'- TCCAGATAGTA GTTGAAGGGCGTC-3'/5'-CTTGCCGACGGGACCACCTTATGTTATT-3' and 5'-GCCGCCCCTTTCTTTGTTTG-3'/ 5'-CACCCAAGGCTCTGCTC CCACAAT-3'. The PCR products were sequence and the sequences were then aligned with *dube3a* genomic DNA sequences using MacVector 9.0 (MacVector, Inc, Cary, NC)

Analysis of *dube3a* mRNA through RT-PCR experiments

dube3a RNA was isolated from desired fly tissues (embryos, larvae, adults or larval eye discs) with TRI reagent Kit (Molecular Research Center, Inc. Cincinnati, OH) according to the user manual. Reverse transcription was done with SuperScript II (Invitrogen) according to the manufacture manual. The cDNA was then used as the PCR templates. The primer pair 5'-GGATCCCAAACAAAGAAAGGGGCGGC-3′/5'-TGAC GGCGTGAGGATAAAGG-3' was used to amplify the 1.7kb 5' *dube3a* RNA sequence. The primer pair 5'-CGGAAACCACTGATACCACTTGA G-3'/ 5'-GGATCCTGGTGGTATCAGTTCCAGATGACAG-3' was used to amplify the 1.4kb 3' *dube3a* RNA sequence.

P element mobilization to generate *dube3a* mutants

dube3a^{8O} and *dube3a*^{6J} attempt: by mobilizing the *EP(3)3124* element with Δ*2-3* transposases (see Figure 2.4 for the cross scheme), ~250 individual hop-out lines were generated. Lines that contained homozygous sub-viable or lethal hop-out chromosomes were discarded, and the remaining 135 lines were divided into 7 pools. Genomic DNA prepared from each pool (2 homozygous flies from each of the 20-25 lines was used) was used as a template for PCR using the primers listed below. The PCR products were electrophoresed and analyzed for the presence of a smaller product indicative of a deletion. Continuation of the process with subpools led to the identification of the single lines 8O and 6J. The precise deletion endpoints in 8O and 6J were identified through DNA sequence determination of the PCR products. Primers used for such group PCR include: Forward primers: F1: 5'-TCCAGATAGTAGTTGAAGGGCGTC-3' (~750bp upstream of the EP insertion site) and F2: 5'-GGCGATTTGGGACTTTGGT-3' (1550bp upstream of the EP insertion site), and Reverse primers: RA: 5'-TGACGGCGTGAGGATAAAGG-3'; RB: 5'-CATCACCGAAAACATCGC-3'; RC: 5'-GGATCCTGGTGGTATCAGTTCCAGATGACAG -3'; RD: 5'-GGGCTAAAGAAGGGAAACA-3'; and RE: 5'-CCCGCAAGAAACTCAGA AACG-3'. PCR from wild-type fly genomic DNA with the primer pair F1/RA results in the amplification of a 3.1kb fragment; with the primer pair F1/RD results in the amplification of a 4.8kb fragment; with the primer pair F2/RA results in the amplification of a 3.9kb fragment; with the primer pair F2/RB results in the amplification of a 4.8kb fragment; with the primer pair F2/RC results in the amplification of a 5.3kb fragment; with the primer pair F2/Re results in the amplification of a 6.0kb fragment. *dube3a*^{6PE} and *dube3a*^{15B} attempt: The isogenic precise (*dube3a*^{6PE}) and imprecise (*dube3a*^{15B}) excision chromosomes were generated with the cross scheme listed in Figure 2.5. Eye disc protein extracts of homozygotes each of the 120 independent lines were analyzed by Western blotting using guinea pig anti-Dube3a. Genomic

DNA of lines that appeared to express no Dube3a protein were analyzed as described above.

Transgene construction and transformation. P element transformation of *w*^{1118} flies was performed using standard techniques.

pUASt-dube3a^{+}

The 1.7kb *dube3a* 5' cDNA fragment and a 1.4kb *dube3a* 3' cDNA fragment were obtained as described above, through RT-PCR with *w*^{1118} adult fly samples. These PCR products were ligated into *pGEMTe* vector (*pGEMTe*, Promega Corporation, Madison, WI) to generate *pGEMT-dube3a*$^{5'}$ and *pGEMT-dube3a*$^{3'}$ respectively. These cloned fragments were confirmed through sequencing. The 1.7kb 5' fragment and the 1.4kb 3' fragments were then isolated as 1.7kb NotI/DraIII and 1.4kb DraIII/BamHI fragments and subcloned together into the NotI/BamHI-digested *pBSAscI* vector (Chen and Fischer 2000) to generate *pBSA-dube3a*$^{e+}$. The 3.1kb *dube3a* cDNA fragment was then isolated from *pBSA-dube3a*$^{e+}$ as a NotI/KpnI fragment and ligated into NotI/KpnI-digested *pUAStAscI* vector (Huang and Fischer-Vize 1996) to generate *pUASt-dube3a*$^{+}$.

pUASt-dube3a^{C941A}

A 1.3kb *dube3a* coding fragment carrying a Cys941Ala substitution was obtained through PCR-mediated mutagenesis using *pGEMT-dube3a*$^{3'}$ as the PCR template and the primer pair 5'-CGGAAACCACTGATACCACT TGAG-3'/ 5'-GAACGTTGAAGGCGGTGTGCGAGGTAGGCAA-3', thus introduces an Ala codon at the place of the 941Cys codon. The 1.3kb Cys941Ala PCR fragment was ligated into *pGEMTe* vector and the presence of the 941Ala codon was confirmed by sequencing. The 1.3kb Cys941Ala fragment was then recovered as a NotI/AclI fragment and subcloned into the NotI/BamHI-digested *pBSAscI* vector, together with a 0.1kb AclI/BamHI fragment isolated from *pGEMT-dube3a*$^{3'}$, to generate a 1.4kb Cys941Ala *dube3a* 3' cDNA fragment. The product is *pBSA-dube3a*$^{3'C941A}$. Isolated from *pBSA-dube3a*$^{3'C941A}$ as a DraIII/BamHI fragment, this 1.4kb Cys941Ala fragment was then pieced together with the 1.7kb NotI/DraIII *dube3a* 5' fragment isolated from *pGEMT-dube3a*$^{5'}$, into NotI/BamHI-digested *pBSAscI* vector to make *pBSA-dube3a*^{eC941A}. The 3.1kb *dube3a* Cys941Ala fragment was then subcloned as a NotI/KpnI fragment into NotI/KpnI-digested *pUAStAscI* vector to generate *pUASt-dube3a*^{C941A}.

pUASt-3mdube3a^{+}

dube3a N-terminal coding fragment was obtained by PCR amplification of *pBSA-dube3a*$^{e+}$ with the primer pair 5'-CAGATCTCAGGATCCATGAA CGGTGGCGGGGGT-3'/ 5'-GCGGCCGCCGTTGATGAGCTGGTCCCT

T-3', which then ligated into *pGEMTe* vector and sequenced. The product is *pGEMT-dube3a*$^{N'}$. A 1.2kb BamHI/AscI fragment was cut out *pGEMT-dube3a*$^{N'}$ and pieced together with a 1.8kb AscI/BamHI fragment from *pBSA-dube3a*$^{e+}$ into BamHI-digested p8036 vector (Harris and Macdonald 2001), from which the 3.0kb full-length *dube3a* coding sequence was recovered as a single BamHI fragment and inserted into the BamHI site of *pBSAscI* vector to make *pBSA-dube3a*$^{+}$. A 1.8kb AscI fragment was then isolated from *pBSA-dube3a*$^{+}$ and inserted into the AscI site of *pUASt-3mdube3a*$^{5'}$ to make *pUASt*-3m*dube3a*$^{+}$. *pUASt-3mdube3a*$^{5'}$ was constructed as following: a BglII site was introduced to replace Dube3a codon5-6 in *pGEMT-dube3a*$^{5'}$ by PCR-based mutagenesis using QuickChange Site-Directed Mutagenesis Kit (Stratagene, La Jolla, CA), with the primers 5'-AAGATGAACGGTGGCAGATCTGGC GAGGATGATCAG-3'/ 5'-CTGATCATCCTCGCCAGATCTGCCACCGTT CATCTT-3' to generate *pGEMT-B2-dube3a*$^{5'}$, which was then restricted with BglII/HindIII to accommodate a 0.1kb BamHI/*3×myc* fragment from *pSPBP4-tsl-3×myc* (Stevens L and Stein D, unpublished data) and a 1.0kb BamHI/HindIII fragment from *pBSA-dube3a*$^{+}$ together thus generating *pGEMT-3mdube3a*$^{5'}$. Finally, a 1.8kb NotI fragment encoding the N-terminal part of Dube3a with a *3×myc* tag fused in-frame was isolated from *pGEMT-3mdube3a*$^{5'}$ and inserted into the NotI site of *pUAStAscI* to generate *pUASt-3mdube3a*$^{5'}$.

***pUASt-3mdube3a*^{C55Y}**

A 0.2kb PCR fragment containing the beginning of *dube3a* coding sequence was amplified from *pGEMT-dube3a*$^{N'}$ with the primer pair 5'-CAGATCTCAGGATCCATGAACGGTGGCGGGGGT-3'/ 5'CAATTGGCA TTGCTGCAGTTGGCGTTCCCGTAGCCGGATTGTAGTTG-3', thus introducing a Tyr codon at the place of the 55Cys codon. This PCR fragment was ligated into *pGEMTe* vector and sequenced. The 0.2kb sequence was then recovered as a SacI/MfeI fragment and subcloned together with a 2.9kb MfeI/XhoI fragment cut out of *pBSA-dube3a*$^{+}$ into the SacI/XhoI-digested *pBSAscI* vector to generate *pBSA-dube3a*^{C55Y}. The 3.1kb *dube3a*^{C55Y} was then recovered from *pBSA-dube3a*^{C55Y} as a BamHI fragment and ligated into EcoRI/ BglII-digested *pUAStAscI*, together with a 0.2kb 3×myc EcoRI/BamHI fragment isolated from *pUASt-UBE3A*$^{iso1\text{S349P}}$ described below.

***pUASt-3mdube3a*^{T447P}**

A 0.9kb *dube3a* coding fragment containing a Thr447Pro substitution was obtained by PCR with *pBSA-dube3a*$^{e+}$ as the template and the primer pair 5'-ATCTTACCCAGAGTGTGCCGCAAC-3'/ 5'-GAAGACAAT

CTTTAAAACTTTGGGGACACTGATTATGGATTC-3', which introduces a Thr codon at the place of the 447Pro codon. It was ligated into *pGEMTe* vector and sequenced to confirm the presence of the 447Thr codon This T447P fragment was then isolated as a 0.6kb BbsI fragment and replaced the correspondent fragment in *pBSA-dube3a*$^{+}$, thus generated *pBSA-dube3a*^{T447P}. A 1.8kb AscI fragment was then isolated from *pBSA-dube3a*^{T447P} and inserted into the AscI site of *pUASt-3mdube3a*$^{5'}$to make *pUASt-3×myc•dube3a*^{T447P}.

***pUASt-3mdube3a*^{R626C}**

A 1.1kb *dube3a* coding fragment carrying a Arg626Cys substitution was obtained by PCR with *pBSA-dube3a*$^{e+}$ as the template and the primer pair 5'-CTTAAGCTGACGGTGCGATGCGACCAGCTCATCAACGAC-3'/ 5'-GGATCCTGGTGGTATCAGTTCCAGATGACAG-3' introducing an Arg codon at the position of 626Cys, and ligated into *pGEMTe* vector and sequenced to verify the presence of the 626Arg codon. This R626C fragment was then recovered as a 0.9kb AflII/MluI fragment and replaced the correspondent fragment in *pBSA-dube3a*$^{+}$, thus generated *pBSA-dube3a*^{R626C}. A 1.8kb AscI fragment was then isolated from *pBSA-dube3a*^{R626C} and inserted into the AscI site of *pUASt-3mdube3a*$^{5'}$ to make *pUASt-3mdube3a*^{R626C}.

***pUASt-3mdube3a*^{I925K}**

A 1.2kb fragment of *dube3a* coding sequence containing a Ile925Lys substitution was obtained by PCR with *pBSA-dube3a*$^{e+}$ as the template and the primer pair 5'-CGGAAACCACTGATACCACTTGAG-3'/5'-ACGC GTCTTTAGCAGACGCAGGCATTTCAG-3', which introduces an Ile codon at the position of the 925Lys codon, and ligated into *pGEMTe* vector. The fragment was then recovered as a 0.9kb AflII/MluI fragment and replaced the corresponding fragment in *pBSA-dube3a*$^{+}$, thus generated the *pBSA-dube3a*^{I925K}. A 1.8kb AscI fragment was then isolated from *pBSA-dube3a*^{I925K} and inserted into the AscI site of *pUASt-3×myc•dube3a*$^{5'}$ to make *pUASt-3mdube3a*^{I925K}.

***pUASt-3mdube3a*^{C941A}**

A 1.8kb fragment of *dube3a* coding sequence containing a Cys941Ala substitution was cut out of *pBSA-dube3a*^{eC941A} and inserted into the AscI site of *pUASt-3mdube3a*$^{5'}$ to make *pUASt-3mdube3a*^{C941A}.

All the *UBE3A* fragments used below were subcloned from various *UBE3A* plasmids kindly provided by Dr. Jon Huibregtse, UT-Austin.

pUASt-UBE3A^{iso1+}

The 2.6kb BamHI/HindIII *UBE3A*$^{iso1+}$ fragment was converted into a BamHI/AscI fragment and linked into *pUASpAscI* vector, where an AscI site is inserted into the XbaI site of *pUASp* vector (Rorth 1998). The *UBE3A*$^{iso1+}$ fragment was then recovered from *pUASp-UBE3A*$^{iso1+}$ as a NotI/AscI fragment and inserted into *pUAStAscI*.

pUASt-UBE3A^{iso2+}

The 2.6kb *UBE3A*$^{iso2+}$ cDNA fragment was converted into a NotI/AscI fragment as above and linked into *pUAStAscI* vector.

pUASt-3mUBE3A^{iso1+}

A 0.2kb *3×myc* BamHI fragment recovered from *pGEMT-3mdube3a*$^{5'}$ was inserted into the BamHI site of *pUASp-UBE3A*$^{iso1+}$, from where the *3mUBE3A*$^{iso1+}$ fragment was isolated and subcloned into *pUAStAscI* as a NotI/AscI fragment.

pUASt-3mUBE3A^{iso1C21Y}

A 0.2kb *3×myc* BamHI fragment recovered from *pGEMT-3mdube3a*$^{5'}$ was pieced in-frame with a 2.6kb BamHI/NotI *UBE3A*^{iso1C21Y} into BglII/NotI-digested *pUAStAscI* vector

pUASt-3mUBE3A^{iso1S349P}

A 0.2kb *3×myc* BamHI fragment recovered from *pGEMT-3mdube3a*$^{5'}$ was pieced in-frame with a 2.6kb BamHI/NotI *UBE3A*^{iso1S349P} into BglII/NotI-digested *pUAStAscI* vector

pCaspeR4-gdube3a^{+}

A 13kb XhoI/BamHI *dube3a* genomic DNA fragment was isolated from BAC clone BACR19G23 (BACPAC Resources, http://bacpac.chori.org) and ligated into XhoI/ BamHI-cut *pBSAscI* to generate *pBSA-gdube3a*$^{+}$, from which the 13kb genomic fragment was subcloned into the *pCaspeR4* vector using KpnI and NotI as the cloning sites to generate *pCaspeR4-gdube3a*$^{+}$.

pCaspeR4-gdube3a^{C941A}

A 0.25kb SphI fragment containing the constructed Cys941Ala substitution was isolated from *pUASt-dube3a*^{C941A} and replaced the corresponding piece in *pBSA-gdube3a*$^{+}$, thus generating *pBSA-gdube3a*^{C941A}, from which the modified 13kb genomic fragment was subcloned into KpnI/NotI-digested *pCaspeR4* to generate *pCaspeR4-gdube3a*^{C941A}.

pCaspeR4-g6mdube3a

Similar to the construction of *pGEMT-B2-dube3a*$^{5'}$ described in *pUASt-3mdube3a*$^{+}$, a *pBSA-gB2-dube3aSA* carrying a subcloned 1.8kb SpeI/AscI fragment from *pBSA-gdube3a*$^{+}$ was generated with a BglII site engineered in replace of codon5-6. *pBSA-gB2-dube3aSA* was then restricted with BglII/AscI to accommodate BamHI/*3xmyc* fragments from *pSPBP4-tsl•3×myc* and a 1.4kb BamHI/AscI fragment amplified from *pBSA-gdube3a*$^{+}$ to generate *pBSA-g6mdube3a-SA*, in which the presence of two tandem *3×myc* fragments was determined. The1.9kb SpeI/AscI fragment from *pBSA-g6mdube3a-SA* was then recovered and replace the corresponding sequence in *pBSA-gdube3a*$^{+}$ to generate *pBSA-g6mdube3a*, from which the 13kb *g6mdube3a* fragment was subcloned into NotI/KpanI digested *pCaspeR4* to generate *pCaspeR4-g6mdube3a*.

pCaspeR4-ggfpdube3a

pCaspeR4-ggfpdube3a was generated following exactly the same steps described in *pCaspeR4-g6mdube3a* construction, except that a 0.75kb BamHI/*GFP* fragment was used in place of the BamHI/*3xmyc* fragment. The BamHI/*GFP* fragment is obtained through PCR from *pUASg-gfpdube3a* (Kracklauer et al. 2007) with the primer pair 5'-GGATCCATG AGTAAAGGAGGAGAAC-3'/ 5'-CTGTTGGCCTCCGATGTGAA-3'. The PCR product was cloned into *pGEMTe* and recovered as a BamHI fragment after the GFP sequence was confirmed.

Dube3a antibodies

The 3.0kb full-length *dube3a* coding sequence as described in *pUASt-3mdube3a*$^{+}$ construction was inserted into the BamHI site of pET-28a vector (Novagen, Madison, WI). Expression of the His•Dube3a recombinant protein was induced in *E. coli* Codon-Plus RIL cells (Stratagene, La Jolla, CA). The recombinant protein was purified with His•Bind Resin (Novagen) following the user protocol. The purified protein was then sent to Pocono Rabbit Farm& Laboratory Inc (Canadensis, PA) for injection in rats and guinea pigs to raise polyclonal anti-Dube3a antisera.

Protein blotting

Western blottings were performed as described (Chen et al. 2002; Fischer et al. 2004). The primary antibodies were used at the following dilutions: rat or guinea pig anti-Dube3a 1:5000; mouse anti-tubulin E7 (Developmental Studies Hybridoma Bank, Iowa city, IA) 1:100; mouse anti-Myc 9B11 (Cell Signaling Technologies, Danvers, MA) 1:5000. The secondary antibodies were used at the following dilutions: HRP-conjugated anti-guinea pig 1: 50,000; HRP-conjugated anti-rat 1:5000; HRP-conjugated anti-mouse 1:5000 (Sigma-Aldrich Corp. St. Louis, MO).

Embryo immunohistochemistry
Embryo immunostaining was done as described (Jones and Macdonald 2007). The primary antibodies were used at the following dilutions: rat anti-Dube3a 1:500 (preabsorbed against *dube3a*^{8O} homozygous embryos); mouse anti-Elav 9F8A9 (DSHB) 1:40; mouse anti-Myc 9B11 1:4000; rat anti-Elav 7E8A10 (DSHB) 1:25. Cross-absorbed secondary antibodies were used at the following dilutions: Alexa Fluro 488 goat anti-mouse 1:500, Alexa Fluro 647 goat anti-rat 1:500 (Molecular Probes, Eugene, OR). Stained embryos were mounted in VectaShield mounting medium (Vector Laboratories, Burlingame, CA). Images were acquired with a Leica SP2 AOBS confocal microscope or a Leica TCS-SP confocal microscope.

Eye disc immunohistochemistry
Third instar larval eye discs were prepared as described (Fischer-Vize et al. 1992; Chen et al. 2002). Images were acquired with a Leica TCS-SP confocal microscope. The antibodies were used as follows: rat anti-Dube3a 1:500; rabbit anti-GFP 1:1000 (kindly provided by Hui Li and Dr. Arturo DeLozanne, UT-Austin); mouse anti-Myc 9B11 1:1000; Cy5 goat anti-rat 1:200 (Jackson Immunoresearch, West Grove, PA); Alexa Fluro 488 goat anti-mouse 1:200; Alexa Fluro 488 goat anti-rabbit 1:200; Phalloidin 568 1:10 (Molecular Probes).

Larval and adult brain immunohistochemistry
Adult or larval brains were dissected in PBS and fixed in 4% paraformaldehyde at room temperature for 50 minutes, incubated in primary antibodies overnight at 4°C. The secondary antibody incubation was done at room temperature for at least 2 hours. PBST washes were done between the fixation and primary, secondary antibody incubations. The fly tissues were mounted with VectaShield mounting medium. Images were acquired with a Leica SP2 AOBS confocal microscope or a Leica TCS-SP confocal microscope. The primary antibodies were used as follows: mouse anti-Myc 9B11 1:4000; rat anti-Elav 7E8A10 1:30; mouse anti-Fasciclin II 1:50. Cross-absorbed secondary antibodies were used at the following dilutions: Alexa Fluro 488 goat anti-mouse 1:600; Alexa Fluro 647 goat anti-mouse 1:600; Alexa Fluro 488 goat anti-rat 1:600; Alexa Fluro 647 goat anti-rat 1:600 (Molecular Probes).

Heat shock assay
Heat shock assays were performed on *dube3a*^{15B} and *dube3a*^{6PE} flies at age 3-4 days and 8-9 days old. Appropriately aged flies were transferred into empty vials and heat shocked in 37C water bath for signs of

paralysis, every 5 minutes. The latest time point is 20 minutes. For each genotype, more than 120 flies were tested each time.

Bang sensitivity assay

Bang sensitivity assay was done with *dube3a*^{15B} and *dube3a*^{6PE} flies as described (Zhang et al. 2002) at age 2-3 or 7-8 days old . For either genotype, more than 120 flies were tested.

Flight test

The ability of *dube3a* flies to initiate flight was tested with a flight assay described (Benzer 1973; Palladino et al. 2002). In brief, flies were dumped through a glass funnel into a glass graduated cylinder with the inside surface coated by mineral oil. Strong fliers would start flight immediately at the opening of the funnel and strike to the side of the cylinder near the top. Weak fliers, on the other hand, would initiate flight later and land near the bottom. The flight tests were done on flies 3-4 days old and 7-8 days old. Approximately 300 flies were tested for each genotype at each time point and the results were counted as described in Palladino et al. (2002). The overall flight abilities of *dube3a* mutant and control flies were analyzed with the student's t-test.

Climbing assay

The locomotor activity of *dube3a* mutants was tested in a climbing assay as described (Orso et al. 2005) with some modifications. The flies tested were collected one day after eclosion. Twenty adult flies were kept in food vials to age. Upon the day of testing, the flies were transferred into empty plastic vials and gently tapped down to the bottom of the vial and the percentage of flies climbing up to the 3cm line in 3 seconds were recorded with a digital camera. The climbing tests were performed on files at day 3-4 and 8-9 after eclosion. For each genotype, ~300 flies were tested and the results were analyzed by the student's t-test.

Analysis of eyes and wings.

Analysis of adult eyes and wings were done as described (Cadavid et al. 2000; Patterson et al. 2004).

REFERENCE:

Albrecht, U., J. S. Sutcliffe, B. M. Cattanach, C. V. Beechey, D. Armstrong, G. Eichele and A. L. Beaudet (1997). Imprinted expression of the murine Angelman syndrome gene, Ube3a, in hippocampal and Purkinje neurons. Nat Genet 17(1): 75-78.

Amerik, A. Y. and M. Hochstrasser (2004). Mechanism and function of deubiquitinating enzymes. Biochim Biophys Acta 1695(1-3): 189-207.

Ardley, H. C. and P. A. Robinson (2004). The role of ubiquitin-protein ligases in neurodegenerative disease. Neurodegener Dis 1(2-3): 71-87.

Arnaud, L., N. K. Robakis and M. E. Figueiredo-Pereira (2006). It may take inflammation, phosphorylation and ubiquitination to 'tangle' in Alzheimer's disease. Neurodegener Dis 3(6): 313-319.

Auluck, P. K. and N. M. Bonini (2002). Pharmacological prevention of Parkinson disease in Drosophila. Nat Med 8(11): 1185-1186.

Auluck, P. K., H. Y. Chan, J. Q. Trojanowski, V. M. Lee and N. M. Bonini (2002). Chaperone suppression of alpha-synuclein toxicity in a Drosophila model for Parkinson's disease. Science 295(5556): 865-868.

Baumer, A., D. Balmer and A. Schinzel (1999). Screening for UBE3A gene mutations in a group of Angelman syndrome patients selected according to non-stringent clinical criteria. Hum Genet 105(6): 598-602.

Benzer, S. (1973). Genetic dissection of behavior. Sci Am 229(6): 24-37.

Bier, E. and R. Bodmer (2004). Drosophila, an emerging model for cardiac disease. Gene 342(1): 1-11.

Bilen, J. and N. M. Bonini (2005). Drosophila as a model for human neurodegenerative disease. Annu Rev Genet 39: 153-171.

Bilen, J., N. Liu, B. G. Burnett, R. N. Pittman and N. M. Bonini (2006). MicroRNA pathways modulate polyglutamine-induced neurodegeneration. Mol Cell 24(1): 157-163.

Boulton, S. J. (2006). Cellular functions of the BRCA tumour-suppressor proteins. Biochem Soc Trans 34(Pt 5): 633-645.

Brand, A. H. and N. Perrimon (1993). Targeted gene expression as a means of altering cell fates and generating dominant phenotypes. Development 118(2): 401-415.

Brooks, C. L. and W. Gu (2006). p53 ubiquitination: Mdm2 and beyond. Mol Cell 21(3): 307-315.

Brown, V., P. Jin, S. Ceman, J. C. Darnell, W. T. O'Donnell, S. A. Tenenbaum, X. Jin, Y. Feng, K. D. Wilkinson, J. D. Keene, R. B. Darnell and S. T. Warren (2001). Microarray identification of FMRP-associated brain mRNAs and altered mRNA translational profiles in fragile X syndrome. Cell 107(4): 477-487.

Brumby, A. M. and H. E. Richardson (2005). Using Drosophila melanogaster to map human cancer pathways. Nat Rev Cancer 5(8): 626-639.

Brummelkamp, T. R., S. M. Nijman, A. M. Dirac and R. Bernards (2003). Loss of the cylindromatosis tumour suppressor inhibits apoptosis by activating NF-kappaB. Nature 424(6950): 797-801.

Burger, J., D. Horn, H. Tonnies, H. Neitzel and A. Reis (2002). Familial interstitial 570 kbp deletion of the UBE3A gene region causing Angelman syndrome but not Prader-Willi syndrome. Am J Med Genet 111(3): 233-237.

Cadavid, A. L., A. Ginzel and J. A. Fischer (2000). The function of the Drosophila fat facets deubiquitinating enzyme in limiting photoreceptor cell number is intimately associated with endocytosis. Development 127(8): 1727-1736.

Carmine Belin, A., M. Westerlund, O. Bergman, H. Nissbrandt, C. Lind, O. Sydow and D. Galter (2007). S18Y in ubiquitin carboxy-terminal hydrolase L1 (UCH-L1) associated with decreased risk of Parkinson's disease in Sweden. Parkinsonism Relat Disord.

Cattanach, B. M., J. A. Barr, C. V. Beechey, J. Martin, J. Noebels and J. Jones (1997). A candidate model for Angelman syndrome in the mouse. Mamm Genome 8(7): 472-478.

Cauchi, R. J. and M. van den Heuvel (2006). The fly as a model for neurodegenerative diseases: is it worth the jump? Neurodegener Dis 3(6): 338-356.

Caudy, A. A., M. Myers, G. J. Hannon and S. M. Hammond (2002). Fragile X-related protein and VIG associate with the RNA interference machinery. Genes Dev 16(19): 2491-2496.

Chan, H. Y., J. M. Warrick, I. Andriola, D. Merry and N. M. Bonini (2002). Genetic modulation of polyglutamine toxicity by protein conjugation pathways in Drosophila. Hum Mol Genet 11(23): 2895-2904.

Chee, F. C., A. Mudher, M. F. Cuttle, T. A. Newman, D. MacKay, S. Lovestone and D. Shepherd (2005). Over-expression of tau results in defective synaptic transmission in Drosophila neuromuscular junctions. Neurobiol Dis 20(3): 918-928.

Chen, X. and J. A. Fischer (2000). In vivo Structure/Function analysis of the Drosophila fat facets deubiquitinating enzyme gene. Genetics 156(4): 1829-1836.

Chen, X., B. Zhang and J. A. Fischer (2002). A specific protein substrate for a deubiquitinating enzyme: Liquid facets is the substrate of Fat facets. Genes Dev 16(3): 289-294.

Ciechanover, A. (2006). The ubiquitin proteolytic system: from a vague idea, through basic mechanisms, and onto human diseases and drug targeting. Neurology 66(2 Suppl 1): S7-19.

Clark, I. E., M. W. Dodson, C. Jiang, J. H. Cao, J. R. Huh, J. H. Seol, S. J. Yoo, B. A. Hay and M. Guo (2006). Drosophila pink1 is required for mitochondrial function and interacts genetically with parkin. Nature 441(7097): 1162-1166.

Clayton-Smith, J. and L. Laan (2003). Angelman syndrome: a review of the clinical and genetic aspects. J Med Genet 40(2): 87-95.

Comery, T. A., J. B. Harris, P. J. Willems, B. A. Oostra, S. A. Irwin, I. J. Weiler and W. T. Greenough (1997). Abnormal dendritic spines in fragile X knockout mice: maturation and pruning deficits. Proc Natl Acad Sci U S A 94(10): 5401-5404.

Cooper, E. M., A. W. Hudson, J. Amos, J. Wagstaff and P. M. Howley (2004). Biochemical analysis of Angelman syndrome-associated mutations in the E3 ubiquitin ligase E6-associated protein. J Biol Chem 279(39): 41208-41217.

Costa, A., Y. Wang, T. C. Dockendorff, H. Erdjument-Bromage, P. Tempst, P. Schedl and T. A. Jongens (2005). The Drosophila fragile X protein functions as a negative regulator in the orb autoregulatory pathway. Dev Cell 8(3): 331-342.

Crowther, D. C., K. J. Kinghorn, E. Miranda, R. Page, J. A. Curry, F. A. Duthie, D. C. Gubb and D. A. Lomas (2005). Intraneuronal Abeta, non-amyloid aggregates and neurodegeneration in a Drosophila model of Alzheimer's disease. Neuroscience 132(1): 123-135.

Deshpande, G., G. Calhoun and P. Schedl (2006). The drosophila fragile X protein dFMR1 is required during early embryogenesis for pole cell formation and rapid nuclear division cycles. Genetics 174(3): 1287-1298.

Dion, M. H., E. J. Novotny, Jr., L. Carmant, P. Cossette and D. K. Nguyen (2007). Lamotrigine therapy of epilepsy with Angelman's syndrome. Epilepsia 48(3): 593-596.

Dockendorff, T. C., H. S. Su, S. M. McBride, Z. Yang, C. H. Choi, K. K. Siwicki, A. Sehgal and T. A. Jongens (2002). Drosophila lacking dfmr1 activity show defects in circadian output and fail to maintain courtship interest. Neuron 34(6): 973-984.

Doss-Pepe, E. W., L. Chen and K. Madura (2005). Alpha-synuclein and parkin contribute to the assembly of ubiquitin lysine 63-linked multiubiquitin chains. J Biol Chem 280(17): 16619-16624.

Eakin, C. M., M. J. Maccoss, G. L. Finney and R. E. Klevit (2007). Estrogen receptor alpha is a putative substrate for the BRCA1 ubiquitin ligase. Proc Natl Acad Sci U S A 104(14): 5794-5799.

Elbaz, A., C. Levecque, J. Clavel, J. S. Vidal, F. Richard, J. R. Correze, B. Delemotte, P. Amouyel, A. Alperovitch, M. C. Chartier-Harlin and C. Tzourio (2003). S18Y polymorphism in the UCH-L1 gene and Parkinson's disease: evidence for an age-dependent relationship. Mov Disord 18(2): 130-137.

Fang, P., E. Lev-Lehman, T. F. Tsai, T. Matsuura, C. S. Benton, J. S. Sutcliffe, S. L. Christian, T. Kubota, D. J. Halley, H. Meijers-Heijboer, S. Langlois, J. M. Graham, Jr., J. Beuten, P. J. Willems, D. H. Ledbetter and A. L. Beaudet (1999). The spectrum of mutations in UBE3A causing Angelman syndrome. Hum Mol Genet 8(1): 129-135.

Fang, S., K. L. Lorick, J. P. Jensen and A. M. Weissman (2003). RING finger ubiquitin protein ligases: implications for tumorigenesis, metastasis and for molecular targets in cancer. Semin Cancer Biol 13(1): 5-14.

Fang, S. and A. M. Weissman (2004). A field guide to ubiquitylation. Cell Mol Life Sci 61(13): 1546-1561.

Feany, M. B. and W. W. Bender (2000). A Drosophila model of Parkinson's disease. Nature 404(6776): 394-398.

Fernandez-Funez, P., M. L. Nino-Rosales, B. de Gouyon, W. C. She, J. M. Luchak, P. Martinez, E. Turiegano, J. Benito, M. Capovilla, P. J. Skinner, A. McCall, I. Canal, H. T. Orr, H. Y. Zoghbi and J. Botas (2000). Identification of genes that modify ataxin-1-induced neurodegeneration. Nature 408(6808): 101-106.

Ferrante, R. J., J. K. Kubilus, J. Lee, H. Ryu, A. Beesen, B. Zucker, K. Smith, N. W. Kowall, R. R. Ratan, R. Luthi-Carter and S. M. Hersch (2003). Histone deacetylase inhibition by sodium butyrate chemotherapy ameliorates the neurodegenerative phenotype in Huntington's disease mice. J Neurosci 23(28): 9418-9427.

Finelli, A., A. Kelkar, H. J. Song, H. Yang and M. Konsolaki (2004). A model for studying Alzheimer's Abeta42-induced toxicity in Drosophila melanogaster. Mol Cell Neurosci 26(3): 365-375.

Fischer-Vize, J. A., G. M. Rubin and R. Lehmann (1992). The fat facets gene is required for Drosophila eye and embryo development. Development 116(4): 985-1000.

Fischer, J. A., S. Acosta, A. Kenny, C. Cater, C. Robinson and J. Hook (2004). Drosophila klarsicht has distinct subcellular localization domains for nuclear envelope and microtubule localization in the eye. Genetics 168(3): 1385-1393.

Flores, S. Y., C. Debonneville and O. Staub (2003). The role of Nedd4/Nedd4-like dependant ubiquitylation in epithelial transport processes. Pflugers Arch 446(3): 334-338.

Freemont, P. S. (2000). RING for destruction? Curr Biol 10(2): R84-87.

Fung, D. C., B. Yu, K. F. Cheong, A. Smith and R. J. Trent (1998). UBE3A "mutations" in two unrelated and phenotypically different Angelman syndrome patients. Hum Genet 102(4): 487-492.

Gabriel, J. M., M. Merchant, T. Ohta, Y. Ji, R. G. Caldwell, M. J. Ramsey, J. D. Tucker, R. Longnecker and R. D. Nicholls (1999). A transgene insertion creating a heritable chromosome deletion mouse model of Prader-Willi and angelman syndromes. Proc Natl Acad Sci U S A 96(16): 9258-9263.

Ghosh, S. and M. B. Feany (2004). Comparison of pathways controlling toxicity in the eye and brain in Drosophila models of human neurodegenerative diseases. Hum Mol Genet 13(18): 2011-2018.

Glickman, M. H. and A. Ciechanover (2002). The ubiquitin-proteasome proteolytic pathway: destruction for the sake of construction. Physiol Rev 82(2): 373-428.

Golic, K. G. (1991). Site-specific recombination between homologous chromosomes in Drosophila. Science 252(5008): 958-961.

Greene, J. C., A. J. Whitworth, I. Kuo, L. A. Andrews, M. B. Feany and L. J. Pallanck (2003). Mitochondrial pathology and apoptotic muscle degeneration in Drosophila parkin mutants. Proc Natl Acad Sci U S A 100(7): 4078-4083.

Greeve, I., D. Kretzschmar, J. A. Tschape, A. Beyn, C. Brellinger, M. Schweizer, R. M. Nitsch and R. Reifegerste (2004). Age-dependent neurodegeneration and Alzheimer-amyloid plaque formation in transgenic Drosophila. J Neurosci 24(16): 3899-3906.

Gstaiger, M., R. Jordan, M. Lim, C. Catzavelos, J. Mestan, J. Slingerland and W. Krek (2001). Skp2 is oncogenic and overexpressed in human cancers. Proc Natl Acad Sci U S A 98(9): 5043-5048.

Gunawardena, S. and L. S. Goldstein (2001). Disruption of axonal transport and neuronal viability by amyloid precursor protein mutations in Drosophila. Neuron 32(3): 389-401.

Haase, V. H. (2006). The VHL/HIF oxygen-sensing pathway and its relevance to kidney disease. Kidney Int 69(8): 1302-1307.

Handley-Gearhart, P. M., A. G. Stephen, J. S. Trausch-Azar, A. Ciechanover and A. L. Schwartz (1994). Human ubiquitin-activating enzyme, E1. Indication of potential nuclear and cytoplasmic subpopulations using epitope-tagged cDNA constructs. J Biol Chem 269(52): 33171-33178.

Handley, P. M., M. Mueckler, N. R. Siegel, A. Ciechanover and A. L. Schwartz (1991). Molecular cloning, sequence, and tissue distribution of the human ubiquitin-activating enzyme E1. Proc Natl Acad Sci U S A 88(1): 258-262.

Harris, A. N. and P. M. Macdonald (2001). Aubergine encodes a Drosophila polar granule component required for pole cell formation and related to eIF2C. Development 128(14): 2823-2832.

Harvey, K. F. and S. Kumar (1999). Nedd4-like proteins: an emerging family of ubiquitin-protein ligases implicated in diverse cellular functions. Trends Cell Biol 9(5): 166-169.

Hattori, N. and Y. Mizuno (2004). Pathogenetic mechanisms of parkin in Parkinson's disease. Lancet 364(9435): 722-724.

Heisenberg, M. (2003). Mushroom body memoir: from maps to models. Nat Rev Neurosci 4(4): 266-275.

Herrmann, J., A. Ciechanover, L. O. Lerman and A. Lerman (2004). The ubiquitin-proteasome system in cardiovascular diseases-a hypothesis extended. Cardiovasc Res 61(1): 11-21.

Hershko, D., G. Bornstein, O. Ben-Izhak, A. Carrano, M. Pagano, M. M. Krausz and A. Hershko (2001). Inverse relation between levels of p27(Kip1) and of its ubiquitin ligase subunit Skp2 in colorectal carcinomas. Cancer 91(9): 1745-1751.

Hershko, D. D. and M. Shapira (2006). Prognostic role of p27Kip1 deregulation in colorectal cancer. Cancer 107(4): 668-675.

Hicke, L. (2001). Protein regulation by monoubiquitin. Nat Rev Mol Cell Biol 2(3): 195-201.

Hicke, L. and R. Dunn (2003). Regulation of membrane protein transport by ubiquitin and ubiquitin-binding proteins. Annu Rev Cell Dev Biol 19: 141-172.

Hockly, E., V. M. Richon, B. Woodman, D. L. Smith, X. Zhou, E. Rosa, K. Sathasivam, S. Ghazi-Noori, A. Mahal, P. A. Lowden, J. S. Steffan, J. L. Marsh, L. M. Thompson, C. M. Lewis, P. A. Marks and G. P. Bates (2003). Suberoylanilide hydroxamic acid, a histone deacetylase inhibitor, ameliorates motor deficits in a mouse model of Huntington's disease. Proc Natl Acad Sci U S A 100(4): 2041-2046.

Hoppe, T. (2005). Multiubiquitylation by E4 enzymes: 'one size' doesn't fit all. Trends Biochem Sci 30(4): 183-187.

Huang, L., E. Kinnucan, G. Wang, S. Beaudenon, P. M. Howley, J. M. Huibregtse and N. P. Pavletich (1999). Structure of an E6AP-UbcH7 complex: insights into ubiquitination by the E2-E3 enzyme cascade. Science 286(5443): 1321-1326.

Huang, Y. and J. A. Fischer-Vize (1996). Undifferentiated cells in the developing Drosophila eye influence facet assembly and require the Fat facets ubiquitin-specific protease. Development 122(10): 3207-3216.

Huibregtse, J. M. and S. L. Beaudenon (1996). Mechanism of HPV E6 proteins in cellular transformation. Semin Cancer Biol 7(6): 317-326.

Huibregtse, J. M., M. Scheffner, S. Beaudenon and P. M. Howley (1995). A family of proteins structurally and functionally related to the E6-AP ubiquitin-protein ligase. Proc Natl Acad Sci U S A 92(11): 5249.

Huibregtse, J. M., M. Scheffner and P. M. Howley (1993). Cloning and expression of the cDNA for E6-AP, a protein that mediates the interaction of the human papillomavirus E6 oncoprotein with p53. Mol Cell Biol 13(2): 775-784.

Huibregtse, J. M., M. Scheffner and P. M. Howley (1993). Localization of the E6-AP regions that direct human papillomavirus E6 binding, association with p53, and ubiquitination of associated proteins. Mol Cell Biol 13(8): 4918-4927.

Huo, X., Z. Hu, X. Zhai, Y. Wang, S. Wang, X. Wang, J. Qin, W. Chen, G. Jin, J. Liu, J. Gao, Q. Wei, X. Wang and H. Shen (2007). Common non-synonymous polymorphisms in the BRCA1 Associated RING Domain (BARD1) gene are associated with breast cancer susceptibility: a case-control analysis. Breast Cancer Res Treat 102(3): 329-337.

Iijima, K., H. P. Liu, A. S. Chiang, S. A. Hearn, M. Konsolaki and Y. Zhong (2004). Dissecting the pathological effects of human Abeta40 and Abeta42 in Drosophila: a potential model for Alzheimer's disease. Proc Natl Acad Sci U S A 101(17): 6623-6628.

Ikeda, F. and I. Dikic (2006). CYLD in ubiquitin signaling and tumor pathogenesis. Cell 125(4): 643-645.

Ingham, R. J., G. Gish and T. Pawson (2004). The Nedd4 family of E3 ubiquitin ligases: functional diversity within a common modular architecture. Oncogene 23(11): 1972-1984.

Inoue, S., M. Shimoda, I. Nishinokubi, M. C. Siomi, M. Okamura, A. Nakamura, S. Kobayashi, N. Ishida and H. Siomi (2002). A role for the Drosophila fragile X-related gene in circadian output. Curr Biol 12(15): 1331-1335.

Irwin, S. A., M. Idupulapati, M. E. Gilbert, J. B. Harris, A. B. Chakravarti, E. J. Rogers, R. A. Crisostomo, B. P. Larsen, A. Mehta, C. J. Alcantara, B. Patel, R. A. Swain, I. J. Weiler, B. A. Oostra and W. T. Greenough (2002). Dendritic spine and dendritic field characteristics of layer V

pyramidal neurons in the visual cortex of fragile-X knockout mice. Am J Med Genet 111(2): 140-146.

Irwin, S. A., B. Patel, M. Idupulapati, J. B. Harris, R. A. Crisostomo, B. P. Larsen, F. Kooy, P. J. Willems, P. Cras, P. B. Kozlowski, R. A. Swain, I. J. Weiler and W. T. Greenough (2001). Abnormal dendritic spine characteristics in the temporal and visual cortices of patients with fragile-X syndrome: a quantitative examination. Am J Med Genet 98(2): 161-167.

Ishizuka, A., M. C. Siomi and H. Siomi (2002). A Drosophila fragile X protein interacts with components of RNAi and ribosomal proteins. Genes Dev 16(19): 2497-2508.

Izzi, L. and L. Attisano (2004). Regulation of the TGFbeta signalling pathway by ubiquitin-mediated degradation. Oncogene 23(11): 2071-2078.

Jackson, G. R., I. Salecker, X. Dong, X. Yao, N. Arnheim, P. W. Faber, M. E. MacDonald and S. L. Zipursky (1998). Polyglutamine-expanded human huntingtin transgenes induce degeneration of Drosophila photoreceptor neurons. Neuron 21(3): 633-642.

Jackson, G. R., M. Wiedau-Pazos, T. K. Sang, N. Wagle, C. A. Brown, S. Massachi and D. H. Geschwind (2002). Human wild-type tau interacts with wingless pathway components and produces neurofibrillary pathology in Drosophila. Neuron 34(4): 509-519.

Jiang, Y. H., D. Armstrong, U. Albrecht, C. M. Atkins, J. L. Noebels, G. Eichele, J. D. Sweatt and A. L. Beaudet (1998). Mutation of the Angelman ubiquitin ligase in mice causes increased cytoplasmic p53 and deficits of contextual learning and long-term potentiation. Neuron 21(4): 799-811.

Jin, P., D. C. Zarnescu, S. Ceman, M. Nakamoto, J. Mowrey, T. A. Jongens, D. L. Nelson, K. Moses and S. T. Warren (2004). Biochemical and genetic interaction between the fragile X mental retardation protein and the microRNA pathway. Nat Neurosci 7(2): 113-117.

Jones, J. R. and P. M. Macdonald (2007). Oskar controls morphology of polar granules and nuclear bodies in Drosophila. Development 134(2): 233-236.

Kaltenbach, L. S., E. Romero, R. R. Becklin, R. Chettier, R. Bell, A. Phansalkar, A. Strand, C. Torcassi, J. Savage, A. Hurlburt, G. H. Cha, L. Ukani, C. L. Chepanoske, Y. Zhen, S. Sahasrabudhe, J. Olson, C. Kurschner, L. M. Ellerby, J. M. Peltier, J. Botas and R. E. Hughes (2007). Huntingtin Interacting Proteins Are Genetic Modifiers of Neurodegeneration. PLoS Genet 3(5): e82.

Kao, W. H., S. L. Beaudenon, A. L. Talis, J. M. Huibregtse and P. M. Howley (2000). Human papillomavirus type 16 E6 induces self-ubiquitination of the E6AP ubiquitin-protein ligase. J Virol 74(14): 6408-6417.

Kazemi-Esfarjani, P. and S. Benzer (2000). Genetic suppression of polyglutamine toxicity in Drosophila. Science 287(5459): 1837-1840.

Ke, Q. and M. Costa (2006). Hypoxia-inducible factor-1 (HIF-1). Mol Pharmacol 70(5): 1469-1480.

Kinghorn, K. J., D. C. Crowther, L. K. Sharp, C. Nerelius, R. L. Davis, H. T. Chang, C. Green, D. C. Gubb, J. Johansson and D. A. Lomas (2006). Neuroserpin binds Abeta and is a neuroprotective component of amyloid plaques in Alzheimer disease. J Biol Chem 281(39): 29268-29277.

Kishino, T., M. Lalande and J. Wagstaff (1997). UBE3A/E6-AP mutations cause Angelman syndrome. Nat Genet 15(1): 70-73.

Kishino, T. and J. Wagstaff (1998). Genomic organization of the UBE3A/E6-AP gene and related pseudogenes. Genomics 47(1): 101-107.

Kovalenko, A., C. Chable-Bessia, G. Cantarella, A. Israel, D. Wallach and G. Courtois (2003). The tumour suppressor CYLD negatively regulates NF-kappaB signalling by deubiquitination. Nature 424(6950): 801-805.

Kracklauer, M. P., S. M. Banks, X. Xie, Y. Wu and J. A. Fischer (2007). Drosophila klaroid encodes a SUN domain protein required for Klarsicht

localization to the nuclear envelope and nuclear migration in the eye. Fly 1(2): 17-27.

Kuballa, P., K. Matentzoglu and M. Scheffner (2007). The role of the ubiquitin ligase E6-AP in human papillomavirus E6-mediated degradation of PDZ domain-containing proteins. J Biol Chem 282(1): 65-71.

Kuhne, C. and L. Banks (1998). E3-ubiquitin ligase/E6-AP links multicopy maintenance protein 7 to the ubiquitination pathway by a novel motif, the L2G box. J Biol Chem 273(51): 34302-34309.

Kumar, S., A. L. Talis and P. M. Howley (1999). Identification of HHR23A as a substrate for E6-associated protein-mediated ubiquitination. J Biol Chem 274(26): 18785-18792.

Lalande, M. and M. A. Calciano (2007). Molecular epigenetics of Angelman syndrome. Cell Mol Life Sci 64(7-8): 947-960.

Latouche, M., C. Lasbleiz, E. Martin, V. Monnier, T. Debeir, A. Mouatt-Prigent, M. P. Muriel, L. Morel, M. Ruberg, A. Brice, G. Stevanin and H. Tricoire (2007). A conditional pan-neuronal Drosophila model of spinocerebellar ataxia 7 with a reversible adult phenotype suitable for identifying modifier genes. J Neurosci 27(10): 2483-2492.

Lee, A., W. Li, K. Xu, B. A. Bogert, K. Su and F. B. Gao (2003). Control of dendritic development by the Drosophila fragile X-related gene involves the small GTPase Rac1. Development 130(22): 5543-5552.

Lee, W. C., M. Yoshihara and J. T. Littleton (2004). Cytoplasmic aggregates trap polyglutamine-containing proteins and block axonal transport in a Drosophila model of Huntington's disease. Proc Natl Acad Sci U S A 101(9): 3224-3229.

Lehner, P. J., S. Hoer, R. Dodd and L. M. Duncan (2005). Downregulation of cell surface receptors by the K3 family of viral and cellular ubiquitin E3 ligases. Immunol Rev 207: 112-125.

Levecque, C., A. Destee, V. Mouroux, E. Becquet, L. Defebvre, P. Amouyel and M. C. Chartier-Harlin (2001). No genetic association of the

ubiquitin carboxy-terminal hydrolase-L1 gene S18Y polymorphism with familial Parkinson's disease. J Neural Transm 108(8-9): 979-984.

Leyssen, M., D. Ayaz, S. S. Hebert, S. Reeve, B. De Strooper and B. A. Hassan (2005). Amyloid precursor protein promotes post-developmental neurite arborization in the Drosophila brain. Embo J 24(16): 2944-2955.

Lim, K. L., V. L. Dawson and T. M. Dawson (2006). Parkin-mediated lysine 63-linked polyubiquitination: a link to protein inclusions formation in Parkinson's and other conformational diseases? Neurobiol Aging 27(4): 524-529.

Liu, C., E. Fei, N. Jia, H. Wang, R. Tao, A. Iwata, N. Nukina, J. Zhou and G. Wang (2007). Assembly of lysine 63 linked ubiquitin-conjugates by phosphorylated alpha-synuclein implies Lewy body biogenesis. J Biol Chem.

Liu, Y., L. Fallon, H. A. Lashuel, Z. Liu and P. T. Lansbury, Jr. (2002). The UCH-L1 gene encodes two opposing enzymatic activities that affect alpha-synuclein degradation and Parkinson's disease susceptibility. Cell 111(2): 209-218.

Lossie, A. C., M. M. Whitney, D. Amidon, H. J. Dong, P. Chen, D. Theriaque, A. Hutson, R. D. Nicholls, R. T. Zori, C. A. Williams and D. J. Driscoll (2001). Distinct phenotypes distinguish the molecular classes of Angelman syndrome. J Med Genet 38(12): 834-845.

Lu, R., H. Wang, Z. Liang, L. Ku, T. O'Donnell W, W. Li, S. T. Warren and Y. Feng (2004). The fragile X protein controls microtubule-associated protein 1B translation and microtubule stability in brain neuron development. Proc Natl Acad Sci U S A 101(42): 15201-15206.

Lu, Y., Y. Lv, Y. Ye, Y. Wang, Y. Hong, M. E. Fortini, Y. Zhong and Z. Xie (2007). A role for presenilin in post-stress regulation: effects of presenilin mutations on Ca2+ currents in Drosophila. Faseb J.

Malzac, P., H. Webber, A. Moncla, J. M. Graham, M. Kukolich, C. Williams, R. A. Pagon, L. A. Ramsdell, T. Kishino and J. Wagstaff (1998). Mutation analysis of UBE3A in Angelman syndrome patients. Am J Hum Genet 62(6): 1353-1360.

Marsh, J. L. and L. M. Thompson (2004). Can flies help humans treat neurodegenerative diseases? Bioessays 26(5): 485-496.

Marsh, J. L. and L. M. Thompson (2006). Drosophila in the study of neurodegenerative disease. Neuron 52(1): 169-178.

Marsh, J. L., H. Walker, H. Theisen, Y. Z. Zhu, T. Fielder, J. Purcell and L. M. Thompson (2000). Expanded polyglutamine peptides alone are intrinsically cytotoxic and cause neurodegeneration in Drosophila. Hum Mol Genet 9(1): 13-25.

Massoumi, R., K. Chmielarska, K. Hennecke, A. Pfeifer and R. Fassler (2006). Cyld inhibits tumor cell proliferation by blocking Bcl-3-dependent NF-kappaB signaling. Cell 125(4): 665-677.

Matsumoto, Y., S. Nakagawa, T. Yano, S. Takizawa, K. Nagasaka, K. Nakagawa, T. Minaguchi, O. Wada, H. Ooishi, K. Matsumoto, T. Yasugi, T. Kanda, J. M. Huibregtse and Y. Taketani (2006). Involvement of a cellular ubiquitin-protein ligase E6AP in the ubiquitin-mediated degradation of extensive substrates of high-risk human papillomavirus E6. J Med Virol 78(4): 501-507.

Matsuura, T., J. S. Sutcliffe, P. Fang, R. J. Galjaard, Y. H. Jiang, C. S. Benton, J. M. Rommens and A. L. Beaudet (1997). De novo truncating mutations in E6-AP ubiquitin-protein ligase gene (UBE3A) in Angelman syndrome. Nat Genet 15(1): 74-77.

McGrath, J. P., S. Jentsch and A. Varshavsky (1991). UBA 1: an essential yeast gene encoding ubiquitin-activating enzyme. Embo J 10(1): 227-236.

Mellick, G. D. and P. A. Silburn (2000). The ubiquitin carboxy-terminal hydrolase-L1 gene S18Y polymorphism does not confer protection against idiopathic Parkinson's disease. Neurosci Lett 293(2): 127-130.

Menzies, F. M., S. C. Yenisetti and K. T. Min (2005). Roles of Drosophila DJ-1 in survival of dopaminergic neurons and oxidative stress. Curr Biol 15(17): 1578-1582.

Merdes, G., P. Soba, A. Loewer, M. V. Bilic, K. Beyreuther and R. Paro (2004). Interference of human and Drosophila APP and APP-like

proteins with PNS development in Drosophila. Embo J 23(20): 4082-4095.

Merry, D. E. (2005). Animal models of Kennedy disease. NeuroRx 2(3): 471-479.

Meulener, M., A. J. Whitworth, C. E. Armstrong-Gold, P. Rizzu, P. Heutink, P. D. Wes, L. J. Pallanck and N. M. Bonini (2005). Drosophila DJ-1 mutants are selectively sensitive to environmental toxins associated with Parkinson's disease. Curr Biol 15(17): 1572-1577.

Mglinets, V. A., L. Levina and L. M. Konstantinova (1996). [Genomic imprinting and its role in Prader-Willi and Angelman syndromes]. Genetika 32(12): 1605-1615.

Michel, C. I., R. Kraft and L. L. Restifo (2004). Defective neuronal development in the mushroom bodies of Drosophila fragile X mental retardation 1 mutants. J Neurosci 24(25): 5798-5809.

Millard, S. M. and S. A. Wood (2006). Riding the DUBway: regulation of protein trafficking by deubiquitylating enzymes. J Cell Biol 173(4): 463-468.

Miller, R. J. and S. M. Wilson (2003). Neurological disease: UPS stops delivering! Trends Pharmacol Sci 24(1): 18-23.

Miura, K., T. Kishino, E. Li, H. Webber, P. Dikkes, G. L. Holmes and J. Wagstaff (2002). Neurobehavioral and electroencephalographic abnormalities in Ube3a maternal-deficient mice. Neurobiol Dis 9(2): 149-159.

Momand, J., D. Jung, S. Wilczynski and J. Niland (1998). The MDM2 gene amplification database. Nucleic Acids Res 26(15): 3453-3459.

Moncla, A., P. Malzac, M. O. Livet, M. A. Voelckel, J. Mancini, J. C. Delaroziere, N. Philip and J. F. Mattei (1999). Angelman syndrome resulting from UBE3A mutations in 14 patients from eight families: clinical manifestations and genetic counselling. J Med Genet 36(7): 554-560.

Monzo, K., O. Papoulas, G. T. Cantin, Y. Wang, J. R. Yates, 3rd and J. C. Sisson (2006). Fragile X mental retardation protein controls trailer hitch expression and cleavage furrow formation in Drosophila embryos. Proc Natl Acad Sci U S A 103(48): 18160-18165.

Morales, J., P. R. Hiesinger, A. J. Schroeder, K. Kume, P. Verstreken, F. R. Jackson, D. L. Nelson and B. A. Hassan (2002). Drosophila fragile X protein, DFXR, regulates neuronal morphology and function in the brain. Neuron 34(6): 961-972.

Mukhopadhyay, D. and H. Riezman (2007). Proteasome-independent functions of ubiquitin in endocytosis and signaling. Science 315(5809): 201-205.

Mutsuddi, M. and I. Rebay (2005). Molecular genetics of spinocerebellar ataxia type 8 (SCA8). RNA Biol 2(2): 49-52.

Nakagawa, S. and J. M. Huibregtse (2000). Human scribble (Vartul) is targeted for ubiquitin-mediated degradation by the high-risk papillomavirus E6 proteins and the E6AP ubiquitin-protein ligase. Mol Cell Biol 20(21): 8244-8253.

Nakao, M., J. S. Sutcliffe, B. Durtschi, A. Mutirangura, D. H. Ledbetter and A. L. Beaudet (1994). Imprinting analysis of three genes in the Prader-Willi/Angelman region: SNRPN, E6-associated protein, and PAR-2 (D15S225E). Hum Mol Genet 3(2): 309-315.

Nijman, S. M., M. P. Luna-Vargas, A. Velds, T. R. Brummelkamp, A. M. Dirac, T. K. Sixma and R. Bernards (2005). A genomic and functional inventory of deubiquitinating enzymes. Cell 123(5): 773-786.

Nuber, U., S. E. Schwarz and M. Scheffner (1998). The ubiquitin-protein ligase E6-associated protein (E6-AP) serves as its own substrate. Eur J Biochem 254(3): 643-649.

Ocorr, K., T. Akasaka and R. Bodmer (2007). Age-related cardiac disease model of Drosophila. Mech Ageing Dev 128(1): 112-116.

Oda, H., S. Kumar and P. M. Howley (1999). Regulation of the Src family tyrosine kinase Blk through E6AP-mediated ubiquitination. Proc Natl Acad Sci U S A 96(17): 9557-9562.

Ohh, M. (2006). Ubiquitin pathway in VHL cancer syndrome. Neoplasia 8(8): 623-629.

Onel, K. and C. Cordon-Cardo (2004). MDM2 and prognosis. Mol Cancer Res 2(1): 1-8.

Orso, G., A. Martinuzzi, M. G. Rossetto, E. Sartori, M. Feany and A. Daga (2005). Disease-related phenotypes in a Drosophila model of hereditary spastic paraplegia are ameliorated by treatment with vinblastine. J Clin Invest 115(11): 3026-3034.

Palladino, M. J., T. J. Hadley and B. Ganetzky (2002). Temperature-sensitive paralytic mutants are enriched for those causing neurodegeneration in Drosophila. Genetics 161(3): 1197-1208.

Park, J., S. Y. Kim, G. H. Cha, S. B. Lee, S. Kim and J. Chung (2005). Drosophila DJ-1 mutants show oxidative stress-sensitive locomotive dysfunction. Gene 361: 133-139.

Park, J., S. B. Lee, S. Lee, Y. Kim, S. Song, S. Kim, E. Bae, J. Kim, M. Shong, J. M. Kim and J. Chung (2006). Mitochondrial dysfunction in Drosophila PINK1 mutants is complemented by parkin. Nature 441(7097): 1157-1161.

Patterson, K., A. B. Molofsky, C. Robinson, S. Acosta, C. Cater and J. A. Fischer (2004). The functions of Klarsicht and nuclear lamin in developmentally regulated nuclear migrations of photoreceptor cells in the Drosophila eye. Mol Biol Cell 15(2): 600-610.

Pesah, Y., T. Pham, H. Burgess, B. Middlebrooks, P. Verstreken, Y. Zhou, M. Harding, H. Bellen and G. Mardon (2004). Drosophila parkin mutants have decreased mass and cell size and increased sensitivity to oxygen radical stress. Development 131(9): 2183-2194.

Petersen, M. B., K. Brondum-Nielsen, L. K. Hansen and K. Wulff (1995). Clinical, cytogenetic, and molecular diagnosis of Angelman syndrome: estimated prevalence rate in a Danish county. Am J Med Genet 60(3): 261-262.

Pickart, C. M. (2001). Mechanisms underlying ubiquitination. Annu Rev Biochem 70: 503-533.

Plafker, S. M., K. S. Plafker, A. M. Weissman and I. G. Macara (2004). Ubiquitin charging of human class III ubiquitin-conjugating enzymes triggers their nuclear import. J Cell Biol 167(4): 649-659.

Plant, P. J., H. Yeger, O. Staub, P. Howard and D. Rotin (1997). The C2 domain of the ubiquitin protein ligase Nedd4 mediates Ca2+-dependent plasma membrane localization. J Biol Chem 272(51): 32329-32336.

Plante, I., L. Davidovic, D. L. Ouellet, L. A. Gobeil, S. Tremblay, E. W. Khandjian and P. Provost (2006). Dicer-Derived MicroRNAs Are Utilized by the Fragile X Mental Retardation Protein for Assembly on Target RNAs. J Biomed Biotechnol 2006(4): 64347.

Rapakko, K., H. Kokkonen and J. Leisti (2004). UBE3A gene mutations in Finnish Angelman syndrome patients detected by conformation sensitive gel electrophoresis. Am J Med Genet A 126(3): 248-252.

Reeve, S. P., L. Bassetto, G. K. Genova, Y. Kleyner, M. Leyssen, F. R. Jackson and B. A. Hassan (2005). The Drosophila fragile X mental retardation protein controls actin dynamics by directly regulating profilin in the brain. Curr Biol 15(12): 1156-1163.

Reiter, L. T., L. Potocki, S. Chien, M. Gribskov and E. Bier (2001). A systematic analysis of human disease-associated gene sequences in Drosophila melanogaster. Genome Res 11(6): 1114-1125.

Reiter, L. T., T. N. Seagroves, M. Bowers and E. Bier (2006). Expression of the Rho-GEF Pbl/ECT2 is regulated by the UBE3A E3 ubiquitin ligase. Hum Mol Genet 15(18): 2825-2835.

Roman, G. and R. L. Davis (2001). Molecular biology and anatomy of Drosophila olfactory associative learning. Bioessays 23(7): 571-581.

Rorth, P. (1998). Gal4 in the Drosophila female germline. Mech Dev 78(1-2): 113-118.

Rosen, D. R., L. Martin-Morris, L. Q. Luo and K. White (1989). A Drosophila gene encoding a protein resembling the human beta-amyloid protein precursor. Proc Natl Acad Sci U S A 86(7): 2478-2482.

Rotin, D., O. Staub and R. Haguenauer-Tsapis (2000). Ubiquitination and endocytosis of plasma membrane proteins: role of Nedd4/Rsp5p family of ubiquitin-protein ligases. J Membr Biol 176(1): 1-17.

Rougeulle, C., H. Glatt and M. Lalande (1997). The Angelman syndrome candidate gene, UBE3A/E6-AP, is imprinted in brain. Nat Genet 17(1): 14-15.

Rougeulle, C. and M. Lalande (1998). Angelman syndrome: how many genes to remain silent? Neurogenetics 1(4): 229-237.

Rubin, G. M., M. D. Yandell, J. R. Wortman, G. L. Gabor Miklos, C. R. Nelson, I. K. Hariharan, M. E. Fortini, P. W. Li, R. Apweiler, W. Fleischmann, J. M. Cherry, S. Henikoff, M. P. Skupski, S. Misra, M. Ashburner, E. Birney, M. S. Boguski, T. Brody, P. Brokstein, S. E. Celniker, S. A. Chervitz, D. Coates, A. Cravchik, A. Gabrielian, R. F. Galle, W. M. Gelbart, R. A. George, L. S. Goldstein, F. Gong, P. Guan, N. L. Harris, B. A. Hay, R. A. Hoskins, J. Li, Z. Li, R. O. Hynes, S. J. Jones, P. M. Kuehl, B. Lemaitre, J. T. Littleton, D. K. Morrison, C. Mungall, P. H. O'Farrell, O. K. Pickeral, C. Shue, L. B. Vosshall, J. Zhang, Q. Zhao, X. H. Zheng and S. Lewis (2000). Comparative genomics of the eukaryotes. Science 287(5461): 2204-2215.

Russo, S., F. Cogliati, M. Viri, F. Cavalleri, A. Selicorni, L. Turolla, S. Belli, A. Romeo and L. Larizza (2000). Novel mutations of ubiquitin protein ligase 3A gene in Italian patients with Angelman syndrome. Hum Mutat 15(4): 387.

Rusu, P., A. Jansen, P. Soba, J. Kirsch, A. Lower, G. Merdes, Y. H. Kuan, A. Jung, K. Beyreuther, O. Kjaerulff and S. Kins (2007). Axonal accumulation of synaptic markers in APP transgenic Drosophila depends on the NPTY motif and is paralleled by defects in synaptic plasticity. Eur J Neurosci 25(4): 1079-1086.

Sahoo, T., C. A. Shaw, A. S. Young, N. L. Whitehouse, R. J. Schroer, R. E. Stevenson and A. L. Beaudet (2005). Array-based comparative genomic hybridization analysis of recurrent chromosome 15q rearrangements. Am J Med Genet A 139(2): 106-113.

Saitoh, S., T. Wada, M. Okajima, K. Takano, A. Sudo and N. Niikawa (2005). Uniparental disomy and imprinting defects in Japanese patients with Angelman syndrome. Brain Dev 27(5): 389-391.

Sakamoto, K. M. (2002). Ubiquitin-dependent proteolysis: its role in human diseases and the design of therapeutic strategies. Mol Genet Metab 77(1-2): 44-56.

Sanchez-Martinez, A., N. Luo, P. Clemente, C. Adan, R. Hernandez-Sierra, P. Ochoa, M. A. Fernandez-Moreno, L. S. Kaguni and R. Garesse (2006). Modeling human mitochondrial diseases in flies. Biochim Biophys Acta 1757(9-10): 1190-1198.

Satoh, J. and Y. Kuroda (2001). A polymorphic variation of serine to tyrosine at codon 18 in the ubiquitin C-terminal hydrolase-L1 gene is associated with a reduced risk of sporadic Parkinson's disease in a Japanese population. J Neurol Sci 189(1-2): 113-117.

Scheffner, M., J. M. Huibregtse, R. D. Vierstra and P. M. Howley (1993). The HPV-16 E6 and E6-AP complex functions as a ubiquitin-protein ligase in the ubiquitination of p53. Cell 75(3): 495-505.

Schenck, A., B. Bardoni, C. Langmann, N. Harden, J. L. Mandel and A. Giangrande (2003). CYFIP/Sra-1 controls neuronal connectivity in Drosophila and links the Rac1 GTPase pathway to the fragile X protein. Neuron 38(6): 887-898.

Seidner, G. A., Y. Ye, M. M. Faraday, W. G. Alvord and M. E. Fortini (2006). Modeling clinically heterogeneous presenilin mutations with transgenic Drosophila. Curr Biol 16(10): 1026-1033.

Shang, F., G. Deng, M. Obin, C. C. Wu, X. Gong, D. Smith, R. A. Laursen, U. P. Andley, J. R. Reddan and A. Taylor (2001). Ubiquitin-activating enzyme (E1) isoforms in lens epithelial cells: origin of translation, E2 specificity and cellular localization determined with novel site-specific antibodies. Exp Eye Res 73(6): 827-836.

Shearwin-Whyatt, L., H. E. Dalton, N. Foot and S. Kumar (2006). Regulation of functional diversity within the Nedd4 family by accessory and adaptor proteins. Bioessays 28(6): 617-628.

Snyder, P. M. (2005). Minireview: regulation of epithelial Na+ channel trafficking. Endocrinology 146(12): 5079-5085.

Snyder, P. M., J. C. Steines and D. R. Olson (2004). Relative contribution of Nedd4 and Nedd4-2 to ENaC regulation in epithelia determined by RNA interference. J Biol Chem 279(6): 5042-5046.

Spencer, C. M., E. Serysheva, L. A. Yuva-Paylor, B. A. Oostra, D. L. Nelson and R. Paylor (2006). Exaggerated behavioral phenotypes in Fmr1/Fxr2 double knockout mice reveal a functional genetic interaction between Fragile X-related proteins. Hum Mol Genet 15(12): 1984-1994.

Starita, L. M. and J. D. Parvin (2006). Substrates of the BRCA1-dependent ubiquitin ligase. Cancer Biol Ther 5(2): 137-141.

Staub, O., I. Gautschi, T. Ishikawa, K. Breitschopf, A. Ciechanover, L. Schild and D. Rotin (1997). Regulation of stability and function of the epithelial Na+ channel (ENaC) by ubiquitination. Embo J 16(21): 6325-6336.

Steffan, J. S., N. Agrawal, J. Pallos, E. Rockabrand, L. C. Trotman, N. Slepko, K. Illes, T. Lukacsovich, Y. Z. Zhu, E. Cattaneo, P. P. Pandolfi, L. M. Thompson and J. L. Marsh (2004). SUMO modification of Huntingtin and Huntington's disease pathology. Science 304(5667): 100-104.

Steffan, J. S., L. Bodai, J. Pallos, M. Poelman, A. McCampbell, B. L. Apostol, A. Kazantsev, E. Schmidt, Y. Z. Zhu, M. Greenwald, R. Kurokawa, D. E. Housman, G. R. Jackson, J. L. Marsh and L. M. Thompson (2001). Histone deacetylase inhibitors arrest polyglutamine-dependent neurodegeneration in Drosophila. Nature 413(6857): 739-743.

Steffenburg, S., C. L. Gillberg, U. Steffenburg and M. Kyllerman (1996). Autism in Angelman syndrome: a population-based study. Pediatr Neurol 14(2): 131-136.

Stephen, A. G., J. S. Trausch-Azar, A. Ciechanover and A. L. Schwartz (1996). The ubiquitin-activating enzyme E1 is phosphorylated and localized to the nucleus in a cell cycle-dependent manner. J Biol Chem 271(26): 15608-15614.

Stokin, G. B., C. Lillo, T. L. Falzone, R. G. Brusch, E. Rockenstein, S. L. Mount, R. Raman, P. Davies, E. Masliah, D. S. Williams and L. S. Goldstein (2005). Axonopathy and transport deficits early in the pathogenesis of Alzheimer's disease. Science 307(5713): 1282-1288.

Strauss, R. (2002). The central complex and the genetic dissection of locomotor behaviour. Curr Opin Neurobiol 12(6): 633-638.

Sun, Y. (2003). Targeting E3 ubiquitin ligases for cancer therapy. Cancer Biol Ther 2(6): 623-629.

Sutcliffe, J. S., Y. H. Jiang, R. J. Galijaard, T. Matsuura, P. Fang, T. Kubota, S. L. Christian, J. Bressler, B. Cattanach, D. H. Ledbetter and A. L. Beaudet (1997). The E6-Ap ubiquitin-protein ligase (UBE3A) gene is localized within a narrowed Angelman syndrome critical region. Genome Res 7(4): 368-377.

Takeyama, K., S. Ito, A. Yamamoto, H. Tanimoto, T. Furutani, H. Kanuka, M. Miura, T. Tabata and S. Kato (2002). Androgen-dependent neurodegeneration by polyglutamine-expanded human androgen receptor in Drosophila. Neuron 35(5): 855-864.

Talis, A. L., J. M. Huibregtse and P. M. Howley (1998). The role of E6AP in the regulation of p53 protein levels in human papillomavirus (HPV)-positive and HPV-negative cells. J Biol Chem 273(11): 6439-6445.

Taylor, J. P., A. A. Taye, C. Campbell, P. Kazemi-Esfarjani, K. H. Fischbeck and K. T. Min (2003). Aberrant histone acetylation, altered transcription, and retinal degeneration in a Drosophila model of polyglutamine disease are rescued by CREB-binding protein. Genes Dev 17(12): 1463-1468.

Torroja, L., H. Chu, I. Kotovsky and K. White (1999). Neuronal overexpression of APPL, the Drosophila homologue of the amyloid precursor protein (APP), disrupts axonal transport. Curr Biol 9(9): 489-492.

Torroja, L., M. Packard, M. Gorczyca, K. White and V. Budnik (1999). The Drosophila beta-amyloid precursor protein homolog promotes synapse differentiation at the neuromuscular junction. J Neurosci 19(18): 7793-7803.

Trompouki, E., E. Hatzivassiliou, T. Tsichritzis, H. Farmer, A. Ashworth and G. Mosialos (2003). CYLD is a deubiquitinating enzyme that negatively regulates NF-kappaB activation by TNFR family members. Nature 424(6950): 793-796.

Troulinaki, K. and N. Tavernarakis (2005). Neurodegenerative conditions associated with ageing: a molecular interplay? Mech Ageing Dev 126(1): 23-33.

Tsai, T. F., A. Raas-Rothschild, Z. Ben-Neriah and A. L. Beaudet (1998). Prenatal diagnosis and carrier detection for a point mutation in UBE3A causing Angelman syndrome. Am J Hum Genet 63(5): 1561-1563.

van Woerden, G. M., K. D. Harris, M. R. Hojjati, R. M. Gustin, S. Qiu, R. de Avila Freire, Y. H. Jiang, Y. Elgersma and E. J. Weeber (2007). Rescue of neurological deficits in a mouse model for Angelman syndrome by reduction of alphaCaMKII inhibitory phosphorylation. Nat Neurosci 10(3): 280-282.

Varela, M. C., F. Kok, P. A. Otto and C. P. Koiffmann (2004). Phenotypic variability in Angelman syndrome: comparison among different deletion classes and between deletion and UPD subjects. Eur J Hum Genet 12(12): 987-992.

Vidal, M. and R. L. Cagan (2006). Drosophila models for cancer research. Curr Opin Genet Dev 16(1): 10-16.

Vu, T. H. and A. R. Hoffman (1997). Imprinting of the Angelman syndrome gene, UBE3A, is restricted to brain. Nat Genet 17(1): 12-13.

Wan, L., T. C. Dockendorff, T. A. Jongens and G. Dreyfuss (2000). Characterization of dFMR1, a Drosophila melanogaster homolog of the fragile X mental retardation protein. Mol Cell Biol 20(22): 8536-8547.

Wang, J., C. Y. Zhao, Y. M. Si, Z. L. Liu, B. Chen and L. Yu (2002). ACT and UCH-L1 polymorphisms in Parkinson's disease and age of onset. Mov Disord 17(4): 767-771.

Wang, M. and C. M. Pickart (2005). Different HECT domain ubiquitin ligases employ distinct mechanisms of polyubiquitin chain synthesis. Embo J 24(24): 4324-4333.

Warrick, J. M., H. Y. Chan, G. L. Gray-Board, Y. Chai, H. L. Paulson and N. M. Bonini (1999). Suppression of polyglutamine-mediated neurodegeneration in Drosophila by the molecular chaperone HSP70. Nat Genet 23(4): 425-428.

Warrick, J. M., H. L. Paulson, G. L. Gray-Board, Q. T. Bui, K. H. Fischbeck, R. N. Pittman and N. M. Bonini (1998). Expanded polyglutamine protein forms nuclear inclusions and causes neural degeneration in Drosophila. Cell 93(6): 939-949.

Weeber, E. J., Y. H. Jiang, Y. Elgersma, A. W. Varga, Y. Carrasquillo, S. E. Brown, J. M. Christian, B. Mirnikjoo, A. Silva, A. L. Beaudet and J. D. Sweatt (2003). Derangements of hippocampal calcium/calmodulin-dependent protein kinase II in a mouse model for Angelman mental retardation syndrome. J Neurosci 23(7): 2634-2644.

Weissman, A. M. (2001). Themes and variations on ubiquitylation. Nat Rev Mol Cell Biol. **2:** 169-178.

Whitworth, A. J., D. A. Theodore, J. C. Greene, H. Benes, P. D. Wes and L. J. Pallanck (2005). Increased glutathione S-transferase activity rescues dopaminergic neuron loss in a Drosophila model of Parkinson's disease. Proc Natl Acad Sci U S A 102(22): 8024-8029.

Whitworth, A. J., P. D. Wes and L. J. Pallanck (2006). Drosophila models pioneer a new approach to drug discovery for Parkinson's disease. Drug Discov Today 11(3-4): 119-126.

Wiemuth, D., Y. Ke, M. Rohlfs and F. J. McDonald (2007). Epithelial sodium channel (ENaC) is multiubiquitinated at the cell surface. Biochem J.

Williams, C. A. (2005). Neurological aspects of the Angelman syndrome. Brain Dev 27(2): 88-94.

Williams, C. A., A. L. Beaudet, J. Clayton-Smith, J. H. Knoll, M. Kyllerman, L. A. Laan, R. E. Magenis, A. Moncla, A. A. Schinzel, J. A. Summers and J. Wagstaff (2006). Angelman syndrome 2005: updated consensus for diagnostic criteria. Am J Med Genet A 140(5): 413-418.

Willis, M. S. and C. Patterson (2006). Into the heart: the emerging role of the ubiquitin-proteasome system. J Mol Cell Cardiol 41(4): 567-579.

Wittmann, C. W., M. F. Wszolek, J. M. Shulman, P. M. Salvaterra, J. Lewis, M. Hutton and M. B. Feany (2001). Tauopathy in Drosophila:

neurodegeneration without neurofibrillary tangles. Science 293(5530): 711-714.

Wood-Kaczmar, A., S. Gandhi and N. W. Wood (2006). Understanding the molecular causes of Parkinson's disease. Trends Mol Med 12(11): 521-528.

Wu, M. Y., K. S. Chen, J. Bressler, A. Hou, T. F. Tsai and A. L. Beaudet (2006). Mouse imprinting defect mutations that model Angelman syndrome. Genesis 44(1): 12-22.

Xu, K., B. A. Bogert, W. Li, K. Su, A. Lee and F. B. Gao (2004). The fragile X-related gene affects the crawling behavior of Drosophila larvae by regulating the mRNA level of the DEG/ENaC protein pickpocket1. Curr Biol 14(12): 1025-1034.

Yamamoto, Y., J. M. Huibregtse and P. M. Howley (1997). The human E6-AP gene (UBE3A) encodes three potential protein isoforms generated by differential splicing. Genomics 41(2): 263-266.

Yang, Y., S. Gehrke, M. E. Haque, Y. Imai, J. Kosek, L. Yang, M. F. Beal, I. Nishimura, K. Wakamatsu, S. Ito, R. Takahashi and B. Lu (2005). Inactivation of Drosophila DJ-1 leads to impairments of oxidative stress response and phosphatidylinositol 3-kinase/Akt signaling. Proc Natl Acad Sci U S A 102(38): 13670-13675.

Yang, Y., S. Gehrke, Y. Imai, Z. Huang, Y. Ouyang, J. W. Wang, L. Yang, M. F. Beal, H. Vogel and B. Lu (2006). Mitochondrial pathology and muscle and dopaminergic neuron degeneration caused by inactivation of Drosophila Pink1 is rescued by Parkin. Proc Natl Acad Sci U S A 103(28): 10793-10798.

Ye, Y. and M. E. Fortini (1999). Apoptotic activities of wild-type and Alzheimer's disease-related mutant presenilins in Drosophila melanogaster. J Cell Biol 146(6): 1351-1364.

Yokoi, S., K. Yasui, M. Mori, T. Iizasa, T. Fujisawa and J. Inazawa (2004). Amplification and overexpression of SKP2 are associated with metastasis of non-small-cell lung cancers to lymph nodes. Am J Pathol 165(1): 175-180.

Yokoi, S., K. Yasui, F. Saito-Ohara, K. Koshikawa, T. Iizasa, T. Fujisawa, T. Terasaki, A. Horii, T. Takahashi, S. Hirohashi and J. Inazawa (2002). A novel target gene, SKP2, within the 5p13 amplicon that is frequently detected in small cell lung cancers. Am J Pathol 161(1): 207-216.

Zarnescu, D. C., P. Jin, J. Betschinger, M. Nakamoto, Y. Wang, T. C. Dockendorff, Y. Feng, T. A. Jongens, J. C. Sisson, J. A. Knoblich, S. T. Warren and K. Moses (2005). Fragile X protein functions with lgl and the par complex in flies and mice. Dev Cell 8(1): 43-52.

Zhang, H., J. Tan, E. Reynolds, D. Kuebler, S. Faulhaber and M. Tanouye (2002). The Drosophila slamdance gene: a mutation in an aminopeptidase can cause seizure, paralysis and neuronal failure. Genetics 162(3): 1283-1299.

Zhang, J., N. Hattori, E. Leroy, H. R. Morris, S. Kubo, T. Kobayashi, N. W. Wood, M. H. Polymeropoulos and Y. Mizuno (2000). Association between a polymorphism of ubiquitin carboxy-terminal hydrolase L1 (UCH-L1) gene and sporadic Parkinson's disease. Parkinsonism Relat Disord 6(4): 195-197.

Zhang, X. D. and M. J. Matunis (2005). Ub in charge: regulating E2 enzyme nuclear import. Nat Cell Biol 7(1): 12-14.

Zhang, Y. Q., A. M. Bailey, H. J. Matthies, R. B. Renden, M. A. Smith, S. D. Speese, G. M. Rubin and K. Broadie (2001). Drosophila fragile X-related gene regulates the MAP1B homolog Futsch to control synaptic structure and function. Cell 107(5): 591-603.

Zhang, Y. Q., D. B. Friedman, Z. Wang, E. Woodruff, 3rd, L. Pan, J. O'Donnell and K. Broadie (2005). Protein expression profiling of the drosophila fragile X mutant brain reveals up-regulation of monoamine synthesis. Mol Cell Proteomics 4(3): 278-290.

Zhang, Y. Q., H. J. Matthies, J. Mancuso, H. K. Andrews, E. Woodruff, 3rd, D. Friedman and K. Broadie (2004). The Drosophila fragile X-related gene regulates axoneme differentiation during spermatogenesis. Dev Biol 270(2): 290-307.

Vita

Yaning Wu is the daughter of Zongyue Wu and Xiuying Geng. She was born on June 9, 1974 in Fushun, Liaoning Province, P. R. China. She graduated from China Medical University in September, 1997 and her major was clinical medicine. After that, she began her study in the National Laboratory of Medical Molecular Biology in Peking Union Medical College & Chinese Academy of Medical Sciences in Beijing, China. There, she worked on the identification of susceptible genes of Alzheimer's disease in the Chinese population, and she received a M.S. in biochemistry and molecular biology in August, 2000. She began her graduate education in molecular biology at the Institute of Cell and Molecular Biology at the University of Texas at Austin in September, 2000. She joined Dr. Fischer's laboratory in summer, 2001. Her project in the Fischer laboratory was to establish a *Drosophila* model for Angelman syndrome.

Permanent address: 503 Building 4, Yumin St., Fushun, Liaoning,

P.R.China

The dissertation was typed by Yaning Wu.